
ALGERIA


BURKINA FASO


MALI


MAURITANIA

Integrated and Sustainable Management of Shared Aquifer Systems and Basins of the Sahel Region

RAF/7/011

TAOUDENI BASIN

2017

EDITORIAL NOTE

REPORT OF THE IAEA-SUPPORTED REGIONAL TECHNICAL COOPERATION PROJECT RAF/7/011

TAOUDENI BASIN

COUNTERPARTS:

Mr Adnane Souffi MOULLA (Algeria)

Mr Abdelwaheb SMATI (Algeria)

Ms Ratoussian Aline KABORE KOMI (Burkina Faso)

Mr Alphonse GALBANE (Burkina Faso)

Mr Sidi KONE (Mali)

Mr Aly THIAM (Mali)

Mr Brahim Labatt HMEYADE (Mauritania)

Mr Sidi Haiba BACAR (Mauritania)

EXPERT:

Mr Jean Denis TAUPIN (France)

Reproduced by the IAEA

Vienna, Austria, 2017

Table of Contents

1. INTRODUCTION

The Taoudeni Basin (1,500,000 km^2) is a major geological sedimentary formation in West Africa named after the Taoudeni village in northern Mali. It covers large parts of the West African Craton in Mauritania, Mali and the south-western part of Burkina Faso (Fig. 1).

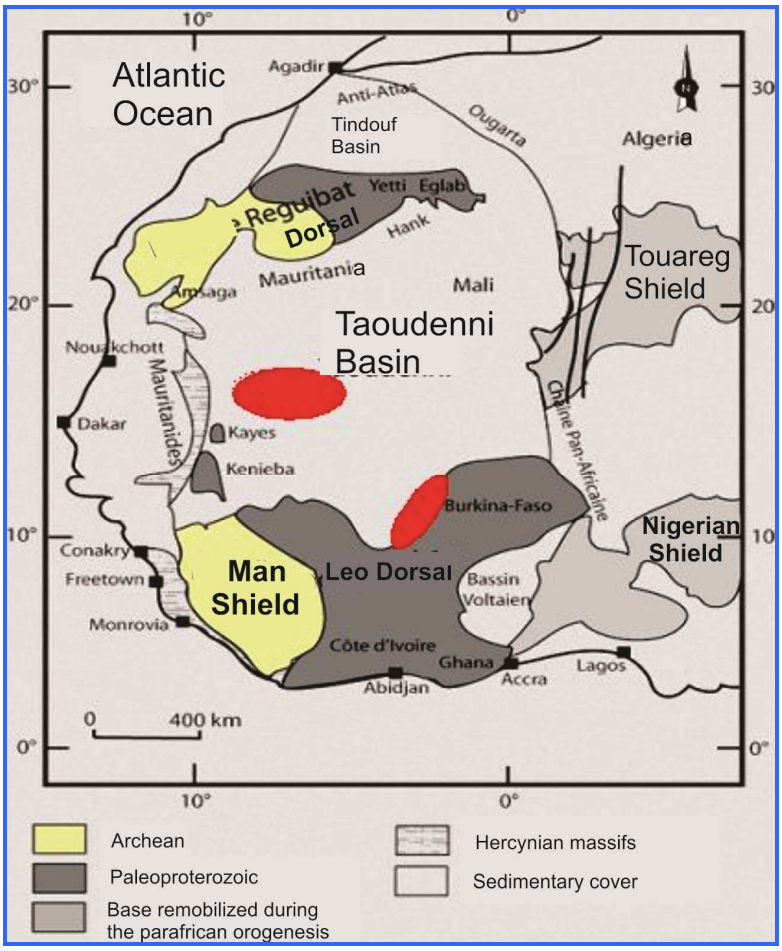

Figure 1: The Taoudeni basin. The study zones included in the IAEA-supported project RAF/7/011 are presented as red ellipses.

The Taoudeni is the largest sedimentary syncline basin in north-west Africa, formed during the mid-late Proterozoic. It continued to subside until the mid-Palaeozoic-age, when Hercynian deformation and uplift occurred. It contains up to 6,000 m of Late Precambrian and Palaeozoic sediments. It is only sparsely covered by thin Mesozoic–Cenozoic continental deposits including Quaternary dunes and lacustrine systems. These last deposits show a spatial continuity between different basins, Taoudeni and Tanezrouft basin in the northern part and Taoudeni and the Iullemeden basin in eastern part. Water reserve in Taoudeni basin are very important, but the current climatic condition from Sahel-Sudanese climate (annual precipitation between 600 to 1000 mm/y) in the southern part to arid climate (< 150 mm/y) in central and northern part does not allow a complete replenishment of water extracted by

human activities. If in the northern part of Taoudeni the population density is low and consumption of water limited, in the central part, and especially in southern part, the population growth rate is about 3% by year, which involves an increasing demand of water, resulting a decrease of water table in numerous aquifers and a water quality degradation due to human activities and the lack of environmental protection.

Two study zones has been investigated for the purpose of this IAEA-supported project RAF/7/011, involving three countries, Mauritania, Mali and Burkina Faso with a limited action for Mali respecting to the initial project due to security problems in northern part (Fig.1).

The study zone is shared between Mali and Burkina Faso in the southern part (SE Mali-SW Burkina Faso) and corresponds to the limit east of Taoudeni sedimentary basin where Infra Cambrian deposit infill unconformable onto the Paleo-Proterozoic crystalline basement at the surface. The total area is 9°30'-15°5' latitude and 1°30'-8°30'W longitude.

Previous studies on isotopes and hydrochemistry in the target area

Concerning existing data or project in Mauritanian Taoudeni basin study zone, accessible bibliography by internet and scientific data does not refer to other studies. Also, some geological elements (map, cross section, stratigraphic profile was given by counterpart in different IAEA meeting concerning the IAEA-supported project RAF/7/011, with a zone covering 15°-17° N ; 6-12°W.

Regarding existing data or project in the study zone, few geochemical and isotopic data are available for the central and western part. However, the eastern part has been the subject of numerous studies and projects in hydrogeology and water quality, since 70's with the decrease of rainfall in Sahelian Sudanian zone:

-The "Mali sud" project (SOGREAH, 1988) which has determined transmissivity parameters on western area of BKF,

-The "Bilan d'eau" project in BKF (Iwago, 1989) which enabled to classify aquifers in three classes depending on the type of porosity,

-The ERES program (close to Bobo Dioulasso) a detailed study of groundwater hydrodynamic in the Kou Basin- 1500 km^2 (SOGREAH, 1994) according to the diversity of Infracambrian sedimentary layers.

-The RESO (1994) and BAD (1999) projects which are an extension of ERES project to develop an extensive data bank on wells location.

The first significant work was done by Ouedrago (1994) with a geological synthesis of BKF part of Taoudeni basin and a description of local groundwater in terms of hydrodynamic and geochemistry. Dakouré (2003) and Huneau et al. (2011), have completed the work of Ouedrago with geochemical and isotopic studies of groundwater on the same zone using different detailed geochemical and isotopic analyses performed over the area since the 1980s through the IAEA-supported Technical Cooperation projects, in particular two projects in Burkina Faso (BKF/8/002 and BKF/8/003) and one in Mali (MLI/8/002). Geochemical and isotopic data from 110 sampling points were selected, among which 98 points for tritium and 39 points for radiocarbon groundwater residence time calculation. The isotopic signature of the recharge was calculated using data from GNIP (IAEA/WMO, 2006) of Bobo-Dioulasso, Barogo and Bamako stations. The main results of this study were to provide a fine hydrodynamic and the geochemical state of the aquifer system and to propose a first model of a single aquifer flowing through the different sedimentary formations in spite of hydraulic local discontinuities. The author brings to light and quantify the decrease of level water (30 m/y in BKF) with respect to increase human consumption and decrease of rainfall. The geochemistry study shows mainly Ca–Mg–HCO_3 type which can shift towards a Na–K–HCO_3 type that indicates developed interactions between groundwater and clay minerals related to the residence time or towards a Cl–NO_3–SO_4–HCO_3 type indicating the anthropogenic influence on groundwater related to the poor sanitary conditions observed around wells. Isotopic study shows in general, over the zone aquifer, weak or null current renewable with locally recent recharge predominant.

The sampling of the IAEA-supported project RAF/7/011 corresponds to the same zone that the study of Dakouré. The last work (Koussobe, 2013) was focused on hydrogeology, hydrochemistry and isotopic study of Gondo plain (Sourou basin) with hydrodynamic modelling. This work is located a little further north to RAF/7/011 project, studying the hydrogeology of Infra Cambrian, Continental Terminal on top of the Infra Cambrian deposit and crystalline basement, geological formation identified in the Gondo plain. The main results has allowed to define the geometric and piezometric characterization of the different aquifers,

to show a recent recharge (superficial aquifers) or deep aquifer on the border of Gondo plain and recharge before 1950 for other deep aquifers below the Continental Terminal (no carbon-14 was analysed to refine dating but one can assume older age as in the Dakouré study, showing stable isotopes more depleted than current rainfall).Due to difference of knowledge level according to the study zone of Mauritania and Mali-BKF, the defined objectives are different.

Objectives of the IAEA-supported project RAF/7/011 in the target aquifer

The objectives of the IAEA-supported project RAF/7/011 in Mauritania Taoudeni basin are to: produce a first evaluation of groundwater potentiality; a first geochemical characterization of spatial variability to linked to geological information; define the flow direction with a potentiometric map showing if there is a relation between superficial and deeper aquifers and showing if current recharge occurs with water stable isotope and tritium. The main difficulty is to compare stable isotopes in groundwater and stable isotope in rainfall, indeed data are very scarce, including limited data in North Senegal (Travi et al., 1987) and recent data (2013-2015) in the Mauritanian coastal section Rosso-Tiguint-Boutilimit-Nouakchott, and with climate conditions different than the RAF/7/011 study zone.

The objectives of the project RAF/7/011 are different in western and eastern study zone of Mali. In western part there are few data it is a first evaluation of groundwater potentiality (west ICT "Infra-Cambrian Tabulaire", CI "Continental Intercalaire and CT "Continental Terminal"), the same objectives for Mauritania could possibly be reached at the end of RAF/7/011 project. In eastern part and Burkina Faso part, there is much data available, with a high sampling density and a scientific value of this work. These new data will strengthen the past interpretation and by comparing data, allow detecting any geochemistry evolution of groundwater (anthropic contribution more important) and adjusting a hydrodynamic model by comparing tritium temporal evolution. The need to develop, in the coming months, a numerical modelling with geochemistry and isotope data is obvious.

2. STUDY SITES

2.1. General presentation of involved countries

The Islamic Republic of Mauritania (Nouakchott as capital) is 1,030,000 km^2, 90% of which is desert. It lies mostly between latitudes 14° and 26°N, and longitudes 5° and 17°W. Mauritania is generally flat, with vast arid plains broken by occasional ridges and cliff-like

outcroppings. Mauritania can be divided into five ecological zones according to climatic characteristics:

- The arid zone covers all the land below the 150 mm isohyet, excluding the littoral band. It corresponds to the Saharan climate.
- The eastern Sahelian zone comprises the land between the 150 mm isohyet and the border of the two Hodhs and Mali. This zone contains half the sylvopastoral potential of the country.
- The west Sahelian zone is between the 150 mm isohyet and the Senegal River.
- The Riverside zone is where most of Mauritania's agriculture is concentrated.
- The sea front is a narrow band of 50 meters between Nouadhibou and N'diago.

Mali, with its capital Bamako, is the largest country in West Africa. It is bordered by seven other states: Mauritania, Algeria, Burkina Faso, Ivory Cost, Guinea, Niger and Senegal. It lies between latitudes 10° and 25°N, and longitudes 13°W and 5°E. It is a vast land of flat plains fed by two major rivers, the Senegal on its western edge and the great River Niger. This river is generally described as Mali's lifeblood, a source of food, drinking water, irrigation, and transportation. On its journey north the Niger converges with the River Bani. The Niger River creates a large and fertile inland delta as it arcs northeast through Mali from Guinea before turning south and eventually emptying into the Gulf of Guinea. On its journey north the Niger converges with the River Bani, and forms a rich inland delta, the marshlands of the Macina, stretching for some 450 km along the River's length, in some places 200 km wide. The central part of the country is arid grazing land, called the Sahel, which has suffered great drought. Mali's size is 1,240,192 km^2. Desert or semi-desert covers about 65% of Mali's area. At Timbuktu, the Niger reaches the desert and here it turns first to the east, then to the southeast at Bourem, where it heads for the ocean. In the desert, near the Algerian and Niger borders in the northeast, the Adrar des Iforas massif rises 800 m. The north of the country is true desert except for the few oases along the ancient trans-Saharan camel routes. The majority of the population lives in the savannah region in the south.

Mali can be divided into four ecological zones according to climatic, soils and topography characteristics:

- The Saharan steppe in the northern part of the Saharan zone with zero to 150 mm of rainfall. Its vegetation of Cornulaca monacantha, Panicum turgidum and Aristida pungens forms pastures. The zone of the sub-Saharan steppe, between the isohyets of 150 and 250 mm, carries vegetation located in the wadis and ravines. That dwarf

vegetation is formed by an herbaceous cover based on short cycle annuals (Aristida hordaceae, Morettia philaeana, Farsetia stylosa ...) and a sparse woody layer of Acacia ehrenbergiana, Acacia tortilis, Balanites aegyptiaca and Maeura crassifolia. Vegetation can be abundant in the depressions and plains corresponding to the beds of wadis like the Adrar, or to zones of spreading spates (Adrar, Tilemsi, Tamesna). On lines of dunes and sandy areas Aristida dominates (A. mutabilis, A. pallida, A. papposa) and Panicum turgidum.

- The Sahelian steppe is situated between 250 and 500 mm of rainfall. Its vegetation on dunes in the north is xerophyllous; the grass component is dominated by Cenchrus biflorus, Aristida mutabilis and Schoenfeldia gracilis while the woody component contains Acacia senegal, Acacia laeta. The vegetation is open on dunes with low water retention and slopes with high runoff. To the south the vegetation is mesophyll steppe. It is localised in the silty depressions with Schoenfeldia gracilis, Panicum laetum, Acacia laeta and Salvadora persica, and in the flood areas of Rivers where aquatic grasslands are formed with perennials like Echinochloa stagnina, Oryza barthii and Vossia cuspidata. On the plateaux, the lateritic cuirasses are colonized by Combretum nigricans, Guiera senegalensis, Lannea acida and Sclerocaraya birrea. Floristically the southern Sahel forms the transition between the Sahelian and Sudanian zones. It contains elements of biogeographical zones with, however, a marked abundance of north Sudanian elements (Combretaceae) and a predominance of tall species in the grass cover.

- The Sudanian zone is the zone between 800 and 1400 mm of rainfall is the “parkland savanna” zone with a full herbaceous cover. This savanna is characterised by Vitellaria paradoxa, Parkia biglobosa, Sclerocarraya birrea and Lannea acida. The herbaceous layer is dominated by perennials of which Andropogon gayanusi is now tending to become scarcer because of clearing. In cultivated areas only fragments of formations of A. gayanus survive with vast areas of the unpalatable Andropogon pseudapricus, Cymbopogon giganteus and Pennisetum perdcellatum.

- The Sudano-Guinean zone which corresponds to area over 1000 mm of rainfall is the domain of the woodland savanna and the light forest. It becomes richer in tall perennial grasses such as several Hyparrhenia. The woody layer is dominated by

Daniellia oliveri and Isoberlina doka, which are associated with grasses like Schizachyrium rupestre, S. semi-herbed and Diheteropogon hagerupii.

Burkina Faso (capital Ouagadougou) is a landlocked country in the heart of West Africa which borders Mali to the west and north, Niger to the east and Côte d'Ivoire, Ghana, Togo and Benin to the south. Burkina Faso lies mostly between latitudes 9° and 15°N (a small area is north of 15°), and longitudes 6°W and 3°E (Fig. 1). The country covers 264 000 km^2, the capital is Ouagadougou. It is made up of two major types of countryside. The larger part of the country is covered by a pen plain, which forms a gently undulating landscape with, in some areas, a few isolated hills, and the last vestiges of a Precambrian massif. The southwest of the country, on the other hand, forms a sandstone massif, where the highest peak, Ténakourou, is found at an elevation of 749 m. The massif is bordered by sheer cliffs up to 150 m high. The average altitude of Burkina Faso is 400 m and the difference between the highest and lowest terrain is no greater than 600 m. Burkina Faso is therefore a relatively flat country. Burkina Faso can be divided into four ecological zones according mainly to climatic characteristics. From north to south, the South Sudanese zone, the North Sudannese Saharan zone, the Sub-Sahelian zone and the Sahelian zone.

2.2. Rainfall and hydrology

In Mauritania, the study zone shows an arid climate with annual rainfall less than 150 mm/y (mainly between June and October) with a gradient south-north (Soule, 2013). The climatic station in the zone are south to north Moudejeria (18,55N-11,43W -188 mm), Tichit (18,43N-9,48W -79 mm), Tidjikia (18,55N-11,43W -126 mm), Chinguetti (20,45N-12,35W -56 mm) and Atar (20,51N-13,05W -70 mm).

Measurement of evaporation Piche method (Griffith, 1972 in Shahin 2006) shows mean values between 14 mm/day (east zone) and 3mm/day (coastal zone). Surface water is very scarce in the north and central part with very limited precipitation. They are some wadies but no perennial. There is also some saline surface water in depression zone linked to direct evaporation of accumulated runoff or evaporation of subsurface aquifer.

In Mali and Burkina Faso, the study zone extends over the same latitude variation, which means, more or less same pluviometry at eastern part or western part only depending on the gradient south/north linked to ITCZ circulation. Annual rainfall is distributed between 1000 and 500 mm. a perennial River system works in the southern part and it is no perennial for

small Rivers in northern part. In western and central part of the study zone, in addition to direct infiltration by rain, the Niger River and their effluents contribute strongly to aquifer recharge process in particular in the inland delta of Niger. In the eastern part (Mali-BKF zone), the Malian part is mainly in the Niger basin and in the Bani Basin an important affluent of Niger River (101,600 km^2), the Burkina Faso part is mainly in the upper Mouhoun basin. In Bani basin the area is flat and the River Bani has created meanders over time and has generated a system of flood plain helping to the recharge process. The River flow is very high between August and November (hydrometric station near Segou located in the study zone) in line with regional rainfall season (Fig. 2).

In the Burkina Faso part, the flow from the Mouhoun River is not so high (mean annual 25 m^3- 20 000 km^2) before the confluence with the Sourou River coming from Mali in northern part of the study zone and other small Rivers feed the area close to Bobo Dioulasso (the Kou River, Houet, Bingbélé and Niamé River). There are also abundant water sources (86 of which 77 perennial) with the most important being the Guinguette source 1820 l/s, and the two ONEA sources (400 l/s), Pesso sources (100 l/s). The south western part of the study zone belongs to Comoé basin with numerous sources.

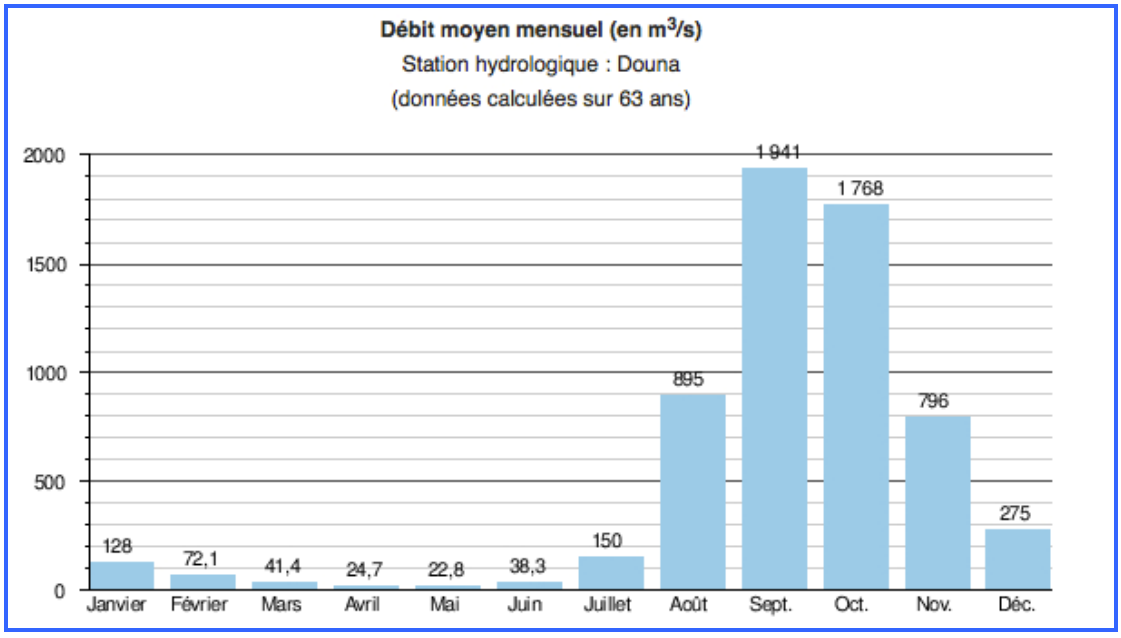

Figure 2: Monthly mean flow at Dona station in the Niger River.

Climate evolution on the last decades is marked by a general decrease of precipitation since the beginning of 70's even if a slight increase is noted early the end on 90's (Fig.3). The increase of temperature also increases evaporation process. The two parameters decreasing rainfall and increasing temperature decrease the total water volume available, if even we can

note that some aquifers in this zone show a rising of water table due to intensification of surface flow and concentration on endorheic system allowing a massive locale infiltration. It is due to deforestation process, changing soil structure with high velocity of rainfall (Leduc et al., 2001). As a result to rainfall decrease, River flow decreases (Fig. 4).

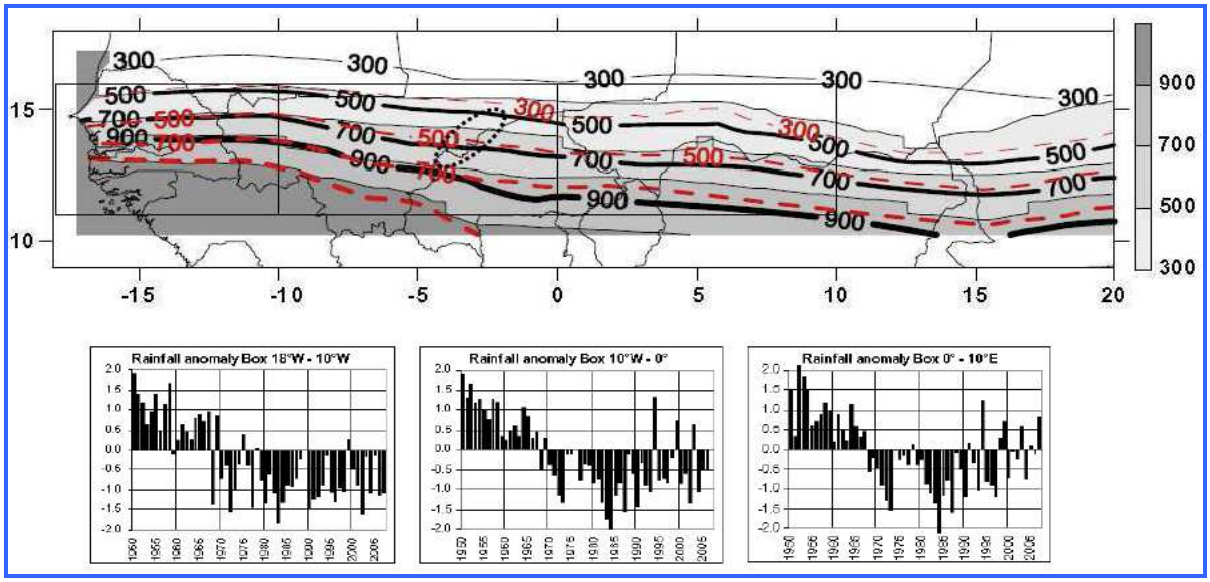

Figure 3: Decrease of precipitation in the Sahel region. Spatial distribution of annual means for the period 1970-1989 in black, and 1990-2006, in red (Lebel et Ali, 2009).

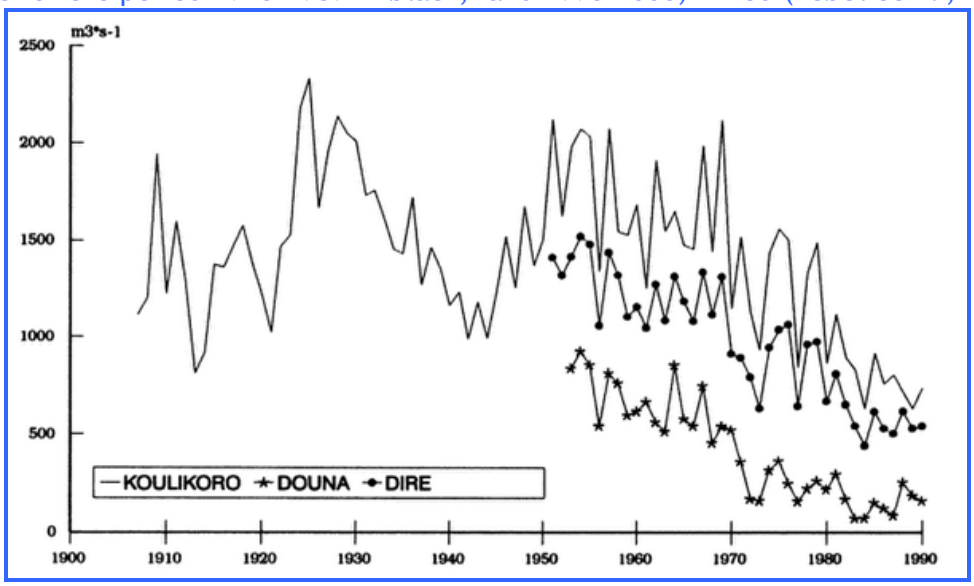

Figure 4: Decrease in the mean flow-rate (m^3/s) in Bani River basin between the years 1900 and 1990.

2.3. Geology and hydrogeology

The geology of the study zone in Mauritania (West edge of Taoudeni basin) at the moment is not well characterized, the available information is a general map of hydrogeological potentiality, a general geological map (Fig. 5) and a study focused on Atar hydrogeological system, north western part of the study zone (Bertone et *al.,* 2007).

In this area, the outcrop limits of the oldest basin formations (Char Group and Atar Group formations) are sites where small parallel valleys have formed, all of them draining into the Seguelil wadi toward the Archaean plain of Amsaga in the south. In these valleys, often partially filled by Quaternary deposits, are the oases of the sector of Atar, irrigated by numerous wells. Moussu and Trompette (1966 a, b) described the hydrogeological setting of this area based on the oasis wells in the Quaternary deposits. Up to the 1970s, these wells exploited the alluvial aquifer. With the decline in rainfall, this aquifer now dries up after the recharge episodes. The oasis wells have very often been deepened to reach the sedimentary formations under the Quaternary alluvium. The main outlet of the system is, at present, still beneath the oases, where more than 6.5 Mm^3/year are extracted, but more and more is pumped from the old sedimentary formations. In this sector, in addition to the 2500 wells, located in the 22 oases, the aquifers have been explored around Atar by drillings. An analysis of these data shows the discontinuous nature of the aquifers. 25% of the boreholes have a yield of less than 1 m^3/h and 20% have a yield greater than 15 m^3/h. Only the most productive wells have been hydraulically tested and the aquifer transmissivities obtained range between $1x10^{-4}$ and $5x10^{-3}$ m^2/s. The sampling was done in Paleozoic and Infracambrian formation, possibly from Quaternary-dune.

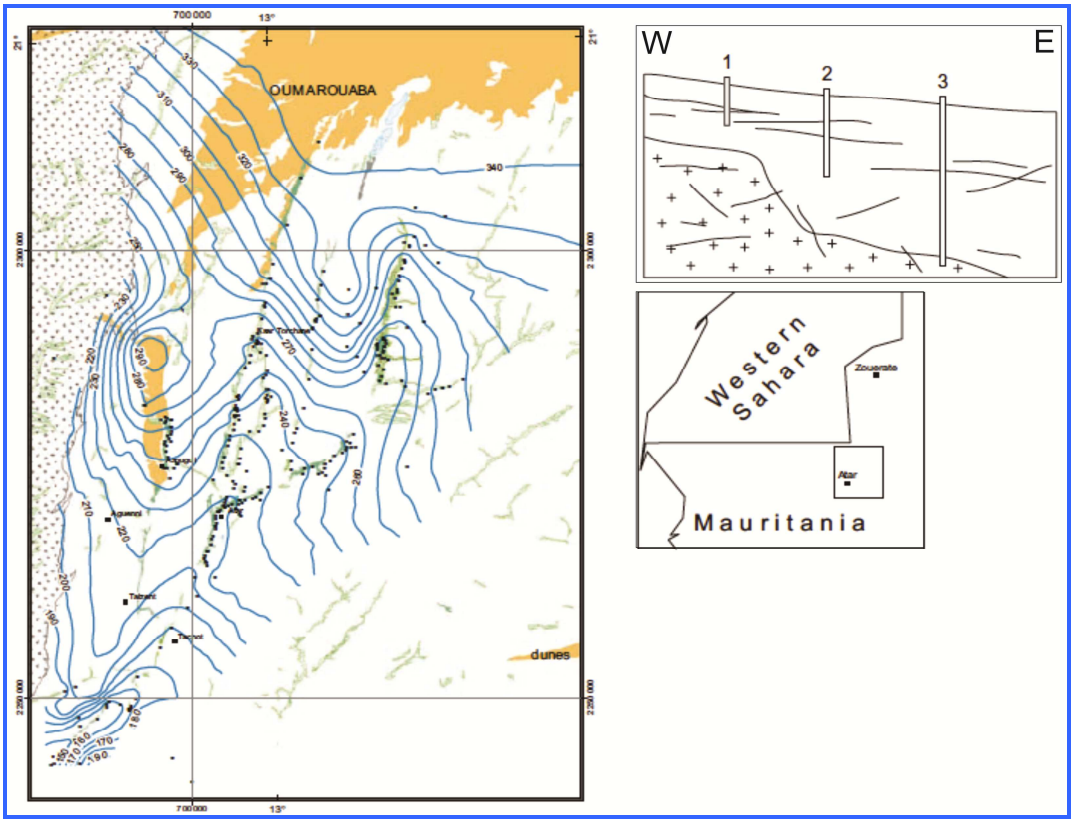

Figure 5: Geological cross-section W-E and potentiometric map, Western edge (Atar zone) of the Taoudeni basin (Bertone, 2007).

The potentiometric map (Fig. 5) constructed from the groundwater levels measured in all the Hodh Super group formations shows a remarkable coherence. It shows at least two major flow systems, separated by a piezometric crest: the Atar system in the south of the Oum Arouaba dunes massif, and the *Bou Talha system* to the north of these dunes. In the south-eastern part of the area, there is an upper aquifer system located within the Adrar Super group, and overlaying the Hodh another which is isolated by a thick aquitard.

For The Atar system, overall, water flows from the north (Oum Arouaba dunes) to the south (Amsaga plain).The groundwater is drained by the oases in the small Adrar valleys. The share of this regional flow that reaches the southern outlet is probably very small, on the order of 0.2 Mm3/year. If part of the recharge of the system can occur during the floods beneath the alluvial deposits, which fill the wadies, and may also occur during rainy episodes between valleys beneath the sandstone and limestone outcrops, whose surface is heavily fractured, the potentiometric map suggests that the system is recharged from the piezometric crest in the North, under the Oum Arouaba dunes massif. On the whole, the recharge by rainfall may be on the order of 5.4 Mm^3/year. The piezometric variations reported by the operators of the oasis wells show that the system refills during very rainy seasons. Depletion is then observed until the following heavy rains, one to four years later. During seasons with heavy rainfall, there charge is intensive and the piezometric levels in the oasis wells are often less than 1 to 2 m below the ground surface. As the withdrawal is limited by the depth of the wells, the system is in a state of unstable equilibrium between maximum recharge during very rainy seasons and maximum drainage after several years without recharge, when the piezometric levels reach the limit of the well depth. In addition to rainfall recharge, the system is also recharged from the overlying system of the Adrar Super group, probably by a volume of around 2.1 Mm^3/year.

The two measurement campaigns are preliminary (Fig. 6) but it would be necessary that Mauritanian group does an extensive analysis of the local geology (geological map with better resolution -1/250 000-1/100 000) and use the large bibliography done on Precambrian-Paleozoic in Mauritania and especially the study of Bertone (2007), to delimit the different formations, to inform each well sampled with depth well, static level, stratigraphy if this information is available, in order to present geological cross sections on the study zone to show the hydrodynamic (continuity or discontinuity) between the geological formations and the regional direction flow (Fig. 7).

The geology and hydrogeology in the study zone of Mali is well known in the eastern part with numerous works on the east Infra Cambrian margin of Taoudeni basin (Fig. 8) In western part some formations has been sampled with a low spatial resolution (CIT, Cambrian, CTQ), it is a preliminary study with few existing data except some areas around Bamako to water supply this city (Alpha et al., 1991; Jerzy Kiewicz, 2011) with geochemical analyses.

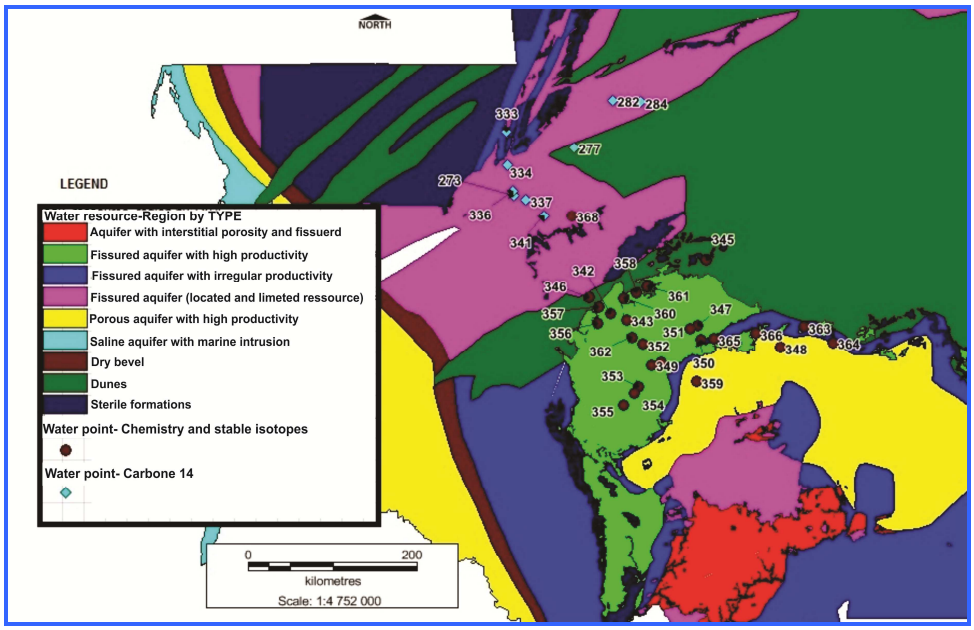

Figure 6: Hydrogeological potentiality in Mauritania

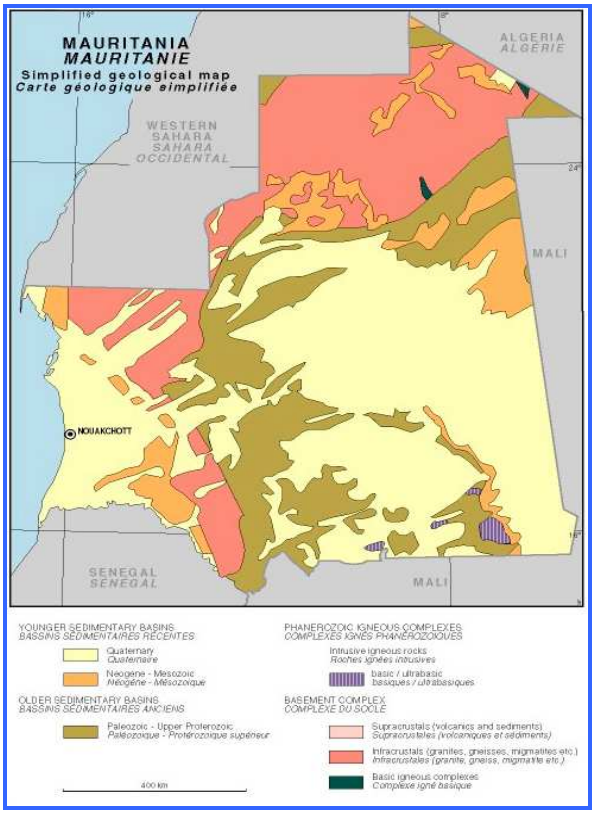

Figure 7: Simplified geological map of Mauritania

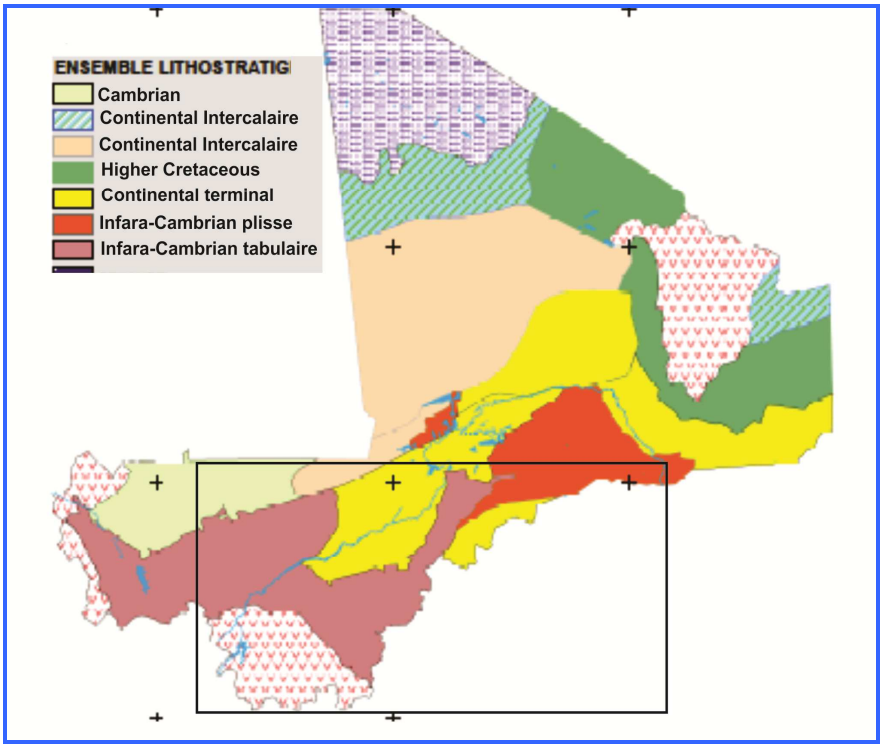

Figure 8: Simplified geological map of Mali

Detailed geological profiles are given in this zone with geoelectric data and stratigraphic data, one example at the north of Bamako (Fig. 9).

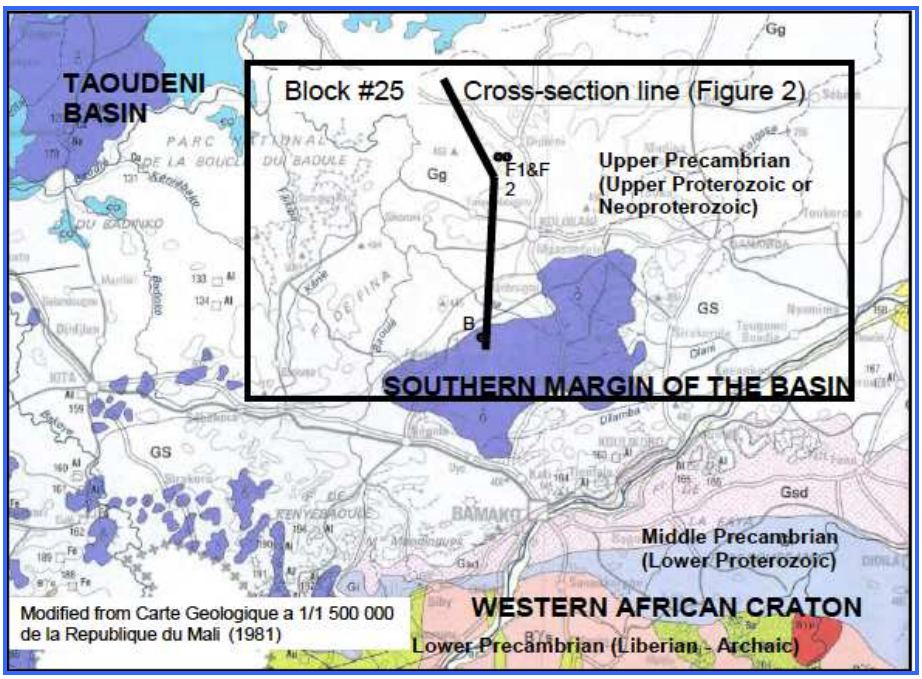

Figure 9a: Location of the geological profiles, north Bamako (Jerzykiewicz, 2011).

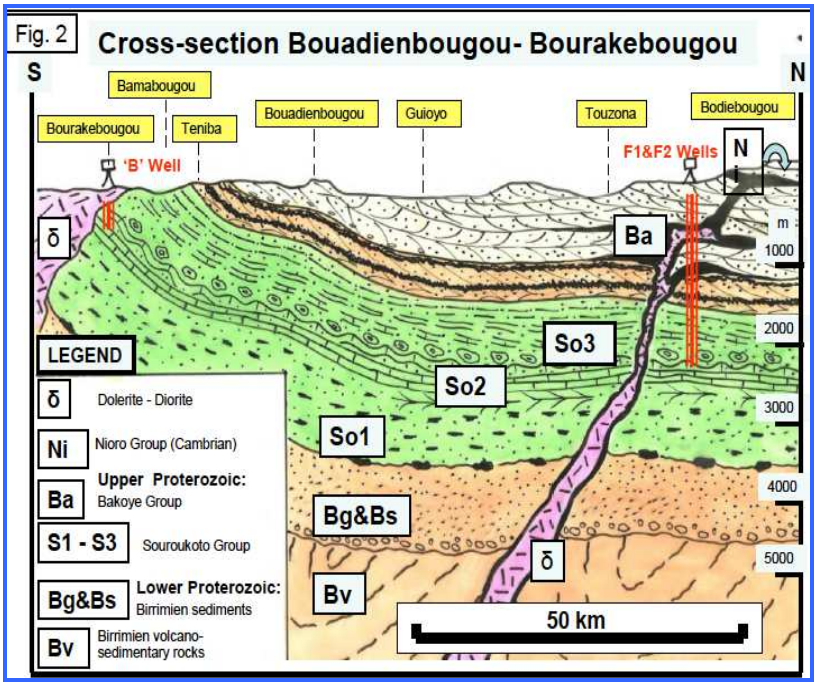

Figure 9b: Geological cross section north of Bamako (Jerzykiewicz, 2011).

The basement belongs to the Leo Shield of the Western African Craton. Its lower part called Liberian is of Lower Precambrian (Archean) age and it is highly metamorphosed, migmatized and granitized about 2700 Ma ago. The Archean is represented by granites, migmatites, anorthosites, charnockites and schists with hyper aluminous and ferruginous horizons (magnetite quartzites). The upper part of the basement is called Birrimian and it is of Middle Precambrian age (metamorphosed and granitized about 1800 Ma ago). It contains volcanic spillitic-keratophyric rock association, and flysch-like rock association marked Bg&Bs (graywackes, conglomerates, quartzites, arkoses and schists). The whole Birrimien succession is intruded by granitic bodies which might be in hypo-volcanic facies. The Neoproterozoic sediments, in our case ICT formation, are subdivided into three groups of formations:
The Sotuba (St), the Souroukoto (So) and the Bakoye Groups (Ba).

The Sotuba strata form bedrock in the Bamako area south of the Niger River valley and the Souroukoto sandstone north of the valley1. The Sotuba strata (St) consists of quartzites and sandstone with glauconite and the basal Souroukoto sandstones are more resistant and form steep escarpments northwest of the Niger River between Sibi and Tabou and Bamako.

In the eastern part of Taoudeni Basin, south east Mali-south west BKF, the aquifer studies have begun in 70's, with the increasing demand and drier climatic conditions. The area is characterized by altitudes from 240 to 790 m a.s.l; the highest areas are located in the south

western zone and the lowest to the north eastern zone. There are two main geological formations in the study zone:

- The Infra Cambrian principal formation which outcrops on a large area in the south of Mali and south-west of BKF where it constitutes the eastern limit of the Taoudeni basin. In BKF, the Infra Cambrian infills unconformably into crystalline basement. Its thickness in the south part is about 600 m (RAF project) and 8000 m in the Gourma zone.
- The Continental Terminal formation located to the northern part of the study zone, (lacustrine fluvial deposit-Upper Eocene-Oligocene) which infills unconformably onto the lower parts of Infra Cambrian formations with more 40 m thickness. CT is composed of alternating sand red ferrous and clay layers. The CT formation together with the recent sandy-clayey alluvium along the main watercourses plays a role in the groundwater recharge. An important lateritic cover can also be observed in most of the area.

In Mali, in the study zone, the infra Cambrian, has been defined in two main groups:

- The sandstone group with:

* The lower sandstone of Massigui-Faya (GI) which contains the sandstones of Kebeni, sandstones of Ningoni, Monkokoro, sandstones of Niamakina, Baba, Zana, sandstones of Sekeyet, Tebena, sandstones of Banco, Bao-Flala.
* The sandstone and Silt-Dolomitic formation (GSD) including the sandstones of Sikasso, pelitic formation of Fana, a level of sandstone clay, a level of red argillite and yellow jasper, a level of fine shale sandstone, argillite, limestone and jasper, a level of fine pink shale sandstone, micaceous argillite, a level of calcareous argillite and the sandstone of Ména.
* The sandstones of Koutiala (GK)
* The sandstones of Bandiagara (GB)

- The schist group with the schists of Toun (ST)

In BKS, the Infra Cambrian has been divided in 9 main formations (Ouédraogo, 1998): from the bottom to the top; the sedimentation is essentially of sandstone type with locally more or less carbonated cement and this covers the Malian nomenclature. In Huneau et al. (2011) four points close to Sikasso are referenced as GKS and SAC1. The other points in northern Malian part (from Koutalia to the north) are referenced as Continental Terminal, but it seems not

consistent with the geological map and sampling made by Malian team, which indicate the Infra Cambrian formation. This point could be clarified.

The nine formations referenced in BKS are (Fig. 10):

– The lower sandstones (GI).

– The Kawara-Sindou sandstones or ‘‘basement sandstones’’ (GKS), 90–350 m.

– The fine-grained sandstones with glauconite or ‘‘Sotuba sandstones’’ (GFG) 100–500 m.

– The quartz granulates sandstones (GGQ) 300–600 m.

– The siltstones, argillites and carbonates of Guena-Souroukoundinga (sandstones, schist, dolomite) (SAC1) 300 m.

– The pink fine grained sandstones (GFR), 100 m.

– The siltstones, argillites and carbonates of Samandeni-Kiébani or ‘‘schist of Toun’’ (SAC2), 400–700 m.

– The siltsones and quartzite of the Fo Pass or ‘‘sandstones of Koutiala’’ (SQ).

– The Fo-Bandiagara sandstones (GFB).

The different formations lie horizontally with a slight northwest dipping of about 2°. The lower formations tend to increase in thickness towards the west in relation with the existence of a positive gravimetric anomaly axed on the Fo-Bandiagara direction. The heterogeneous stratigraphy of sandstones in all the formations indicates very changing sedimentation conditions with an alternation of marine, littoral and continental phases. Numerous doleritic and gabbro-doleritic intrusions of probably Permian origin can also be found in form of sills, necks or km-long dykes. To date, no deep boreholes exist through the complete sedimentary cover to the basement. South of the area, close to Banfora, the sedimentary formations of the lower sandstones appear as folded. The cliff of Banfora, which is the most important feature in the landscape of the region, is affected by numerous faults and fractures particularly towards the West (most common directions: SSE–NNW, SW–NE). The global tectonics of the sedimentary zone is rather complex and greatly modifies the pseudo tabular organization of the deposits with important fault throws of about 100 m. Along the Banfora cliff, an important sub-meridian fault, also affects the basement and obviously limits the extension of the sediment deposits towards the East. Other major faults were identified in the region of Bobo-Dioulasso. They are dominantly of smaller extent, NW-SE oriented and they cut the sedimentary cover in many parallel lowered or uplifted compartments (Ouédraogo, 1998.

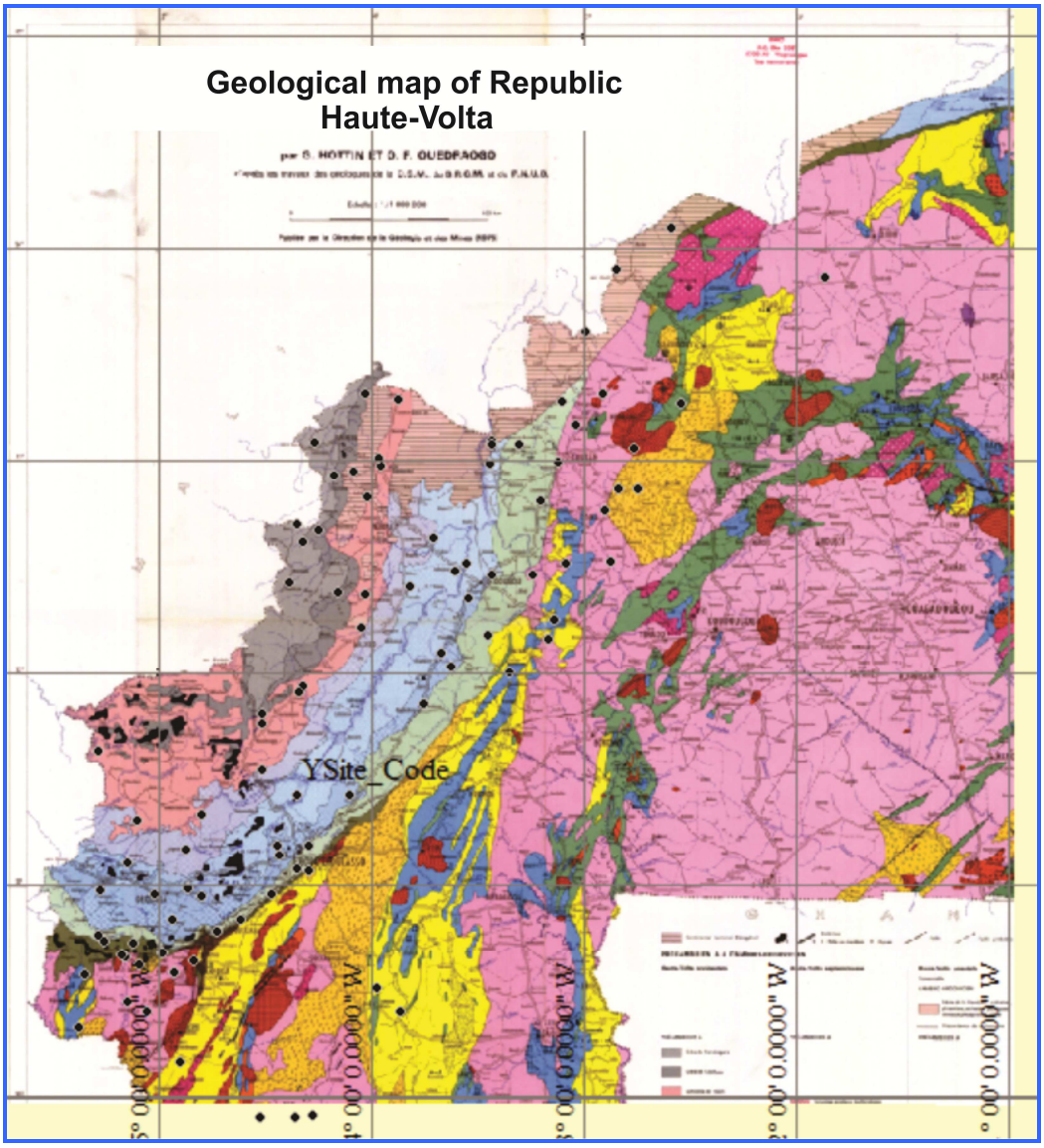

Figure 10: Geological map of the study zone in Burkina Faso

Some geological cross sections in the northern part of the study zone close and on the Continental Terminal are showed in figure 14; the older formation (GI) is not present in this zone. Two aquifers are considered in the study zone, the Continental Terminal and the Infra Cambrian aquifer considered as a multi-layer connected aquifer. The main results of studies and synthesis (in Dakouré, 2003; Huneau et *al.,* 2011; Koussobé, 2013).The hydrogeological parameters available on the sedimentary deposits of the Taoudeni system were compiled by Gombert (1998), using around 1000 boreholes (table 1). The permeability of the sandstones is rather high, around 1.8 10^{6} m/s, and favorable to the development of an important aquifer. The estimated storage coefficient was of around 1x.1 10^{-4}.

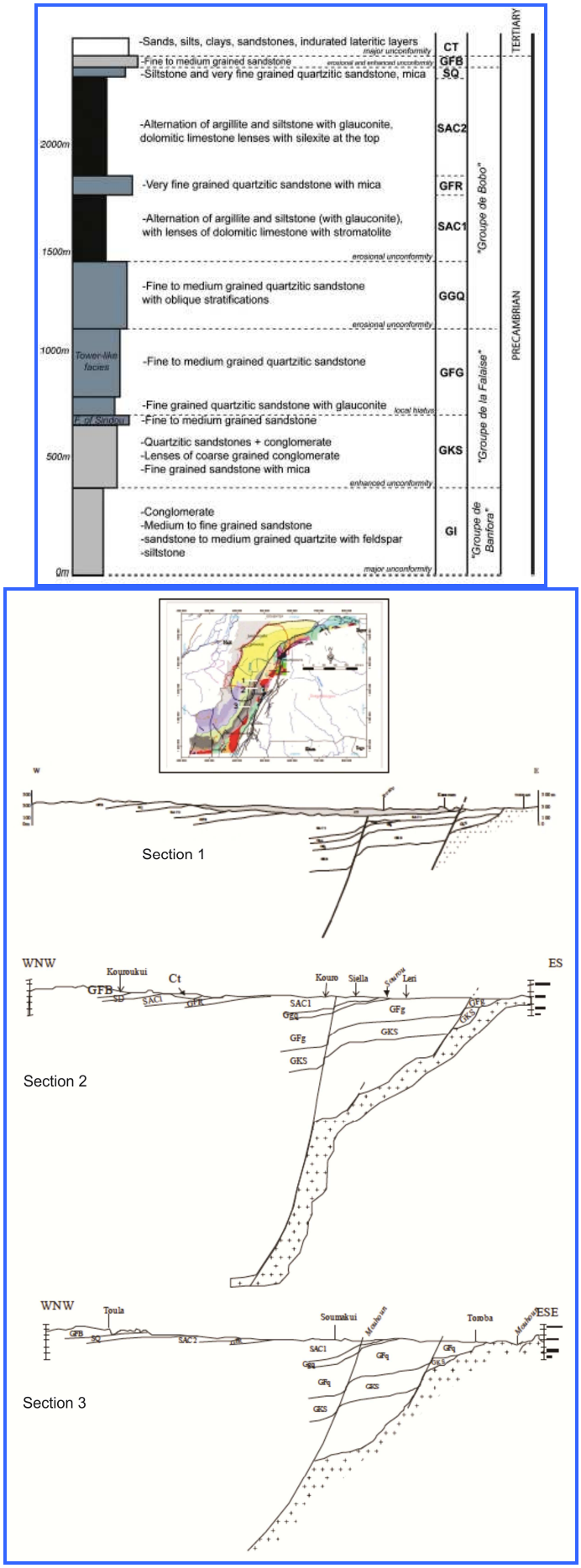

Figure 11: Some geological cross sections in the northern part of the study area and a simplified stratigraphic profile.

Table 1: Hydrogeological parameters for Infra Cambrian formations (Gombert, 1998)

Unit	No. of borehole	Depth (m)	Mean yield (m^3/h)	Mean specific yield ($m^3/h/m$)	T (10^{-4} m^2/s)	K (10^{-6}m/s)
GI	21	75	5.1	0.6	0.5	0.2
GKS	69	48	5.1	0.4	2.7	1.2
GFG	166	80	9.1	0.5	2.8	0.5
GGQ	271	62	13	1	8.5	3
SAC1	179	66	13.4	1.4	4.9	2.2

The Continental Terminal is in lowest position with static level lower and a piezometric level lower than the Infra Cambrian outcrop, with probably hydraulic connection (Table 2).

Table 2: Piezometric data of the different formations

Unit	Nbre	Min depth	Max depth	Mean depth	Mean NS	Mean Q	Qs	Mean NP
GI	6	76	196	129	8	9		293
GKS	67	37	196	83	10	6	0.43	342
GFG	134	41	196	94	16	8	0.78	405
GGQ	269	37	142	70	14	12	1.31	434
SAC1	158	43	190	82	12	10	0.51	345

No clear confining or low permeability layer can be identified at the regional scale and therefore the system can be conceptually considered as one unitary aquifer. Numerous discontinuities encountered at different depths (faults, fractures, horizontal discontinuities) are at the origin of a secondary fracture porosity which potentially increases both flow and storage capacity of the sediments and facilitate the circulation of water through low-permeable rocks such as the argillites.

The groundwater flow direction is mainly oriented SW–NE. The potentiometric map (Fig. 12) of the area also shows that the south-western and central elevated zones seem to behave as recharge areas (about 500-600 m a.s.l.) and that the Mouhoun River can be considered the main drainage axis of the region (lowest points about 180 m a.s.l.). The Mouhoun River is in equilibrium with the groundwater level along the major part of its course. Strong interaction between surface water and groundwater was already mentioned by Mahé (2009) in the Bani River basin in Mali (tributary of the Niger River). In the topographically very contrasting area located between Bobo-Dioulasso and Sikasso most of the deep boreholes produce artesian waters. Important springs can also be observed within the study area, amongst them the famous ‘‘Nasso-Guinguette’’ spring near Bobo-Dioulasso. For the Bobo-Dioulasso area Dakouré (2003) proposes an effective infiltration value of about 74-120 mm per year for the period 1981-1990. For the north-eastern area (Gondo depression) a lower infiltration rate of

about 20-38 mm per year should be considered (Dakouré, 2003). Since the 1960s the potentiometric evolution shows a clear tendency to decreasing levels (Saad, 1970). For example, the decrease in the Dedougou area (Gondo potentiometric depression) has reached about 30 m and can be correlated to the decrease in the precipitation amount. Chemical and isotope results of past studies will be discussed in the next chapter.

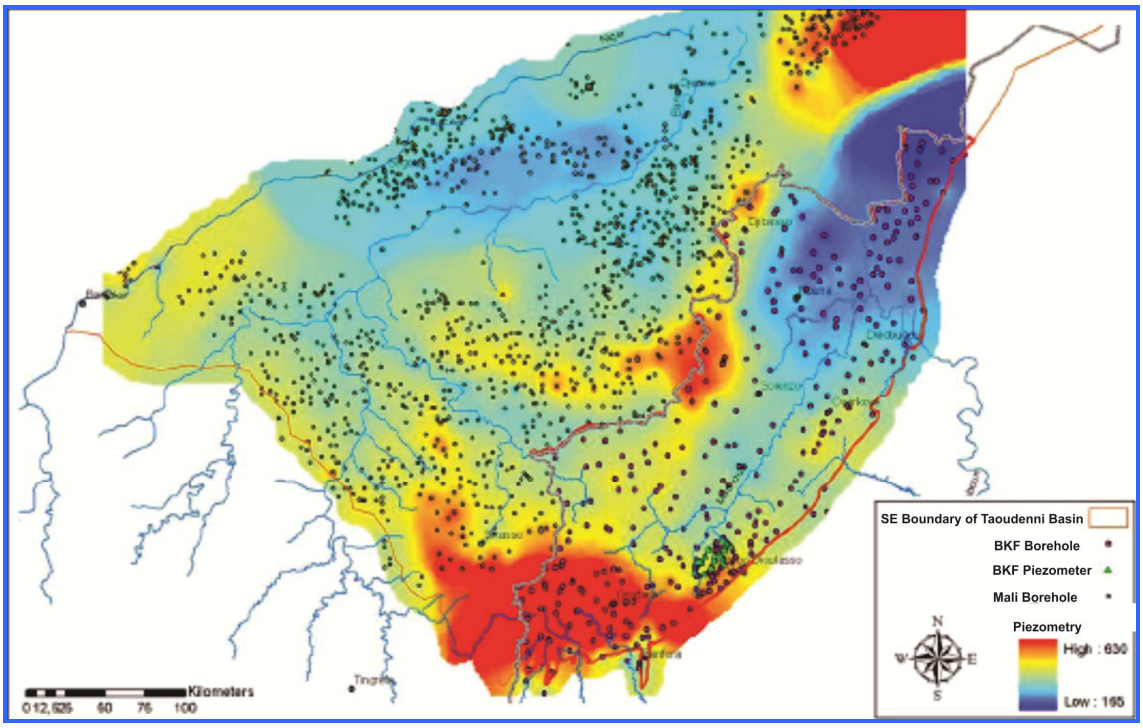

Figure 12: Potentiometric map of the whole zone IC and CT aquifers (Dakouré, 2010)

3.DATA ACQUISITION AND METHODOLOGY USED

Sampling

- **Mauritania**

In Mauritania, two geochemical sampling campaigns (September 2015: 19 samples and July 2016: 14 samples) were carried out. Laboratory measurement, concerns major chemistry, water stable isotope and Tritium (Fig .13). Unfortunately, at this time, only field measurements (location, EC, pH, T, Alkalinity) are available and water stable isotope and Tritium for the first campaign (September 2015). These two campaigns are preliminary and have to be completed by hydrodynamic data (piezometric level) and geological data (information about geological formation for each well, depth of well, etc.). A preliminary interpretation has been done in this report.

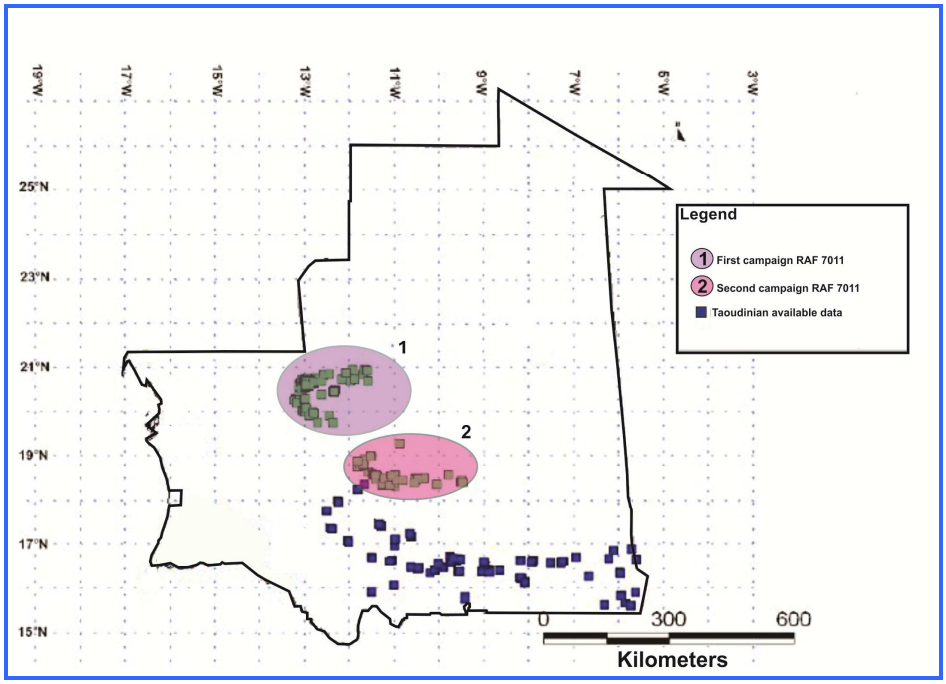

Figure 13: Sampling sites in Mauritania.

- **Mali**

During the implementation of the IAEA-supported project RAF/7/011, three campaigns (June 2013, May 2014, and March 2015) were carried out by Malian counterpart (Fig. 14). Field measurements include location, EC, pH, TDS, dissolved oxygen, depth of well, and some measurement of alkalinity. 108 points in different aquifers have been sampled since 2013: 58 samples in ICT, 34 (CTQ), 7 (CAM), 4 (CIT), 5 (ICP). The laboratory analyses include major chemistry, silica, some traces (Fe), dissolved oxygen, water stable isotopes and Tritium. EC and pH were controlled in laboratory. The ionic balance shows generally good analysis. However few samples present ionic balance more than 5%.

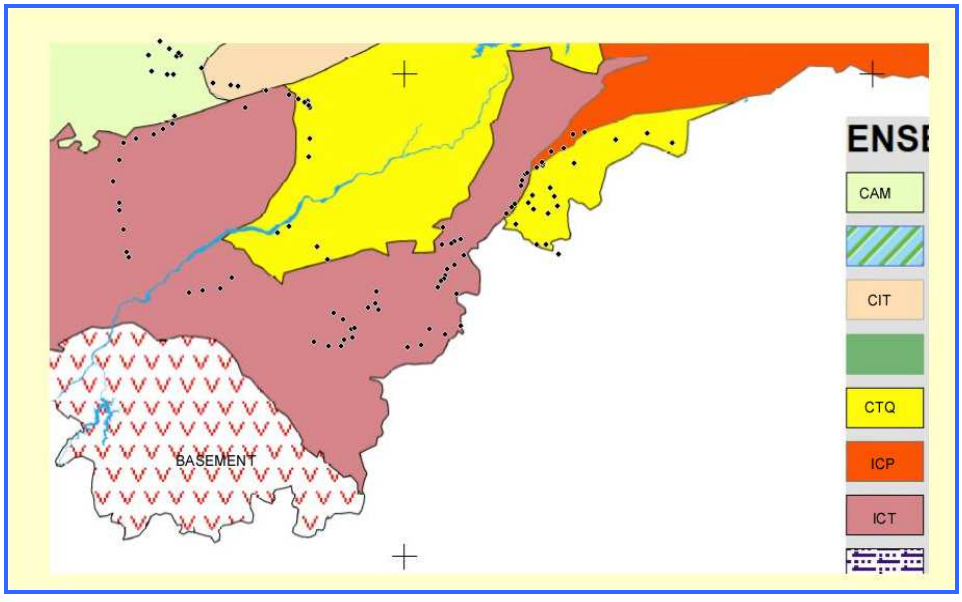

Figure 14: Sampling sites in Mali.

Monthly rainfall 2014 and 2015 from Bamako, Sevare, Koufiala, Mopti and Bankass stations were also collected and water stable isotope (IAEA), tritium (Hydrosys Labor-Budapest) were measured.

- **Burkina Faso**

A total of 140 water samples were collected during two campaigns in December 2013, January 2014 and May 2016 by Burkina Faso group. In laboratory, major chemistry and silica, some traces (Fe), dissolved oxygen water stable isotopes were analyzed. EC and pH were controlled in laboratory (Fig.15).

94 points in different geological formation have been sampled for the first campaign, 25 (crystalline), 10 (Continental Terminal Quaternary CTQ), 59 (Infra Cambrian Tabulaire-ICT). The samples in ICT were classified following the oldest to youngest lithology formation relevant to the location: GI (3)/GKS (8) / GGQ (11) /GFR (3) /SAC2 (6) /GFG (12) /SAC1 (7) /SQ (2) /GFB (7).

The analytical results for the last campaign has been given after the delivery of this report, the points was sampled in the same zone than the first campaign and show similarity in chemistry and isotope variation, we can note 13 points representing surface water. The dating with Tritium also confirms the same repartition of age.

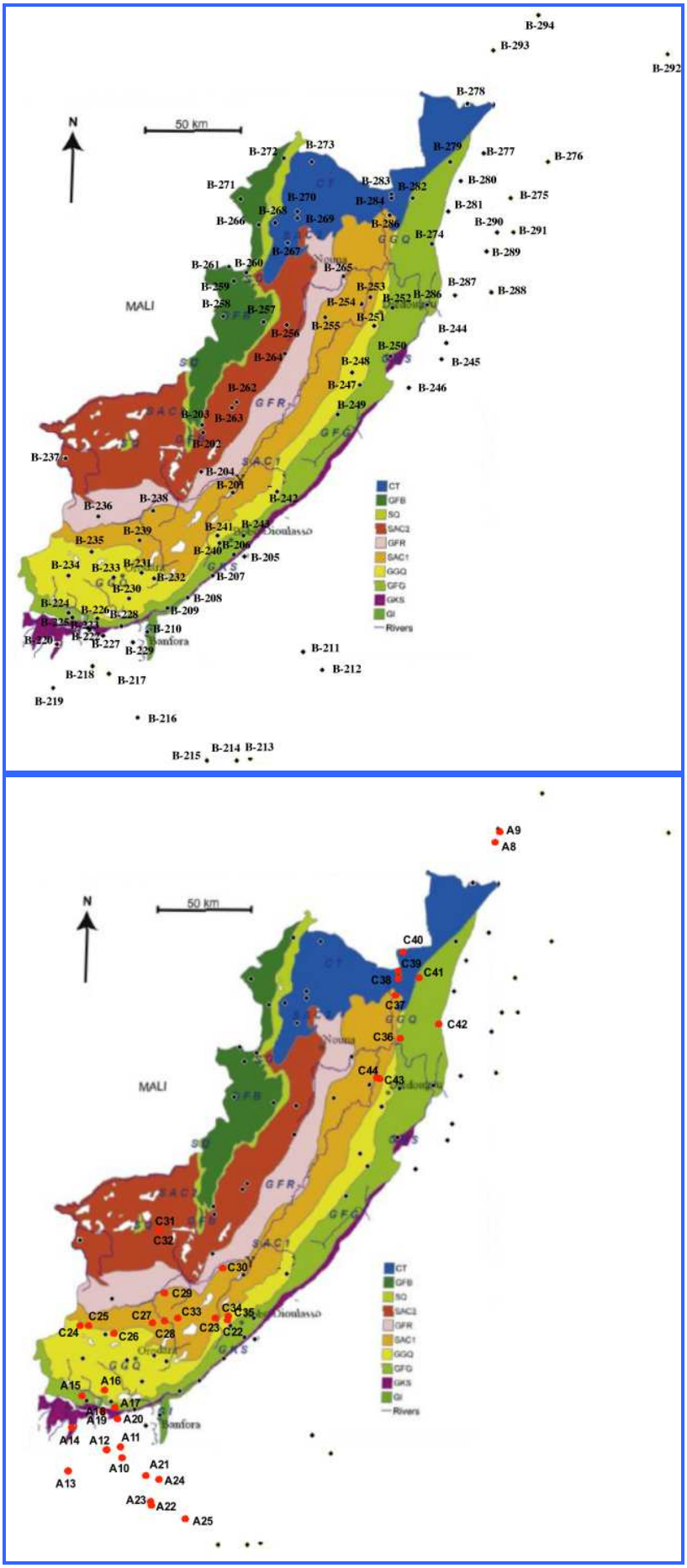

Figure 15: Location of sampling sites for campaigns 1 and 2 in BKF

All chemical and stable isotopes analyses were performed in the LRAE in Tunisia. Tritium was measured in the Hydrosys Labor-Budapest. This first synthesis of geochemical data should be completed with other basic data otherwise hydrogeological interpretation and knowledge of groundwater system will be incomplete. In the first place, it is necessary to have water level of sampling points (Mali and BKF). For Burkina Faso there is no geological information on sampling points given in the data base, the geology of study zone is complex (multiple geological layers form the edge of sedimentary syncline with high variation in stratigraphic facies, with discontinuities of permeability even if the total series could be considered as a multilayer aquifer). In the first way, in order to overcome this difficulty the sampling points were located on a geological map to separate, in this geochemical analysis, the different layers to avoid doing a simplistic analysis, but it would be necessary to make a check in the field to verify points on the limit of two layers. It may be noted that 20 samples are referenced as crystalline basement, without other geological information they were analysed as a homogeneous group.

4. RESULTS AND INTERPRETATION

4.1. Results and discussion: Mauritania study zone

Without adequate geologic information, the partial field data were processed by campaign.

- Electrical Conductivity

The Electrical Conductivity (EC) varies from 395 to 3331 µS/cm for the first campaign and from 178 to 1906 µS/cm for the second. Except the higher point from the first campaign, the EC distribution is more or less equal with an EC low to medium values (Fig. 16).

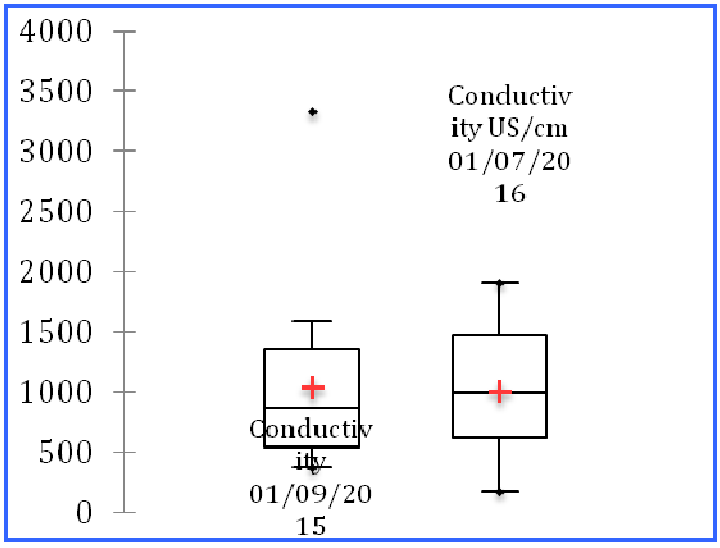

Figure 16: Distribution of Electrical Conductivity values in groundwater samples.

- pH

In opposite to EC, pH shows a difference between the 2 groups, the first shows basic pH values while the second neutral pH values. The total alkalinity is coherent with higher values for the pH basic group. It is probably due to a mineralogical source of Na (K) given alkaline bicarbonate or dissolved hydroxide in the water (Fig. 17).

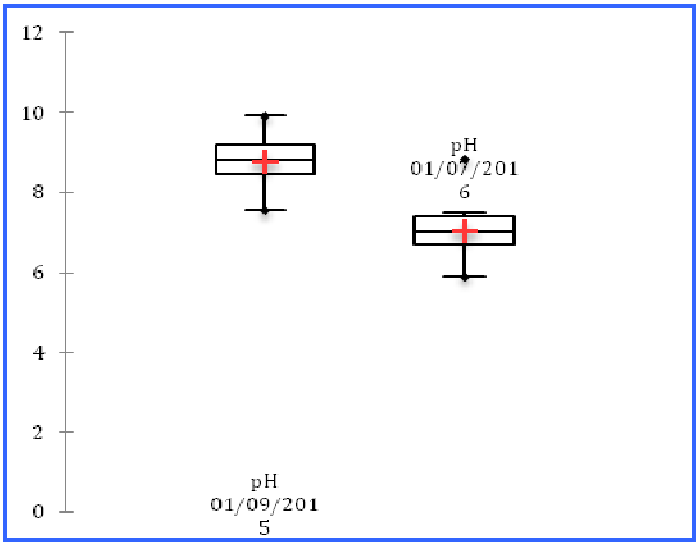

Figure 17: Distribution of pH values in groundwater samples.

- Temperature

Distribution of temperature values in groundwater samples shows small variations and are consistent with annual atmospheric temperature in this zone. There is a systematic small bias on temperature measurement between the two campaigns. But, it seems measured in good enough condition without too atmospheric temperature contact, except one (Bir lechkeb 1) with 39.4 °C. This point shows a low mineralization and local thermal point is highly unlikely, then an error measurement is possible (Fig. 18).

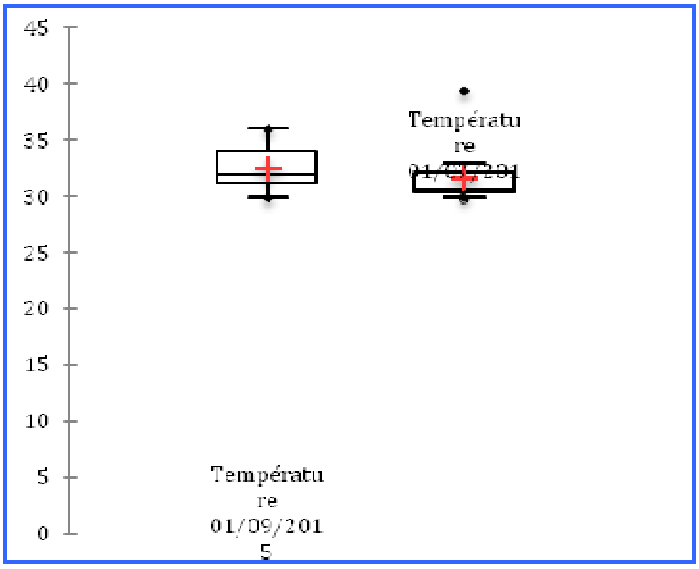

Figure 18: Distribution of temperature values in groundwater samples.

- Alkalinity

As mentionned pH is linked with alcalinity in this samples. Under the assumption that alcalinity represents mainly HCO_3 and CO_3 in these waters, considering the relation between TDS and EC in this range of values (TDS =0.75 EC), the part of bicarbonate in anionic balance seems relatively high for the majority of water but not predominantly (Figs. 19, 20), chloride or/and SO_4 have to higly contribute to the geochemistry of waters.

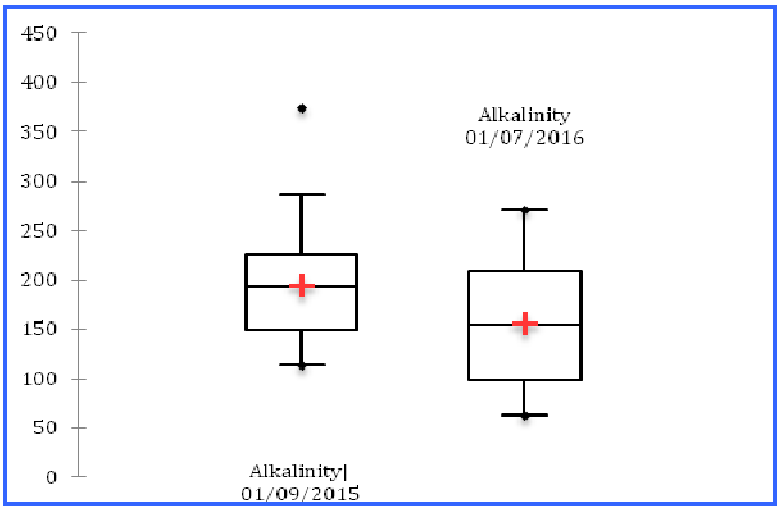

Figure 19: Distribution of alkalinity values in groundwater samples.

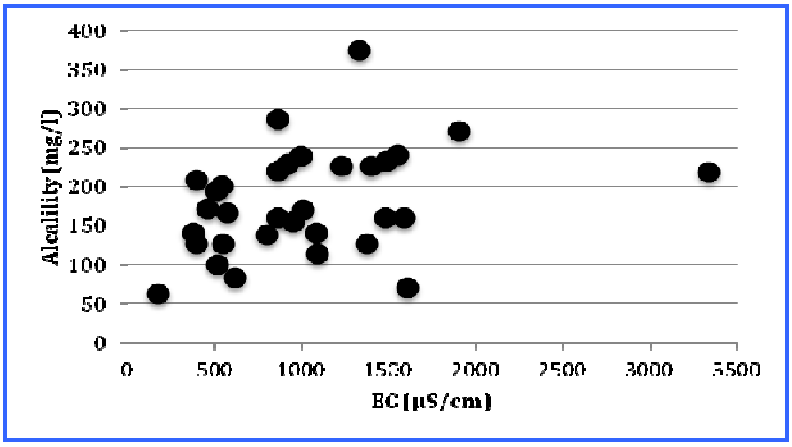

Figure 20: Relationship between Electrical Conductivity and Alkalinity

- Oxygen 18 and deuterium

We have results only for the first campaign, the range of value is smaller than 3‰ (oxygen-18) with a mean value of -4,32 ‰ and 18‰ (deuterium) with a mean of -30,0 ‰ , that is a normal variability for a phreatic aquifer. There is no very enriched values detected and the samples are in the range of current rainfall isotope content found in the regional zone (Figs. 21, 22).

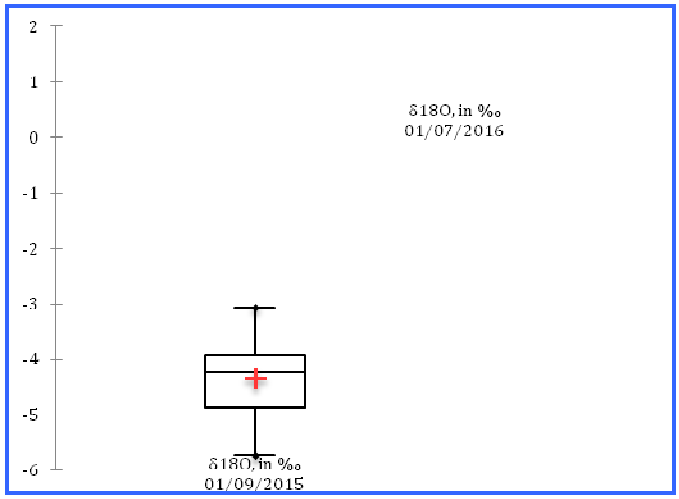

Figure 21: Distribution of ^{18}O contents in groundwater samples.

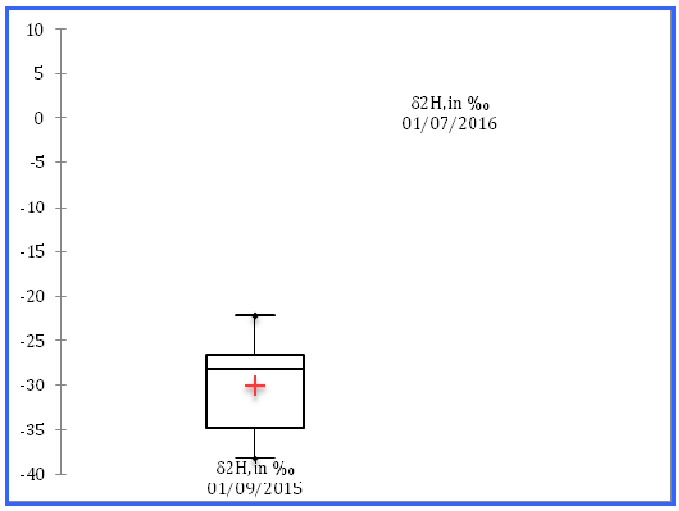

Figure 22: Distribution of ^{2}H contents in groundwater samples.

- **Deuterium excess**

The samples show a low deuterium excess (< 9‰) for all waters, between -0.5 and 8.5‰, showing potentially an evaporation process during the infiltration assuming that the sampling rules for isotopes has been followed (Fig. 23). To take the analysis one step further, we have compared the isotopes values in groundwater with some isotope content of rainfall closer of the study zone. Three sources of data exist, some partial monthly data in 4 stations in southern part of Senegal (Travi and al., 1987), one complete year (2013) of monthly sampling in Louga (northern part of Senegal) and 3 years of daily measurements at two coastal stations in Mauritania (Rosso and Nouakchott, IRD network in coll. with EMIM) (table 3).

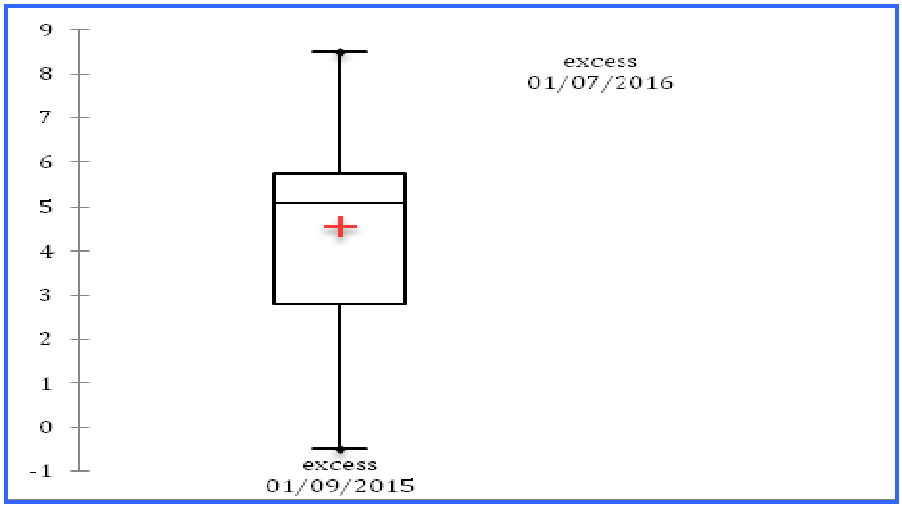

Figure 23: Distribution of deuterium excess values in groundwater samples.

It is obvious that the climate conditions are different comparing to the study zone but it is a first approximation allowing draw up hypothesis regarding the origin of water. The isotope variability of rainfall events over the three years of daily isotope sampling is high (9‰ for oxygen 18 and 68‰ for deuterium) measurement at Rosso and Nouakchott (Fig. 24).

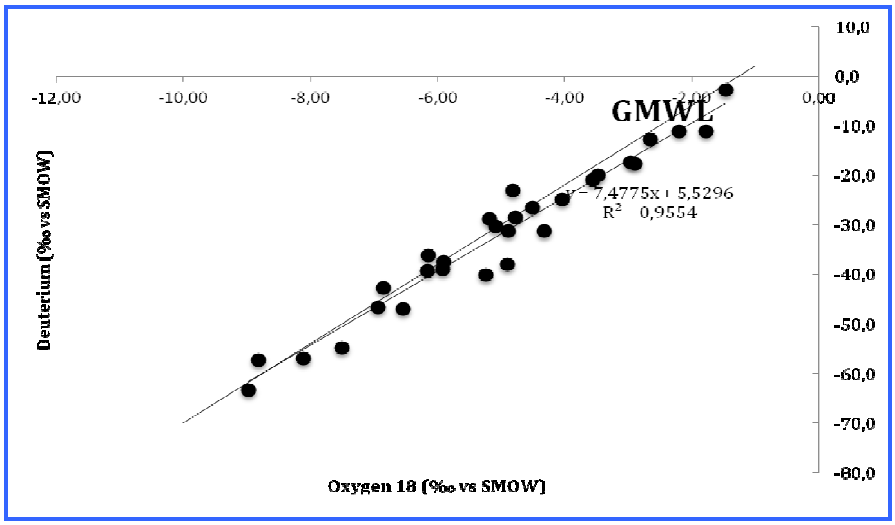

Figure 24: Relation $\delta^{18}O$ *versus* $\delta^{2}H$ in daily precipitation events (2013-2015-Rosso and Nouakchott).

The meteoric line ($\delta^{2}H = 7.48\ \delta^{18}O + 5.53$) is close to Global Meteoric Water Line. The mean annual weighted value shows a great variability, between -2.92 and -6.80 ‰ for the 3 years, then it in not possible on a short time measurement to define a realistic value of annual isotope content of rainfall to have enabling an reference to compare with isotope content in groundwater. However it is a same range of values observed in groundwater and the contribution of current rainfall is a strong hypothesis that tritium values confirm (Fig. 25).

Table 3: Isotopic content of rainfall in Mauritania and Senegal.

	Station	P	$\delta^{18}O_w$ (‰)	$\delta^{2}H_w$ (‰)
2013	ROSSO	239	-6.80	-45.4
	NOUKCHOTT	154	-5.16	-32.6
2014	ROSSO	55	-2.92	-21.8
	NOUKCHOTT	43	-4.93	-12.3
2015	ROSSO	241	-3.98	-24.8
	NOUAKCHOTT	103	-5.82	-40.9
Travi 1987	July-Aug			
	Mbour		-4.05 /	-22.7/
	Diafilon		-8.08/-6.66	-54.3/-42.6
	Tambacouda		-6.33/-6.60	-42.4/-41.9
	Toll		-5.83/-5.38	-32.9/-33.1
GNIP, 2013	Louga	412	-4.78	-33.5

It may be noted that groundwater points are remarquably on a line parallel to the metoric line with a slope of 6.61. If an important part of water in aquifer comes from an old period recharge, it would be necessary to compare with another groundwater studies in the regional zone to find out if the old climate conditions have or not change the air circulation pattern as a result a modification of intercept (lower than 10‰) of $\delta^{18}O/\delta^{2}H$ linear relation.

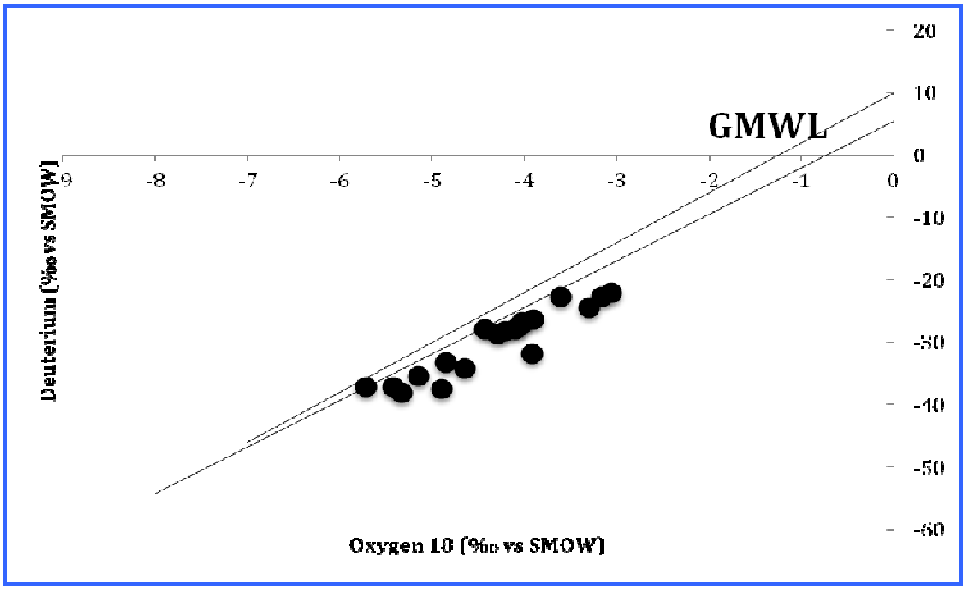

Figure 25: Relationship between $\delta^{18}O$ and $\delta^{2}H$ in groundwater samples.

- **Tritium**

All samples show a significant tritium content (0.7-2.8) except five samples (F13 Atar, Lemoilih POO7, N'Tomadi, Oued Amlellek P012, AD63) into the error limit measurement. Then there is a current recharge in spite of arid conditions and it appears to be consistent with hypothesis issue from stable isotope analysis (Fig. 26). This infiltration processes are probably diffuse if water level is close to surface, or by concentration of water in endoreic depression (local infiltation) as shown in arid south Tunisia (Dhaoui et *al.,* 2016). The current spatial recharge rate is low and probably ground waters results from a mixing between old water and modern water. Comparing with Tritium content in rainfall at climatic stations closer to the study zone (Bamako, Koutiala, Mopti and Bankass station from Mali), the monthly Tritium content rainfall for the 2015 rainy season is between 2.9 and 4.8 TU and a annual value estimated close to 4 TU repesenting the atmospheric natural level in this area. All tritium values in groundwater is smaller, the hydrodynamic conditions of a phreatic aquifer is closer to a mixing model than a piston one. Then, this range of values implies clearly a contribution of older water (before 1950).

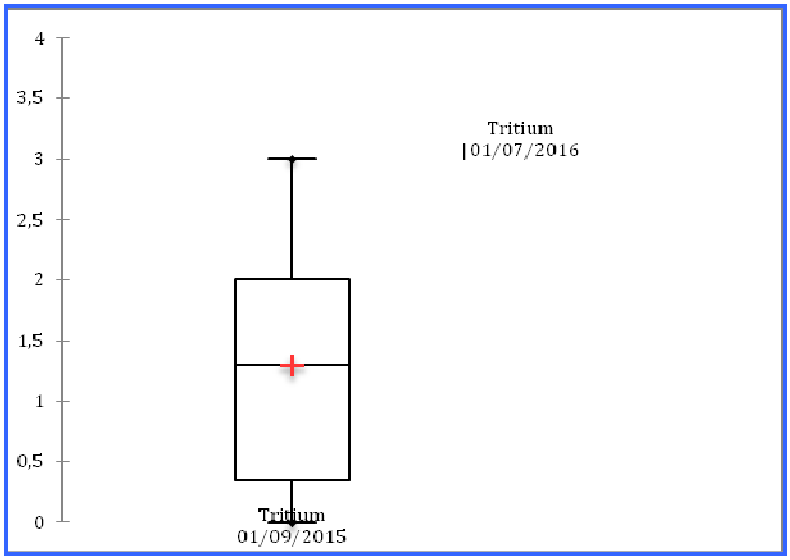

Figure 26: Distribution of tritium contents in groundwater samples.

4.2. Results and discussion: Mali study zone

The compiled data has been processed for each aquifer. In the whole large study area five geological formations have been sampled. Except the eastern part where enough studies and information exist to make assumptions about hydrodynamic relation between the different formations (ICT, CTQ and ICP), the western part with ICT, CAM and west CTQ formation, in this presentation, will be considered as isolated aquifer systems (Fig. 14). It was also noted that some point locations on the geological map, given by the Mali group, seems approximate and may not correspond to the geological formation provided in the data bank.

- Depth of the sampled wells

Groundwater sampling has been carried out mainly in shallow wells (< 100m) but with specificities for each aquifer. The depth is mainly homogeneous for CAM, CIT and ICP, the average is 30, 50 and 45 m respectively. CTQ and ICT show a higher variability (but with a higher number of wells) with deeper wells (80 and 105 m). The depth average is 40 and 55 m. CTQ shows wells with depth close to surface (Fig. 27).

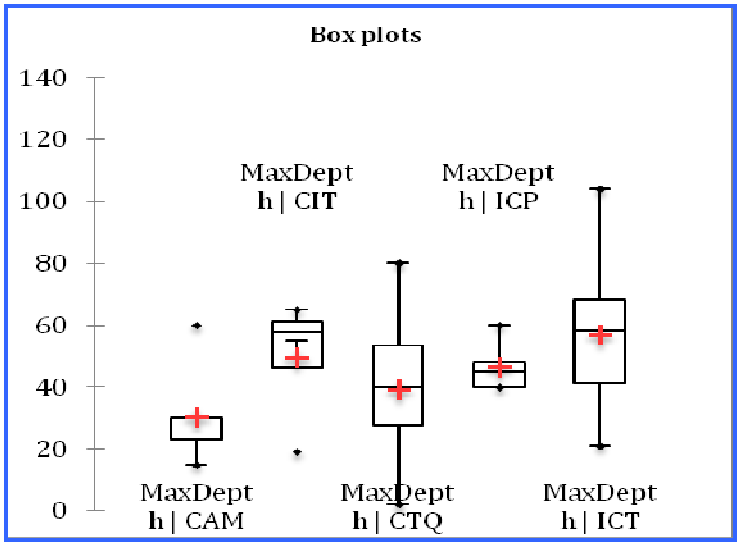

Figure 27: Variability and distribution of the depth of sampled wells in the different geological formations.

- Electrical conductivity and TDS

Groundwaters from the five geological formations show differences in the Electrical Conductivity (EC) in terms of both mineralization and variability. ICT ground waters shows the lowest mineralization and few variability with a mean of 182 µS/cm, except two points 1418 and 1490 µS/cm, which seems contaminated showing a high level of nitrate and sulfate. ICP ground waters which is the same formation that ICT but subjected to a folding, shows low mineralization (slightly higher than ICT and with few variation) with a mean of 357 µS/cm. CTQ ground waters, shows intermediary values with a mean of 535 µS/cm, the variability is more important than ICT with two maximum values about 2500 µS/cm. The last aquifers (CIT and CAM) have an average mineralization higher (700 and 1400 µS/cm) but with a strong variability for CIT (4 samples between 36 and 1847 µS/cm) this result is no significant for this formation, however CAM (7 samples) is more homogeneous and significant (860 to 2660 µS/cm) (Fig.28).

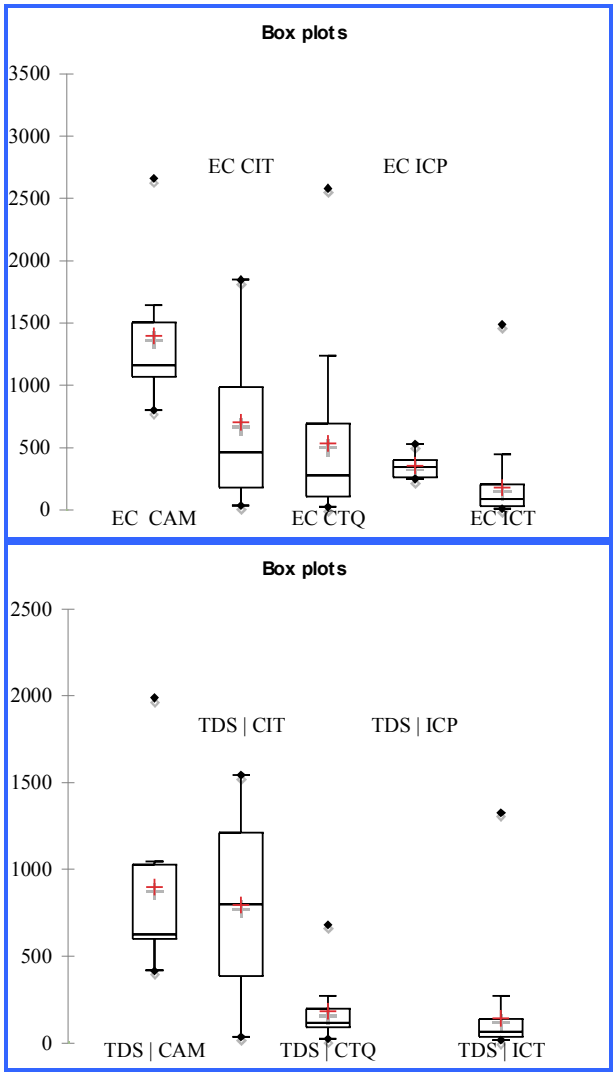

Figure 28: Variability and distribution of EC and TDS in the different geological formations.

The comparing between Total Dissolved Salts (TDS) and EC show a good agreement except for 2 points which present high contents in bicarbonate, sulfate and sodium (Fig.29).

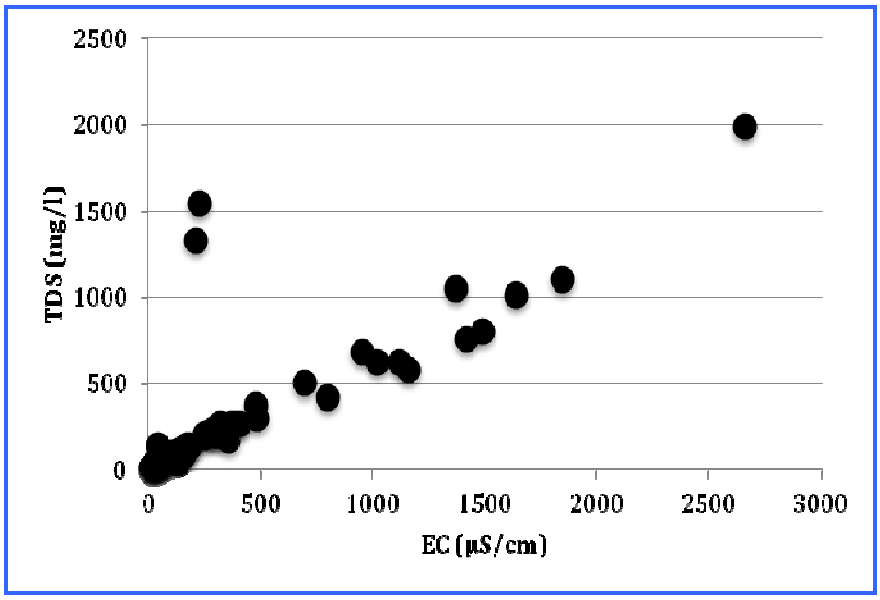

Figure 29: Electrical Conductivity *versus* TSD for all collected samples.

- Temperature

Mean groundwater temperatures show few variations among the aquifers, and are in the range of the annual atmospheric temperature values. Some maximum values (CTQ and ICT) should be viewed cautiously in the computation of thermodynamic equilibrium, due to a re equilibrium of groundwater temperature with the atmospheric temperature in the measurement (Fig.30).

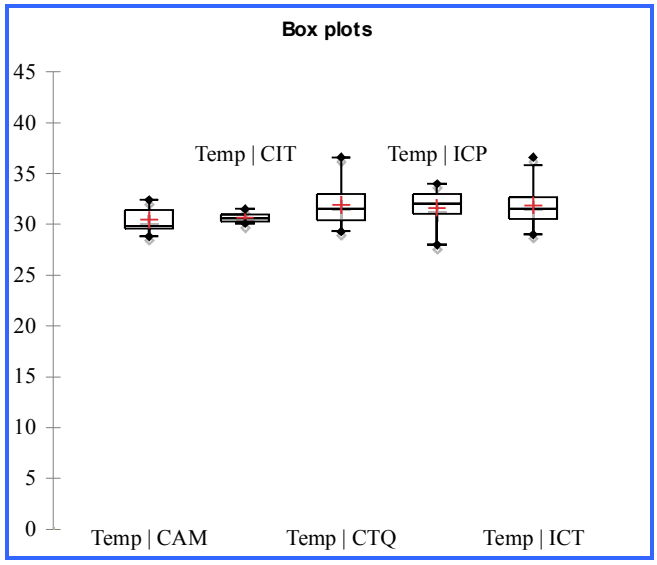

Figure 30: Variability of temperature in the different geological formations.

- pH

Except for ICP ground water, pH is globally (5.5 to 8.5) in the range of normal values in accordance with sandstone or limestone facies. Values with pH above and under these limits, the pH should be viewed cautiously. In the case of basic pH of ICP groundwater (average pH=10), the major ion chemistry does not show a particular excess in alkaline ions (HCO_3-Ca/Mg) and the alkalinity measurement seems linked to bicarbonate (Fig. 31).

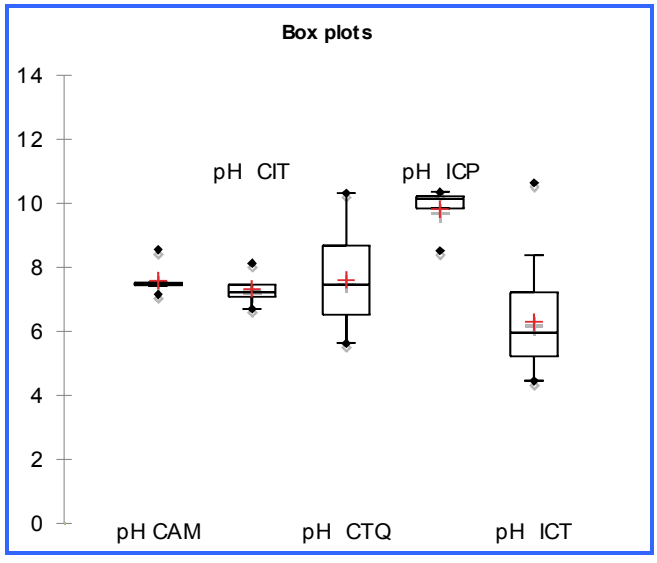

Figure 31: Variability and distribution of pH in the different geological formations.

- Dissolved oxygen

The whole set of groundwater samples (except ICP, with no measurements) shows a normal DO level (5 mg/l) in accordance with the proximity of shallow aquifers with the atmosphere (Fig. 32).

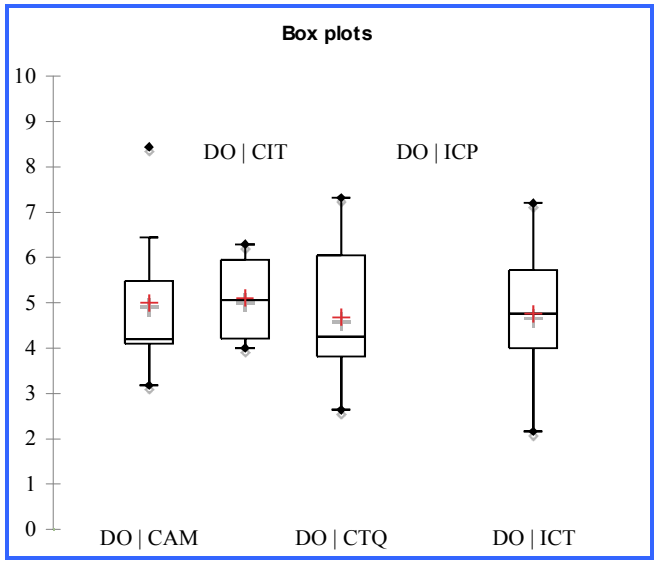

Figure 32: Variability and distribution of Dis. oxygen in the different geological formations.

- Cations

Calcium shows lower values in ICT formation with a low variability (mean=12.2 mg/l). This low heterogeneous is found in ICP formation but with higher values (mean=35.3 mg/l). The others ground waters from CTQ, CIT and CAM have more or less a mean calcium content around 30 mg/l, the mean of calcium for CAM waters is not representative, one point with 250 mg/l increase the mean calcium level (Fig. 33).

Magnesium shows lower contents in mg/l for the whole formations except CIT (mean about 20 mg/l). ICT follows the same behaviour than for Ca, lower values with respect to ICP waters and low variation (mean= 7.2 mg/l) (Fig. 34).

Sodium shows mainly lower content in ICP, ICT and CTQ with a median smaller value than 10 mg/l (except one point for CTQ D509 with the highest EC 2580 µS/cm- and ICT B554 which shows a high level of contamination with 105 mg/l de nitrate) (Fig. 35).

Potassium shows a general low level (median values between 2.1 and 9.7 mg/l). One sample (B571) from CTQ has a values of 130.8 mg/l, which does not seem consistent, values of the others ions do not increase, except nitrate which is high (81 mg/l), an anthropogenic input seems linked to this K content (Fig. 36).

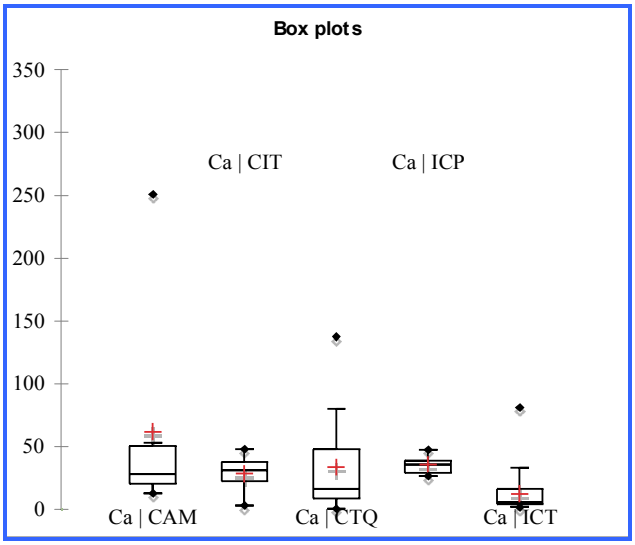

Figure 33: Variability and distribution of Ca in the different geological formations.

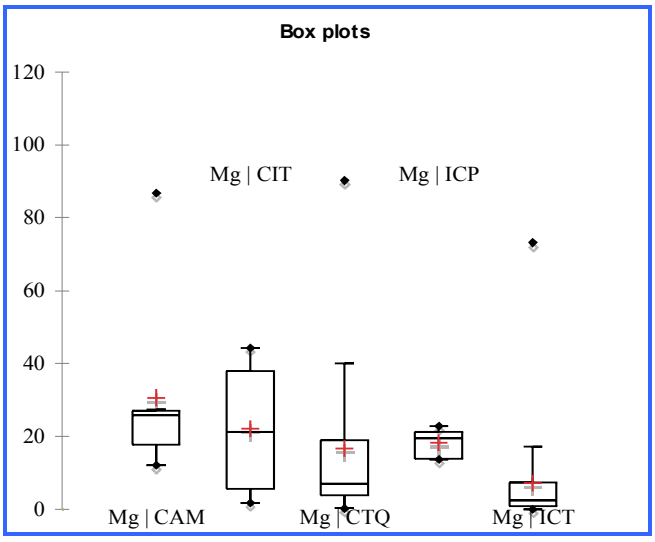

Figure 34: Variability and distribution of Mg in the different geological formations.

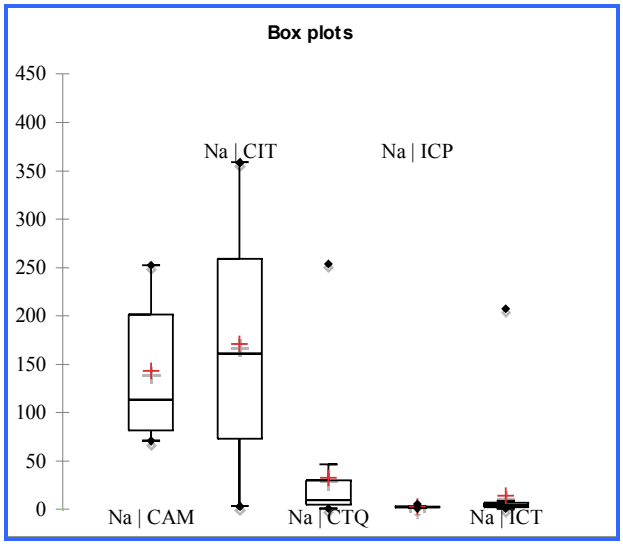

Figure 35: Variability and distribution of Na in the different geological formations.

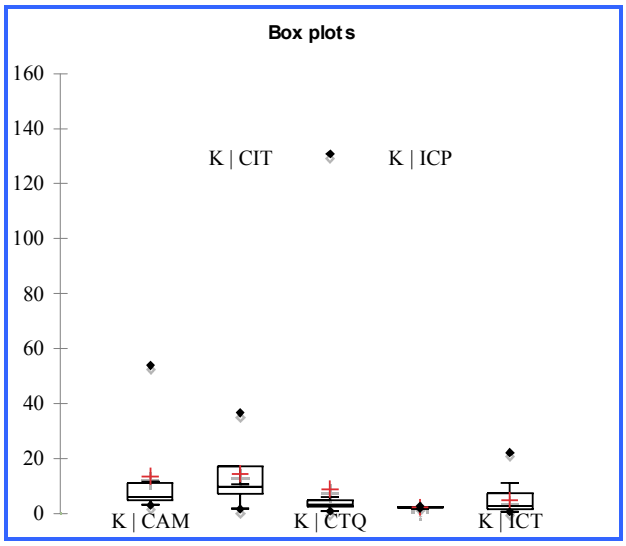

Figure 36: Variability and distribution of K in the different geological formations.

- Anions

Bicarbonate is the predominant anion in the ground waters with content exceeding 50 mg/l for 50% of samples. ICT groundwater show lower values due to lower EC. CAM and CIT show higher values with an average of 200 mg/l. We have no geological information about these two formations in the study zone but it seems obvious limestones in sandstone formation contribute to water mineralization (Fig.37).

Chloride contents are often low (< 10 mg/l) as natural level, as revealed for ICT, ICP and CTQ groundwater (Fig. 38). Above this limit, a strong correlation exists between nitrate and chloride (Fig. 39) linked mainly to an anthropogenic input. For CIT and CAM almost all values are higher (30-210 mg/l). These geological formations have a higher content in sodium linked to bicarbonate (r^2=0.71) but also with chloride (r^2=0.66) (Fig.40).

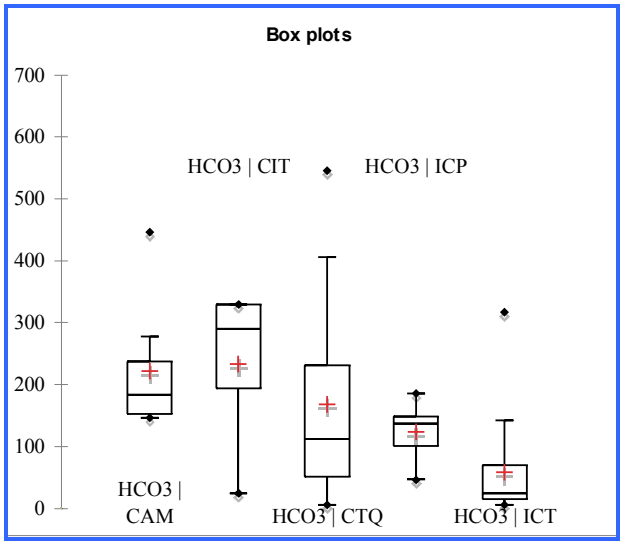

Figure 37: Variability and distribution of HCO_3 in the different geological formations.

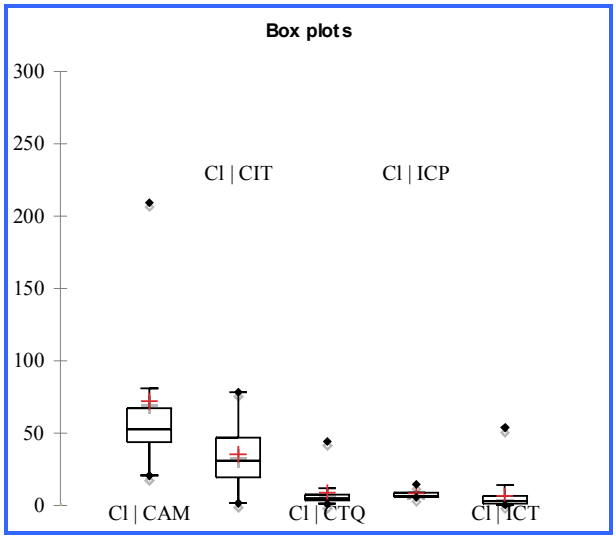

Figure 38: Variability and distribution of chloride in the different geological formations.

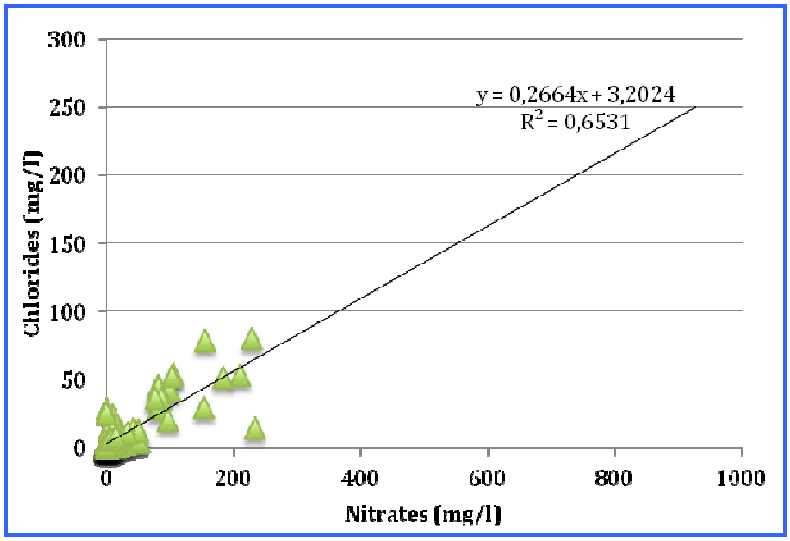

Figure 39: Nitrate *versus* chloride in all groundwater samples.

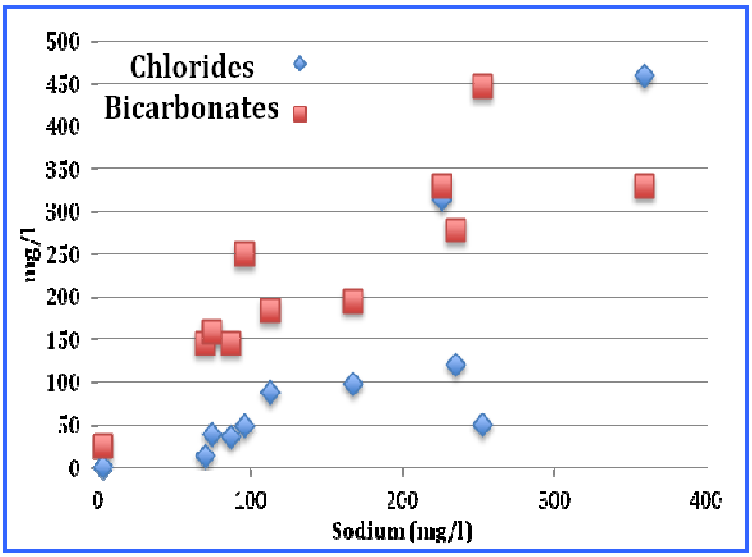

Figure 40: Sodium *versus* chloride and bicarbonate in all groundwater samples.

Sulfate ion shows low levels for ICP, ICT and CTQ groundwaters (median values < 6 mg/l) except some points from CTQ and ICT which have the highest EC, all cations and anions increase and sulfate in this case seems linked to natural dissolution. In CAM formation but especially in CIT formation, sulfate contents reach 458,7 mg/l (D528), anion prevailing in this water in this case associated with a high content in sodium, may be linked to evaporitic minerals locally (thenardite or glauberite). Another sample (D531) from CIT shows the same chemistry. In contrast, another CIT point shows one of the lowest sulfate content of total sampling with only 0.3 mg/l, highlighting the great mineralogic heterogeneity (Fig. 41).

Nitrate ions in Sahelian region are naturally occurring in the soil with specific vegetation like acacias which is a nitrogen-fixing tree, termite also can produce nitrogen and as result, groundwater can show high nitrate contents (Ngugi and Brune, 2012). In the study zone (Fig. 42), 45% of samples have nitrate content smaller than 10 mg/l, 30% are values greater than 25 mg/l, with a maximum of 927 mg/l in CAM formation where it represents the major anion (either sampling problems or bad storage in high temperature?). The whole aquifers show locally high nitrate content; CAM and CIT are most affected. The good relationship between nitrate and chloride supports the hypothesis that an important part of nitrate comes from anthropogenic contamination.

Silica (Fig. 43) content shows values between 3 and 37 mg/l, the highest values concern the CAM CIT and CTQ ground waters with a high variability in each group. ICT ground waters show more homogeneous and low values, the low EC observed shows that mineral dissolution is limited for ions and also silica linked probably to time residence younger.

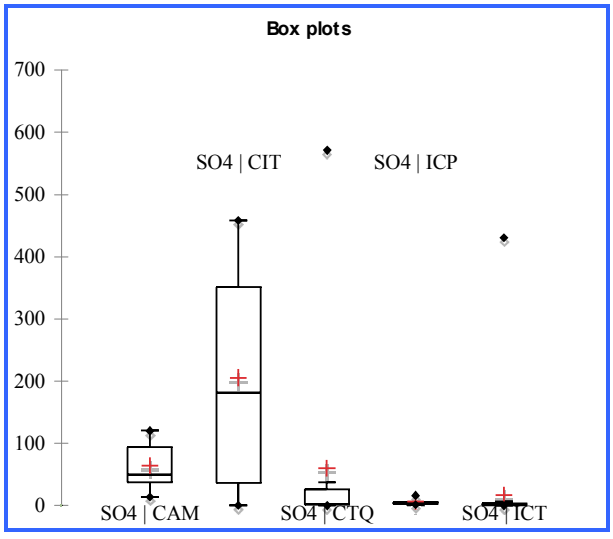

Figure 41: Variability and distribution of SO_4 in the different geological formations.

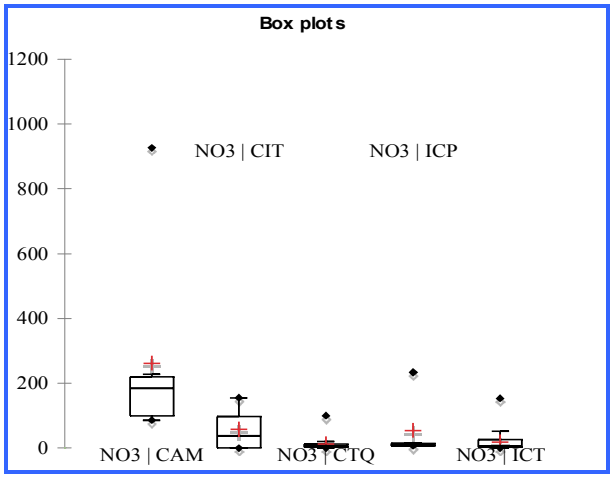

Figure 42: Variability and distribution of NO_3 in the different geological formations.

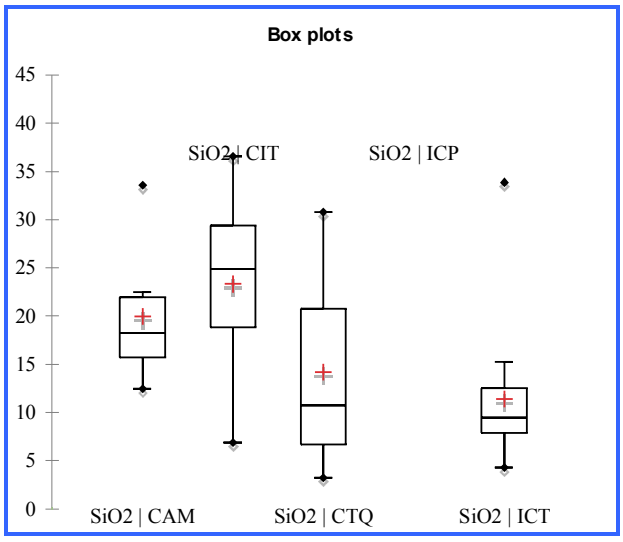

Figure 43: Variability and distribution of SiO_2 in the different geological formations.

- Oxygen-18 and deuterium

The range of values in the whole aquifer is from -6.7 to 1.4 ‰ for $\delta^{18}O$ (Fig. 44) and -52 to +1‰ for $\delta^{2}H$ (Fig. 45). However the comparison of median value for each group shows a low variability 1‰ (^{18}O) and 8‰ (^{2}H) and these values are consistent with the weighted isotopic value of annual rainfall. The variability observed for ICT, ICP, CIT and CAM shows a normal variability for shallow aquifer (more or less 3‰ for $\delta^{18}O$). In contrast the high variability observed in CTQ aquifer reveals another process, evaporation shown by enriched values. This evaporation could occur before the infiltration (endorheic local zone collecting surface runoff), during the infiltration depending on soil conditions helping or not, direct infiltration from the upper water level close to the surface (or direct from open well). Many wells in CTQ formation are shallow and the depth/isotope graphic confirms this process (Fig.46).

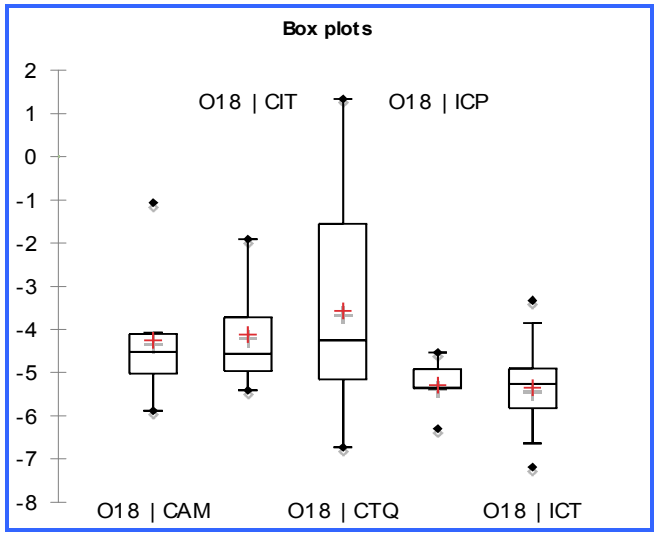

Figure 44: Variability and distribution of oxygen 18 contents in the different geological formations.

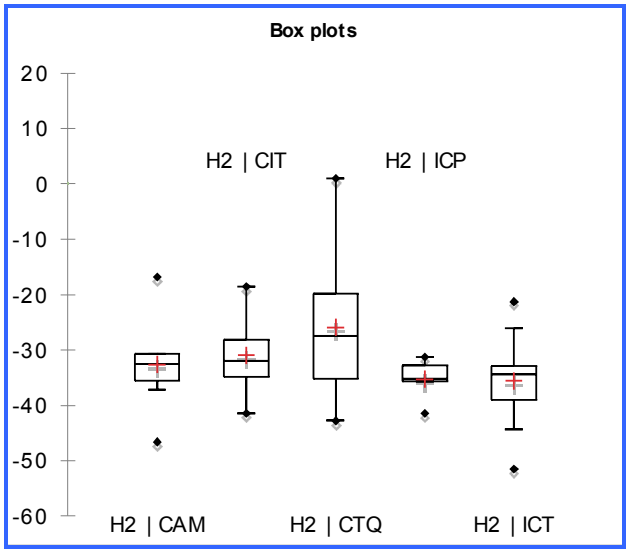

Figure 45: Variability and distribution of deuterium contents in the different geological formations.

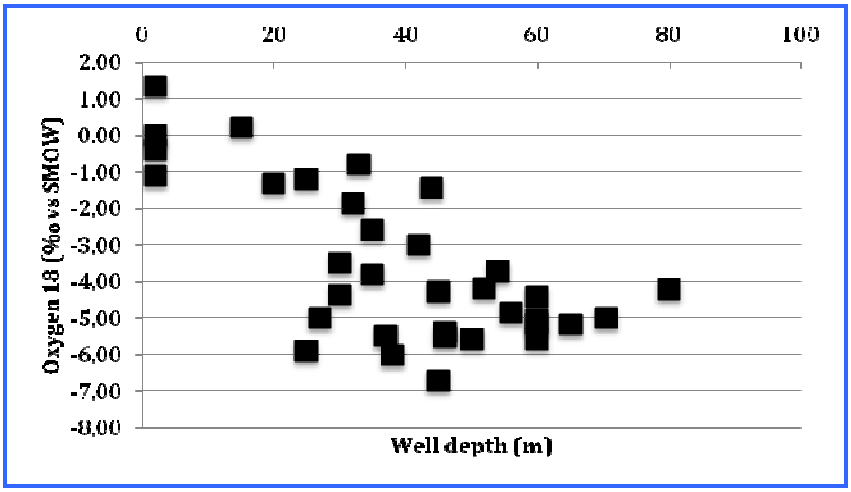

Figure 46: Well depth *versus* Oxygen 18, CTQ samples.

- Deuterium excess

The evaporation process in CTQ groundwater is evidenced by the high variability of deuterium excess and low or negative values. But the others aquifers show a low deuterium excess, especially CAM and CIT waters with "d' smaller than 6 ‰ (Fig. 47). ICT and ICP show mean values around 7.5‰ with points close to 13‰ probably linked to continental vapour recycling (Taupin et al., 2000). Besides the problem of sampling and its conservation before analysis, the deuterium excess behaviour of CAM and CIT is not so easy to understand as a general evaporation of groundwater, except an aquifer with subsurface water level does not seem possible. Water from old recharge with atmospheric circulation being different from current conditions and affecting the deuterium excess is an another hypothesis. Carbon 14 analysis could shed light on this discussion.

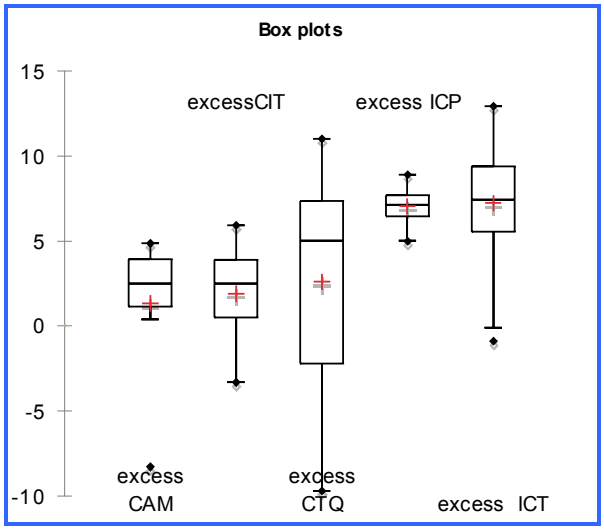

Figure 47: Variability and distribution of deuterium excess values in the different geological formations

- Tritium content

The total samples measured for tritium was 108. Most groundwaters show significant tritium contents, except a few points without detectable tritium. The figure takes into account sample with significant tritium content. ICT shows the greater variation (0.3-9,1) and higher values with mean value of 3.3 UT. ICP and CIT waters show lower values smaller than 1.6 TU and 2.95 TU. CTQ waters show intermediary values between 0.3 and 6.3 TU. From the tritium data in 2015 to Bamako, Koutiala, Mopti and Bankass stations (monthly JJA), the estimated annual value (natural level) is 4 TU. As a result, ICP, CIT, CTQ and CAM groundwaters show a mixing water with on the hand a current contribution and the other hand waters older than 1950. In contrast ICT groundwater show in most points a recent recharge over the last 65 years, with a tritium content close to 4 TU, the last 10-20 years and a content > 5-6 TU

during the period of tritium peak (1955-1980). It can note ICT samples show lower EC; in this case it is linked to rapid renewable water (Fig. 48).

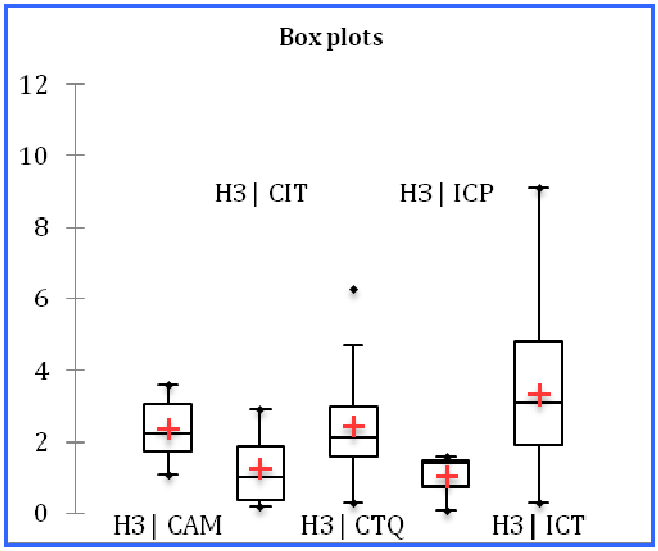

Figure 48: Variability and distribution of tritium contents in the different geological formations.

- Hydrochemical facies

The water chemistry expressed in meq/l is used to define chemical facies, Table 4 shows HCO_3^- as the dominant anion an Ca^{2+} as the dominant cation for ICT, CIT and ICP groundwaters. In some samples, Mg^{2+} and Na^+ can be dominant with HCO_3^- (Mg^{2+}) or SO_4^{2-} (Na^+) for ICT and CTQ ground waters. ICP ground water have a mixing facies HCO_3^- - Ca^{2+}/Mg^{2+}. CAM and CIT ground waters show mainly a HCO_3^- - Na^+. Nitrate is the dominant anion in some samples and mainly the second anion. These higher nitrate contents seem questionable, so it is necessary to verify the sampling protocol (good sampling conditions, strictly observe cold chain integrity between the field and laboratory, sampling conservation in freezer or cold storage and chemical analysis within a reasonable time). The main risk with these climatic conditions (hot dry or hot humid) is the development of the algae or bacteria and the increasing of nitrate content in water.

Table 4:Cation and Anion en meq/l (first campaign)

	Ca^{2+}	Mg^{2+}	Na^+	K^+	HCO_3^-	SO_4^{2-}	Cl^-	NO_3^-
ICT	42	8	11		50	4		13
CTQ	16	7	11	1	31	2	1	2
CAM	1		6		6		1	2
CIT	1	1	3		2	2		
ICP	5	5			5			1

The Piper diagram with all the samples (Fig. 49) allows showing the main chemical facies characteristics. We can note a clear evolution (CTQ and ICT) between components HCO_3^- - Ca^{2+}/Mg^{2+} towards HCO_3^- - Na^+. The diamond shape shows a high dispersion of ground water samples, but it is not due to particular mineral dissolution but due to the influx of nitrate and should be ignored to identify the geological dissolution processes. There is another evolution in CTQ and ICT aquifers for few points towards a component HCO_3^-/SO_4^{2-} - Na^+. ICP ground waters show an individual chemical facies $HCO_3^-Ca^{2+}$ad HCO_3^- - Na^+. CIT and especially CAM (ground waters shows an evolution from HCO_3^-- Ca^{2+}/Na^+ to HCO_3^- - Na^+.

The relationship of $(Ca^{2+} + Mg^{2+})$ - $(HCO_3^- + SO_4^{2+})$ versus $(Na^+ + K^+ - Cl^-)$ (Garcia et al. 2001) reveals that the waters from ICT, CTQ, CIT, CAM as we had expected, are involved in a cation exchange process, some ground waters are displaced towards positions that represent a gain in Na^+ contents against a loss in Ca^{2+} and Mg^{2+} contents. In the case of the absence of this phenomenon all the points are positioned on the origin (Fig. 50).

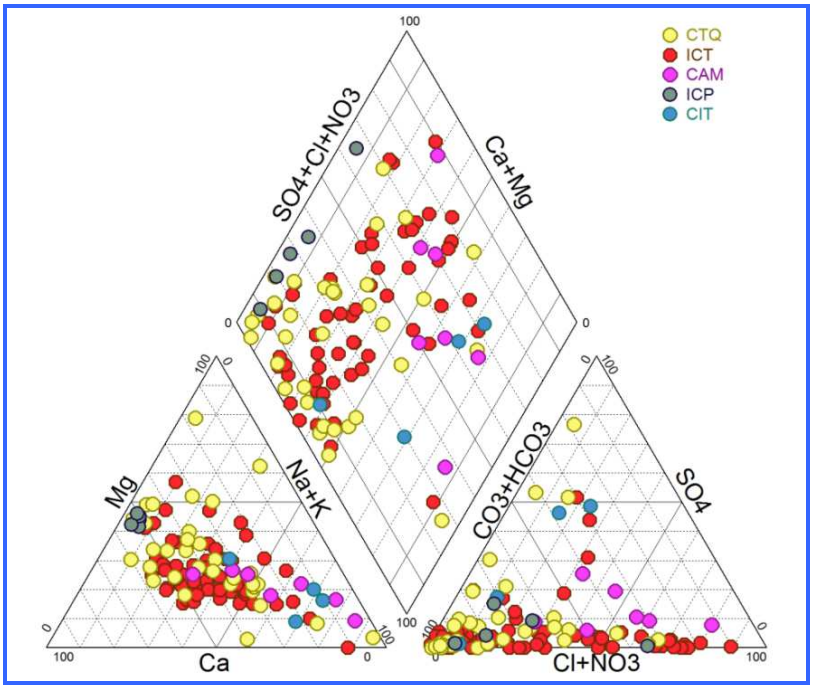

Figure 49: Piper diagram for all groundwater samples.

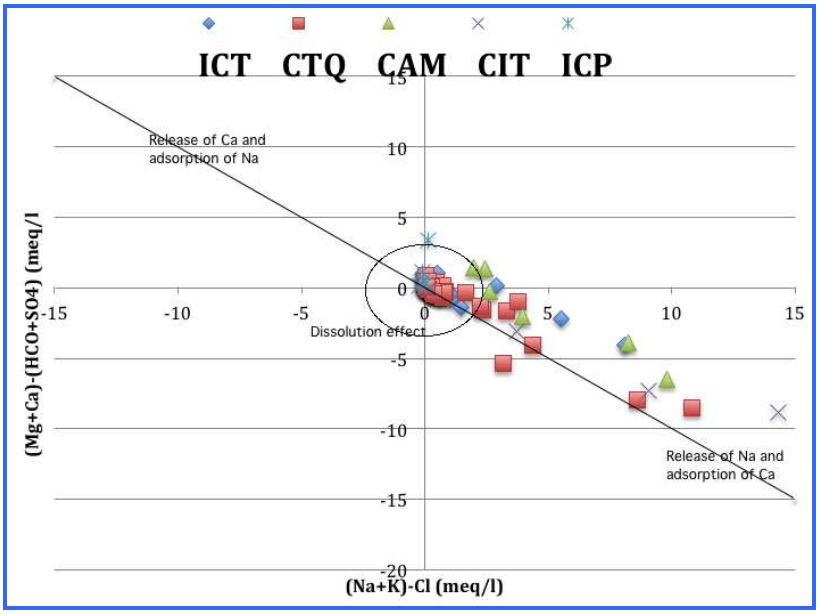

Figure 50: Cation exchange affecting groundwater.

- Equilibrium between groundwater and minerals (no data for ICP waters)

With the software PHREEQC, it has been calculated the Saturation Index (SI) of water with respect to various classical minerals. It can be noted in IAEA data base that the almost ICT samples and some CTQ samples present total iron measurements with as result a systematic value of 0.01 mg/l. With these values, water mainly show an over saturation with respect to hematite and goethite. The others major minerals, which could interact in our geochemical environment, are calcite, dolomite and quartz. The ICT, CIT and CTQ show ground waters mainly under saturated with respect to calcite and few samples show a saturation level or a very light over saturation. The samples from CAM aquifer are inside the saturation range (Fig. 51). The index saturation graphic for dolomite shows similar results (Fig. 52).

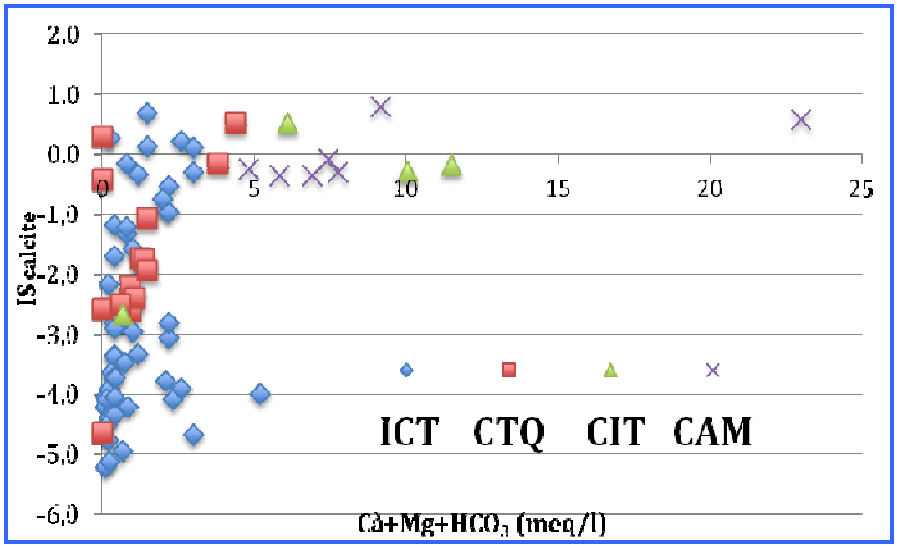

Figure 51: Saturation indices with respect to calcite in groundwater samples from various aquifers.

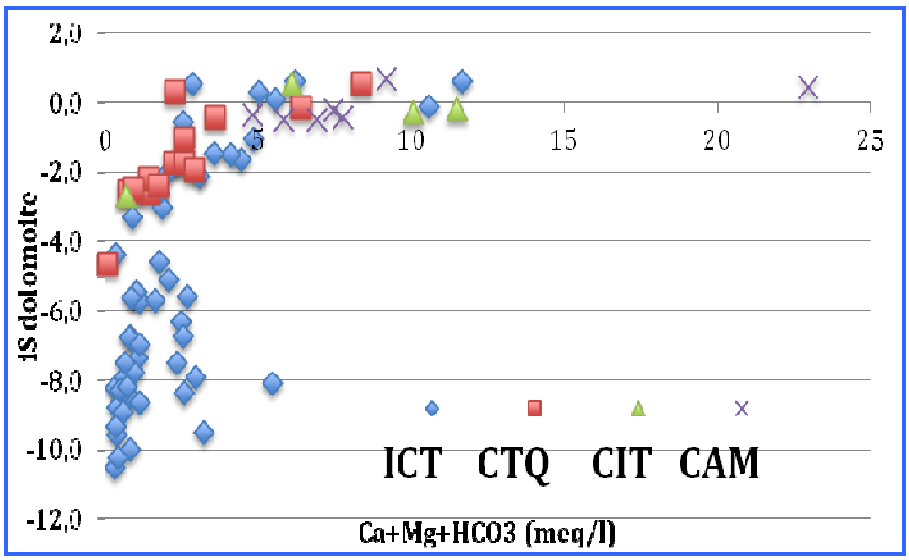

Figure 52: Saturation indices with respect to dolomite in groundwater samples from various aquifers.

With respect to quartz (Fig. 53), all ground waters are in the stability zone, the main rocks in the study zone are composed by sandstones with quartz mineral inside or silica cement.

The figure 54 shows the equilibrium state of waters with respect to silicate minerals. This water mainly is in equilibrium with kaolinite towards an evolution to smectite clays domain or feldspar. CAM and CIT groundwater show an equilibrium state close to or inside the smectite clay domain; these waters have a dissolution state more developed.

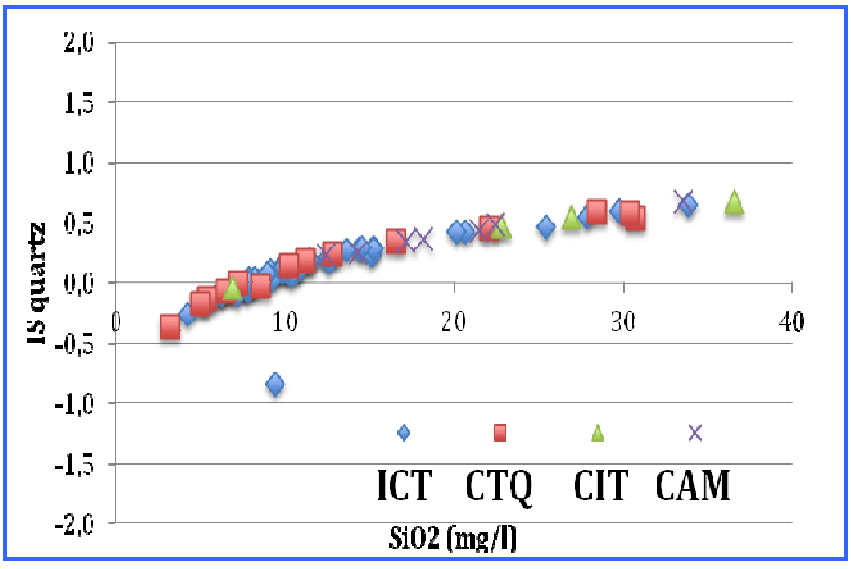

Figure 53: Saturation indices with respect to quartz in groundwater samples from various aquifers.

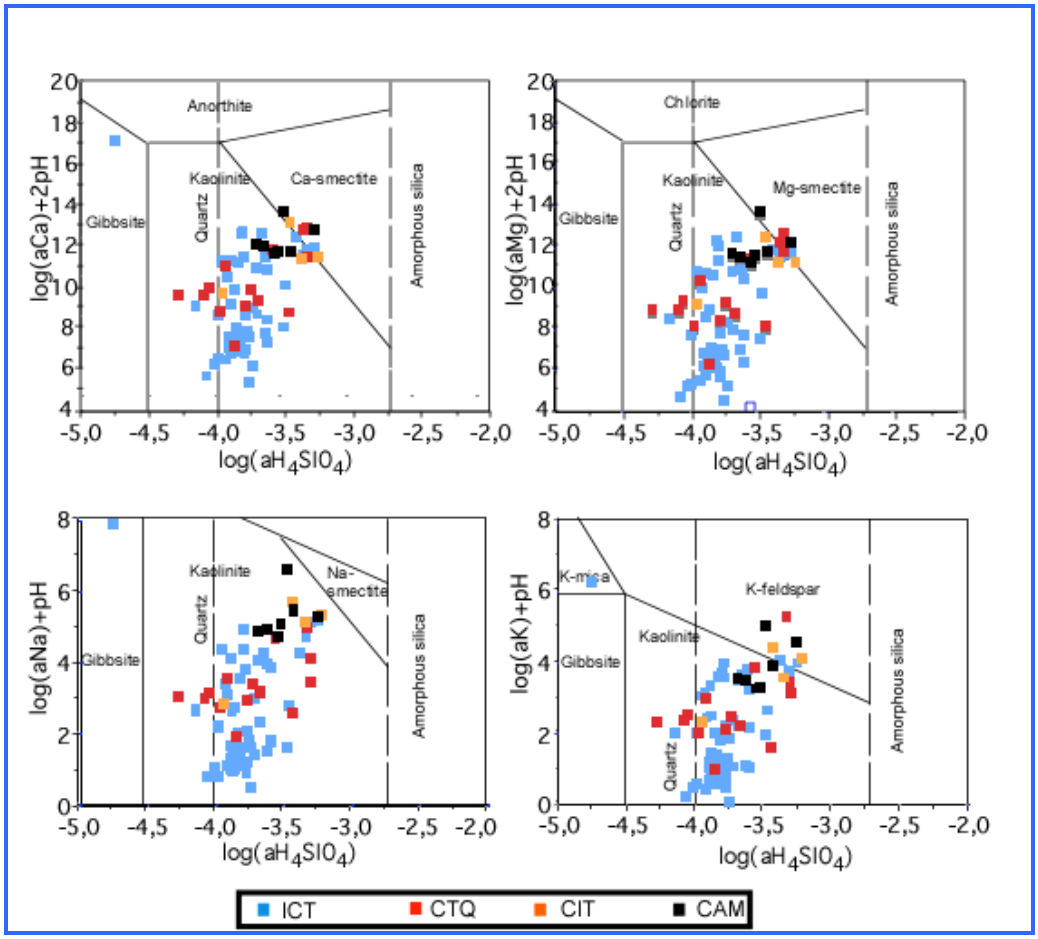

Figure 54: Korjinsky diagram, stability field diagram of silicate minerals.

- Multi correlation analysis

The aim of a principal component analysis (PCA) tool is allowing proposing a visualisation of multidimensional data, in our case the analysed or field measured parameters of ground waters, and the structure of variables through a bi dimensional graphic. Each axis corresponds to a composition of n analysed elements; then the coordinates X and Y of each sample are calculated by:

X = a1 + b1 [Param1] + c1. [Param2] + d1.[Param3]+ ….+ n1.[ParamN]
Y = a2 + b2. [Param1] + c2.[Param1] + d2.[Param1] + ….+ n2.[ParamN]

In this case, the parameters used are the chemistry elements, the field measurement and isotope and Tritium measurements.

Waters with similar profile are close in the graphic.
The results are presented in table 5 and figures 55 and 56 (complete analysis on 78 observations).

ACP total

Table 5: Total Variance measured by axis

	F1	F2	F3	F4	F5
Value	8,176	2,755	1,601	1,355	1,187
Variability (%)	45,424	15,303	8,896	7,529	6,596
Cumulative percentage	45,424	60,727	69,623	77,152	83,748

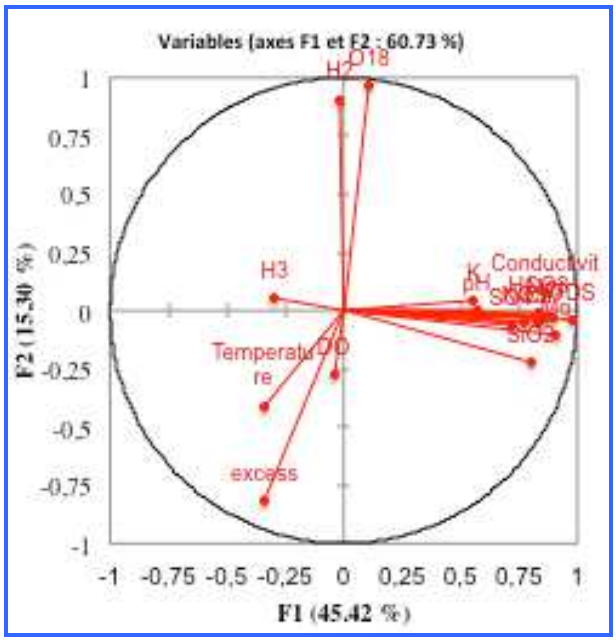

Figure 55: Principal component analysis of ground waters (parameters).

F1 represents all the mineralization and chemical elements of ground waters and F2 the water stable isotopes and in opposite correlation the deuterium excess. F3 do not add new information.

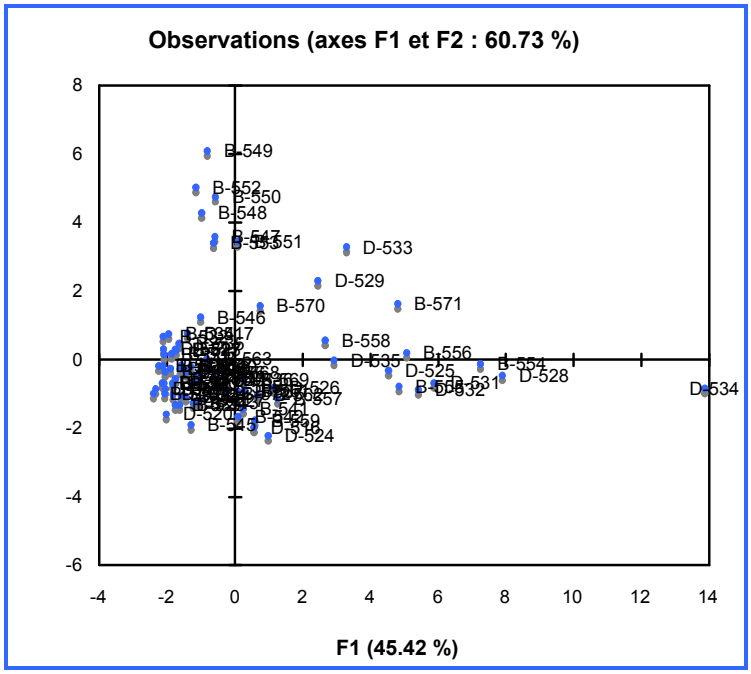

Figure 56: Principal component analysis of all sampled groundwaters.

Two groups of samples can be identified separately for each axis depending on F1, F2 parameters. F1 shows the samples more mineralized and F2 the samples which show the more enriched isotopic value and as a result the deuterium excess lower. PCA does not distinguish with respect to the geological formations which are mainly similar in term of geochemistry, but all the points on F2 axes come from CTQ formation because we have seen that they show the most enriched values in stable isotopes, and low deuterium excess, linked to shallow water level.

- Spatial distribution of groundwater parameters (preliminary work)

There are not enough points in CIT, ICP and CAM to point a spatial relation, in this case to show a flow direction marked by a chemical, or age evolution linked to a contact water-rock longer.

For ICT formation, the study zone is too large with a network few suitable and a poor knowledge of geological context. However if we can make the general hypothesis that circulation flow follows the direction from edge to center of basin, with in our case two cross section, at the western part a cross section S to N and at the eastern part a cross section S-SE to N-NW. We can see (with caution) a spatial organization East-West, with lower values in south eastern part a higher EC in north western part. Bicarbonate and calcium show a similar behavior, this comes as no surprise, because these ions strongly contribute to the total water mineralization. The pH also shows this evolution from acid to neutral-basic water that could be explained by a chemical buffer effect, with mineral dissolution neutral or alkaline ions

increase and decreases the initial acidity. Stable isotopes show a pattern less obvious but in south eastern part the values between -4 and -6‰ prevail and in northern part the values are mainly -more depleted (-5 and -7‰) due may be to a mixing more important with older water?. The spatial distribution of Tritium follows this hypothesis with younger water in the south eastern part (between >3 TU and in the north western part a strong decrease of tritium and water without tritium.

Concerning the CTQ formation, there is (a priori) no hydrodynamic continuity between eastern and western part, CTQ is separated by ICP formation. The western and eastern part show differences, more mineralized (EC and bicarbonate) and pH basic in eastern part.
The pattern of oxygen 18 with enriched values and low deuterium excess in north western part of the aquifer is due in part to a shallow depth well with water level close to the surface. For Tritium, no obvious pattern is shown, high Tritium content and water without Tritium occurs in the same geographical zone.

- Isotopic results

We have analysed all available isotopic data in the zone to synthetize the isotopic information of RAF/7/011 project in a global context long term. We have used isotopic data from GNIP and GNIR programme in Mali and Burkina Faso (Fig. 57).

- **Isotope contents in rainfall**

For Bamako station we have used only data after 1990, the first set (1962-1980) showing many errors due to sampling problems (deuterium excess too lower - 60% of samples).

In the first instance we have estimated the weighted isotopic mean annual from some stations and some years where 90% of annual rainfall were collected and analysed. The results are shown in the table 6. Unfortunately, in the IAEA-supported project RAF/7/011, the collection of rainfall in Bankass, Mopti, Bamako and Koutiala has been partial and less of 90% of rainfall has been collected except Mopti in 2014.

Figure 57: Isotopic data from GNIP and GNIR stations used in this study; black rectangles GNIP stations (Bamako, Koutiala, Nasso, Hounde, and Bobo Dioulasso) and GNIR (Sele) stations.

Table 6: Isotopic annual values

Bamako 1992	-4,94	-31,3
Bamako 1993	-4,97	-26,2
Bamako 1994	-6,12	-38,7
Bamako 1996	-4,45	-26,8
Bobo Dioulasso 2010	-4,70	-29,8
Bobo Dioulasso 2011	-3,37	-17,9
Bobo Dioulasso 2012	-5,09	-29,7
Bobo Dioulasso 2013	-2,11	-9,7
Mopti-Sevaré 2014	-3,75	-21,7

The annual isotopic content variability is high (-2.11 -/ -6.12 ‰ $\delta^{18}O$; -9.7 / -38.7 ‰ $\delta^{2}H$) with a mean of -4.39 and -25.8 ‰ respectively for $\delta^{18}O$ and $\delta^{2}H$. These values are consistent with other long term studies in the Sahelian zone at Niamey (Taupin et al., 2000, 2002) with -4.2 ‰ and -23.5 ‰ respectively for ^{18}O and ^{2}H. Mathieu et al.(1993) calculated a weighted mean value of -3.7 ‰ (^{18}O) and -23.8 ‰ (^{2}H) at Barogo station, located about 50 km northeast from Ouagadougou (1988–1989 period). The intra-annual variations are affected by climatic conditions. Sahelian rainfalls (April to October) depends on the position of the

InterTropical Front (ITF). About 80% of annual rainfall is due to convective systems. During humid years, the average isotopic composition of local precipitation is more negative because low temperature and high relative humidity can reduce the evaporation effect (Gourcy et al., 2000). The isotopic composition is also influenced by the rainfall origin. In the Sahelian region of western Africa, the rain comes from the Guinean monsoon or Easterly waves carried by the African Easterly Jet and Tropical Easterly Jet (Gourcy et al., 2000). The predominance of one of these phenomena during the rainy season directly influences the amount precipitated and the isotopic content of rainwater (Gourcy et al., 2000; Taupin et al., 2002).

At the monthly scale (Bobo Dioulasso – 2010-2013), isotope content and deuterium excess in rainy season is characterized by a V shape (Taupin et al., 2000, 2003). At the beginning and at the end of the rainy season, isotopic contents are enriched by high temperatures and by the desaturation of the atmosphere due to the instability of the monsoon. In the middle of the rainy season, when the monsoon is well established, isotopic contents become depleted because the atmosphere is saturated with water, temperatures are lower and numerous convective systems develop to a great height (Figs. 58 and 59).

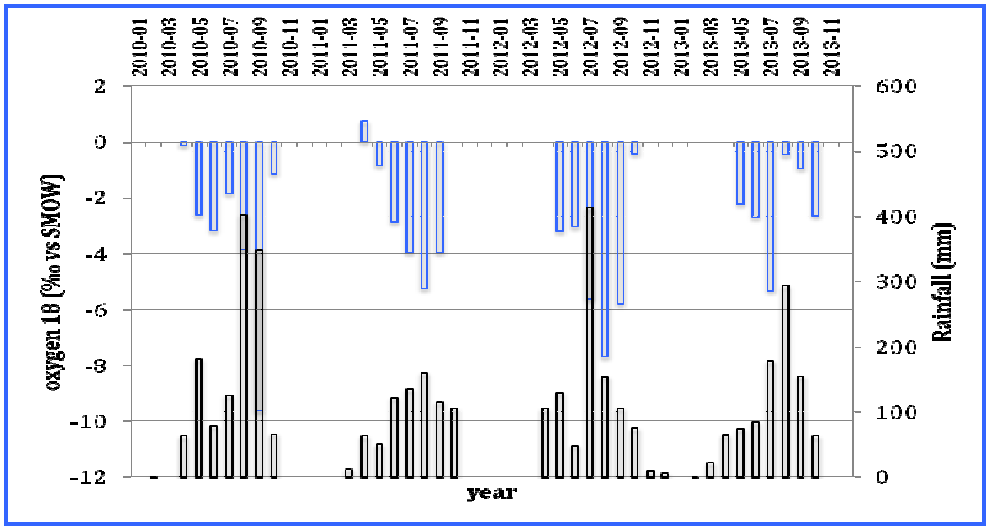

Figure 58: Isotopic monthly variability at Bobo-Dioulasso.

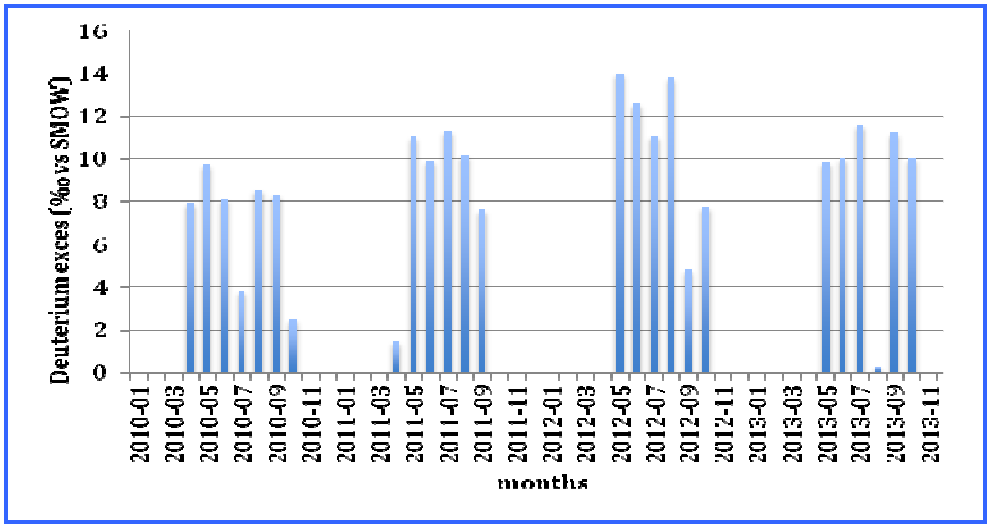

Figure 59: Monthly evolution of deuterium excess at Bobo-Dioulasso station.

To define the relation between oxygen 18 and deuterium, we have used all monthly data set available from the 5 rainfall stations (Fig. 60). The Local Meteoric Water Line is close to the GMWL. If we delete evaporated points, the LMWL the line is: $\delta^2H=7{,}866\ \delta^{18}O + 8.87$, very similar to the GMWL and also similar to the relationship found in long term series at Niamey (Taupin, 2002), and closer to the study zone:

- Barogo station, Mathieu et al. (1993):

$$\delta^2H = 7.7\ (\pm 0.3)\ \delta^{18}O + 7.8\ (\pm 4.0)$$

- Bobo-Dioulasso, 1997-1998 (Huneau et al., 2011):

$$\delta^2H = 8.0\ (\pm 0.5)\ \delta^{18}O + 10.2\ (\pm 2.1)$$

- Bamako, period 1991-1998 (Gourcy et al., 2000):

$$\delta^2H = 8.1\ (\pm 0.2)\delta\ ^{18}O + 11.9\ (\pm 2.1)$$

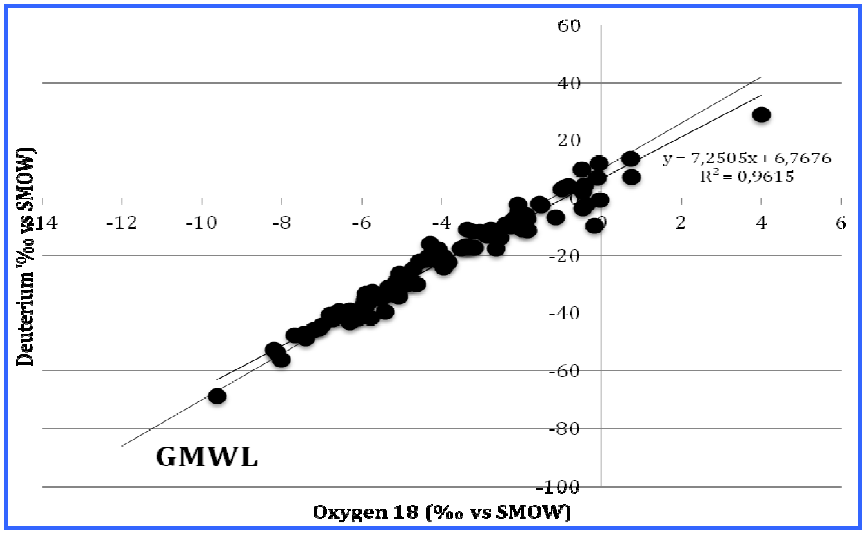

Figure 60: Relationship between oxygen 18 and deuterium in monthly rainfall samples from 5 stations.

- **Isotope contents of groundwater samples**

To complete and finalise the discussion about the isotope contents in groundwater, we have compared isotope contents in current rainfall and isotope contents in the 5 aquifers (Fig. 61). With an estimated inter annual isotope content of -4.4 ‰ ($\delta^{18}O$) and -25.8‰ ($\delta^{2}H$) in rainfall, isotopes in precipitation are strongly enriched with respect to 77 % of groundwater samples. Even assuming a mean value of -5‰ in $\delta^{18}O$ for rainfall 45% of samples are yet isotopically more depleted. Comparing with the isotope content of groundwater in Burkina Faso, these waters show values more enriched than -6 ‰ ($\delta^{18}O$); in Mali $\delta^{18}O$ values more depleted than -6‰ constitute 14% of the analysed samples.

If we compare $\delta^{18}O$ contents and tritium (Fig. 62) there is no clear relationships showing older age linked to more depleted values. However, the paleoclimatology studies have shown that the Sahel region has endured, in the past, many different climate phases which have influenced the infiltration and recharge processes in a great manner (Beyerle et al., 2003).

Before 4500 years B.P, the Western African climate was characterised by several humid phases during the Holocene within optimum in the Sahara region around 8500-6500 years B.P, interrupted by short dry periods (Gasse, 2000). In the Sahelian belt the monsoon reactivation after the dry and cold Last Glacial Maximum (LGM, 23-18 kyr B.P) took place in two steps at around 15,000 and 11,500 years B.P (Gasse, 2000), separated by a return to drier conditions coincident with the Younger Dryas. Palaeoclimatic records from Western Africa that extend beyond the LGM indicate that prior to 23,000 years B.P humid climate conditions alternated with arid phases while the average temperature remained lower than today (Gasse, 2000).

Huneau et al. (2011), in the eastern edge of Taoudeni basin in BKF part, suggested, through carbon 14 dating, a continuous recharge of the system through time from Actual to Pleistocene, but the aquifer was prominent recharged during humid periods up to 4500–5000 years B.P.

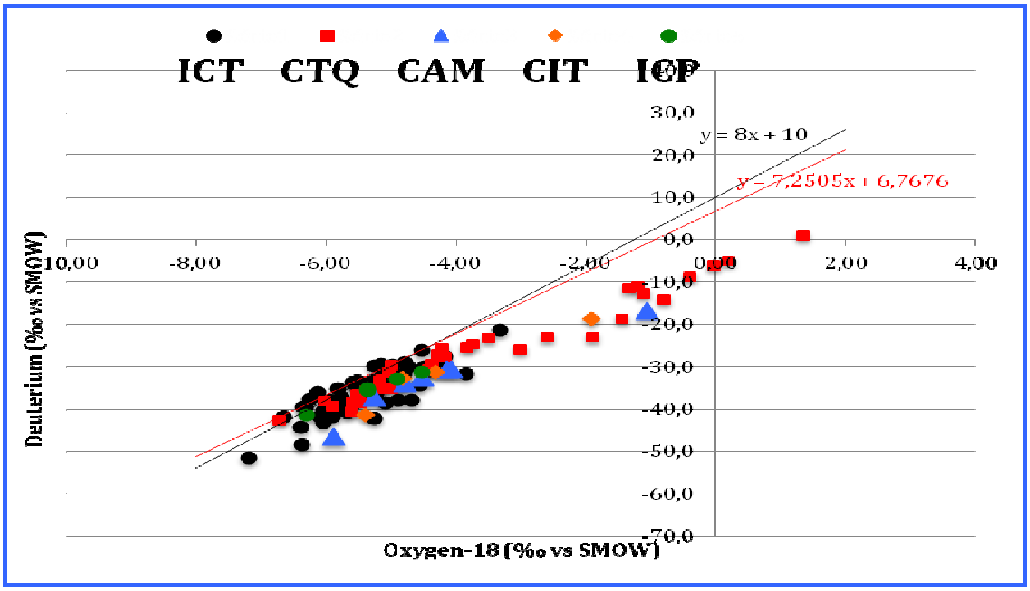

Figure 61: Oxygen 18 *versus* deuterium contents in groundwater samples.

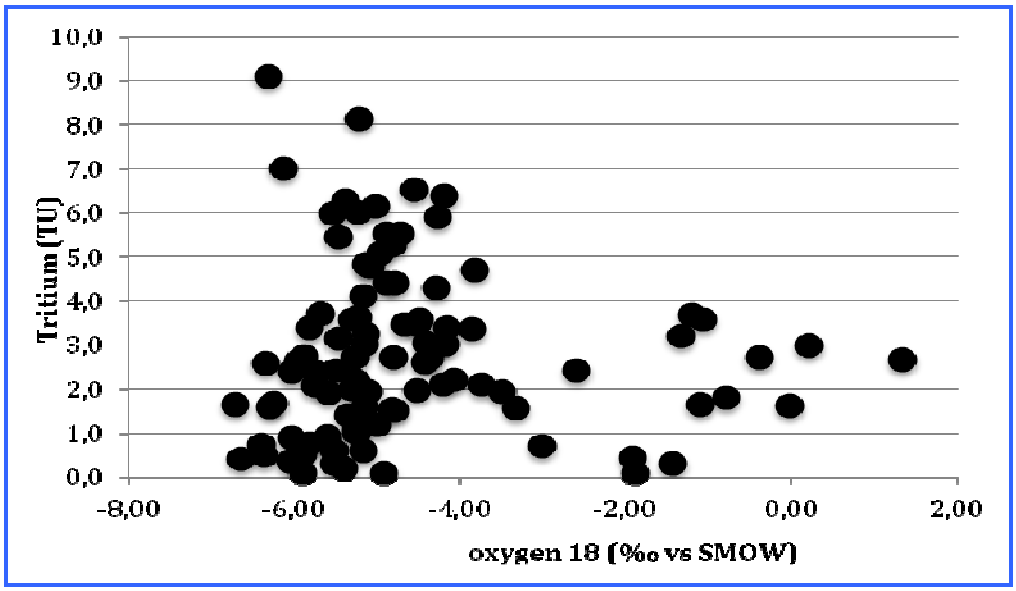

Figure 62: Oxygen 18 versus tritium contents in groundwater samples.

- **Isotope contents in surface waters**

Three surface waters were sampled during the project: 24/6/2013 Niger River at Bamako; 25/05/2014 Bani River at Douna and 18/03/2015 Niger River at Markala (Fig. 63). The EC is between 49 and 81 µS/cm with a neutral pH (6.7-7.6). The chemical facies is HCO_3^- - Ca^{2+}/Mg^{2+}or HCO_3^- - Na^{2+}/Mg^{2+}. Nitrate contents are low in river waters (0.09-3,8mg/l). The dissolved oxygen shows high levels in all cases (7-8 mg/l).

The isotope measurements in Niger River (Sele) show a high variability (> 8 ‰ in oxygen-18) during the year showing a cycle similar to the isotope rainfall cycle with a light temporal

diphase shift (one month) This curve is correlated to the river flow-rate and in the dry season the Niger river is subjected to a strong evaporation (Fig. 63), (high isotope enrichment and low deuterium excess).

The isotopic contents in the three river samples show a similar temporal variation between them even if the values are different (more depleted) which depends on the annual rainfall conditions:

24/6/2013 Niger River at Bamako -3.00 ‰ -18.3‰ respectively for $\delta^{18}O$ and $\delta^{2}H$
25/05/2014 Bani River at Douna +0.48 ‰ -8.5 ‰
18/03/2015 Niger River at Markala -1.14 ‰ -11.7 ‰

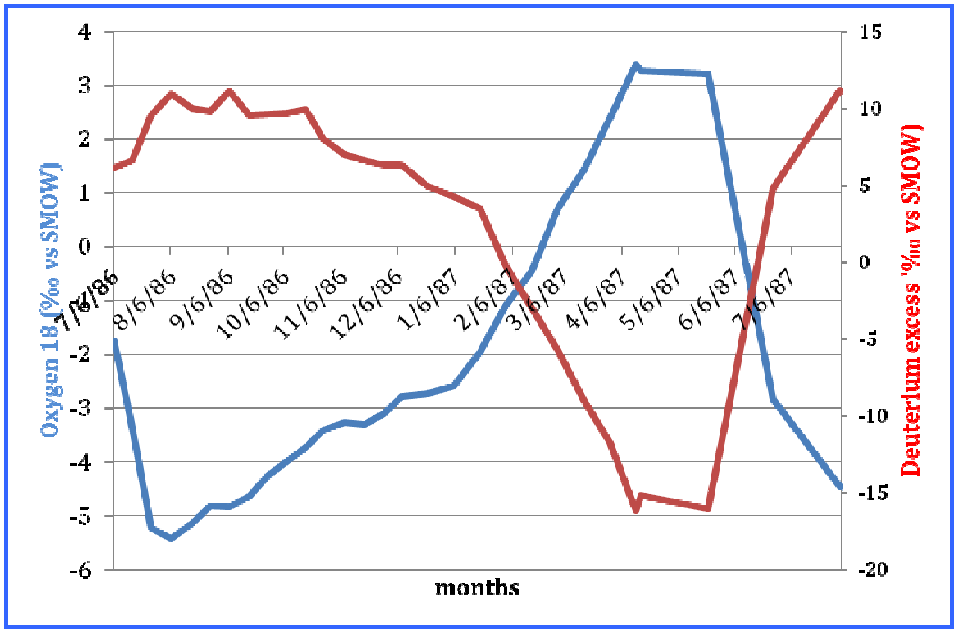

Figure 63: Oxygen 18 and deuterium excess in 1990-1991 at Sele river station

4.3. Results and discussion: Burkina Faso study zone

The available data has been processed by lithology types (Fig. 15).

-Depth of the sampled wells

Groundwater sampling has been carried out in wells deeper on average than those sampled in the south eastern part of Mali. On average the depth wells is between 60 and 80 m, except for GFR formation with has a depth around 50 m (Fig. 64). In the study zone there are few shallow wells between 25 and 40 m depth. Two formations show great depth variability, GFG and SAC1, with 80 and 90 m. In contrast, the depth wells shows in the crystalline formations

a depth wells homogeneous, despite its extensive area and its geological diversity, may be due to a generalized alteration and fractured process which limits the depth of productive zone.

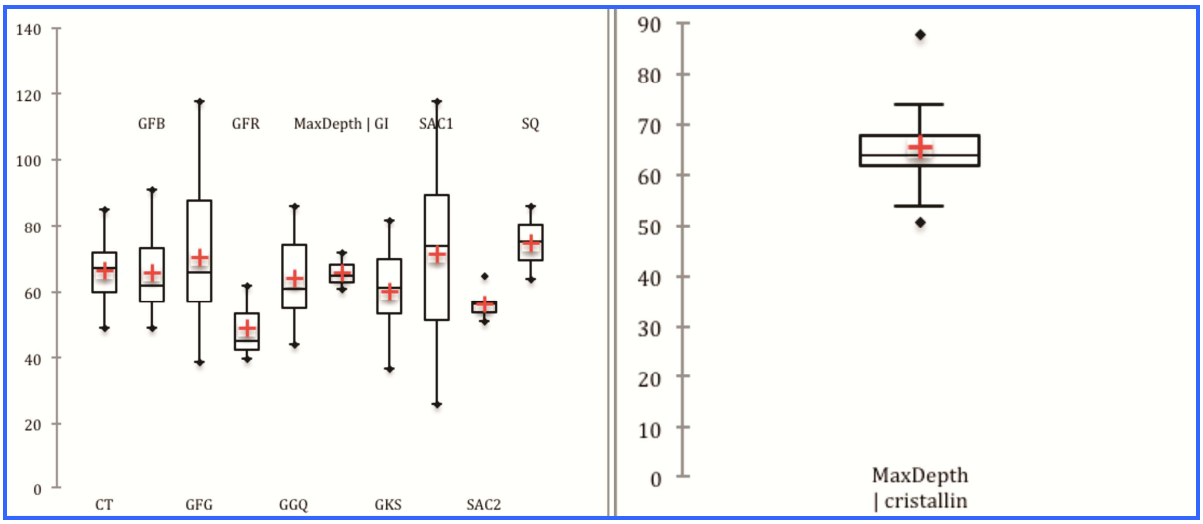

Figure 64: Variability and distribution of the depth of the sampled wells in the different geological formations

-Electrical conductivity

EC in the crystalline formations is highly fluctuating (58-1856 µS/cm) with a mean value of 513 µS/cm (Fig. 65). The highest values are not linked to a natural process of mineralogical dissolution; it's the high content in nitrate which contributes to the increase of EC and not only for the crystalline formations (Fig. 66). In this context all samples (except one sample in a crystalline formation) with an EC greater than 800 µS/cm are highly contaminated by nitrate, related also to a higher content in potassium. It is important to know if this anomaly is the result of a sampling problem (probably) or to a high contamination level in the well. Outside this issue, all samples on average show low (GFB, GI, GGQ, SAC2 < 200µS/cm) to medium (others IC formations and CTQ < 400µS/cm) EC. Comparing with the south eastern part of Mali, CTQ shows values lower in BKF (average 390 µS/cm - 535 µS/cm), in Mali 60% of samples located in eastern CTQ show values between 500 and 2000 µS/cm (Annex II).

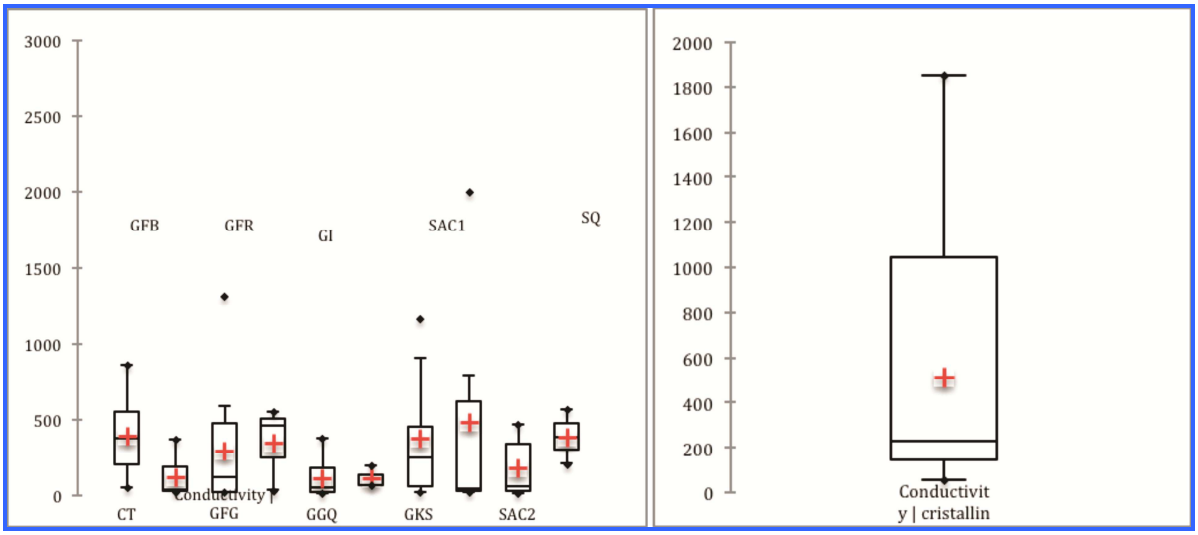

Figure 65: Variability and distribution of EC in the different geological formations.

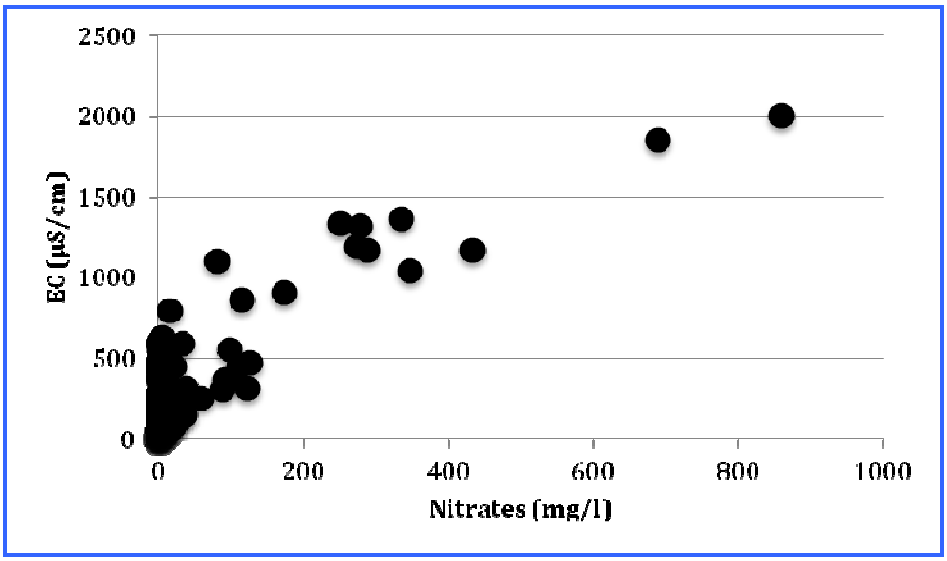

Figure 66: Relationship between nitrate contents and Electrical Conductivity.

Comparing TDS and Electrical Conductivity (Fig. 67), there is a very good agreement.

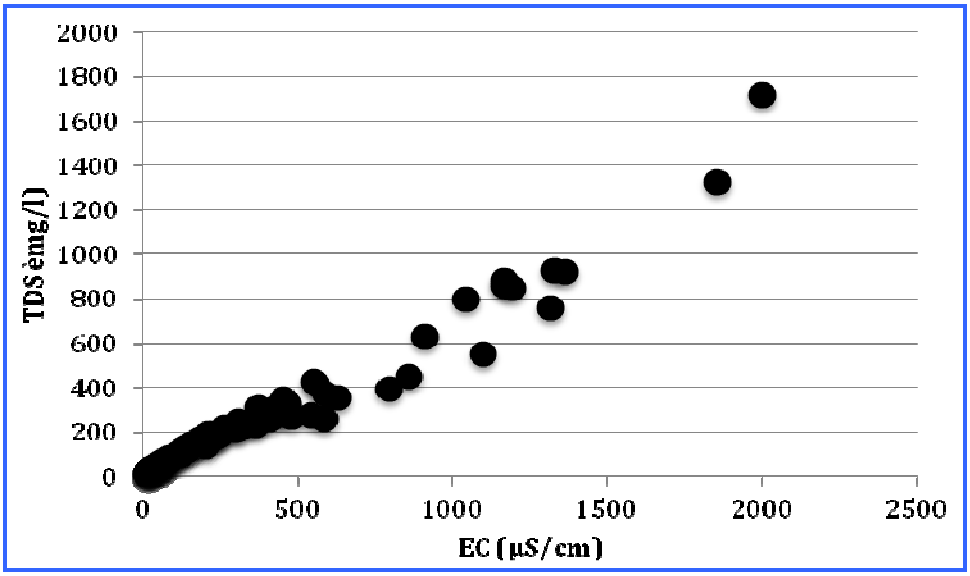

Figure 67: Electrical Conductivity *versus* TDS-for all samples.

- Temperature

Mean water temperatures show few variations between the geological formations, and are in the range of the annual atmospheric temperature value (30-31°C). Some maximum values (CTQ and GKS) should be viewed cautiously in the use of the computation of thermodynamic equilibrium, it should be due to a re equilibrium of groundwater temperature with the atmospheric temperature at the time of the measurement (Fig. 68).

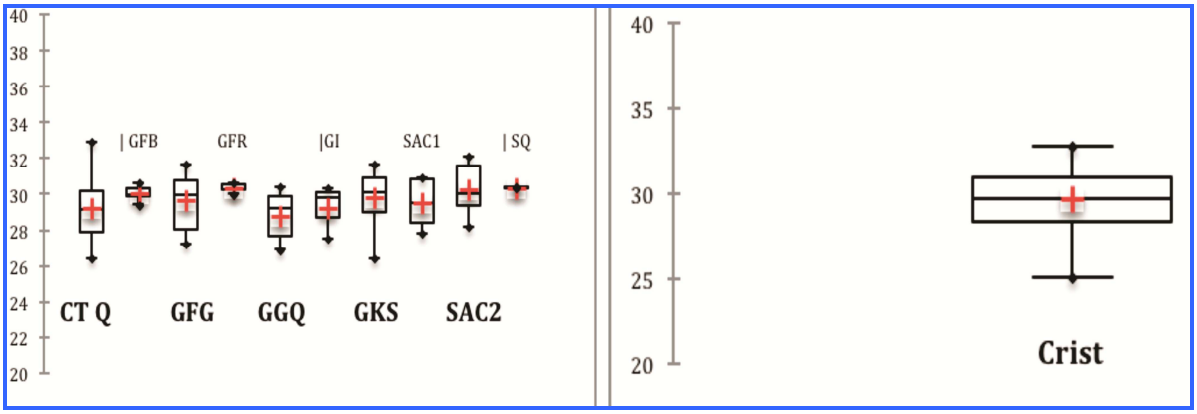

Figure 68: Variability and distribution of temperature in the different geological formations.

In accordance with Huneau et al. (2011), GGQ groundwater provide on average the lowest temperatures about 28–30°C probably translating the deep origin of water. SAC2 shows higher groundwater temperatures related to a more superficial origin of the water in the central basin.

- pH

The range values seems normal globally (5.0 to 7.5) for the whole formations, may be some points with a pH acid (<4.5) have to be revised (Fig. 69). The pH values correspond to sandstone or limestone facies. In accordance with Huneau (2011), most of the samples originating from carbonated levels pH values are close to neutral pH as CT and GFR. Water from the most siliceous levels show a clear tendency toward more acidic pH (GFB, GI). Even if in the two studies the results mainly agree, it can noted that in Huneau et al. (2011) pH are systematically higher (0.5 to 1 pH). In crystalline formation pH is very stable, slightly acid in accordance with its content in silica.

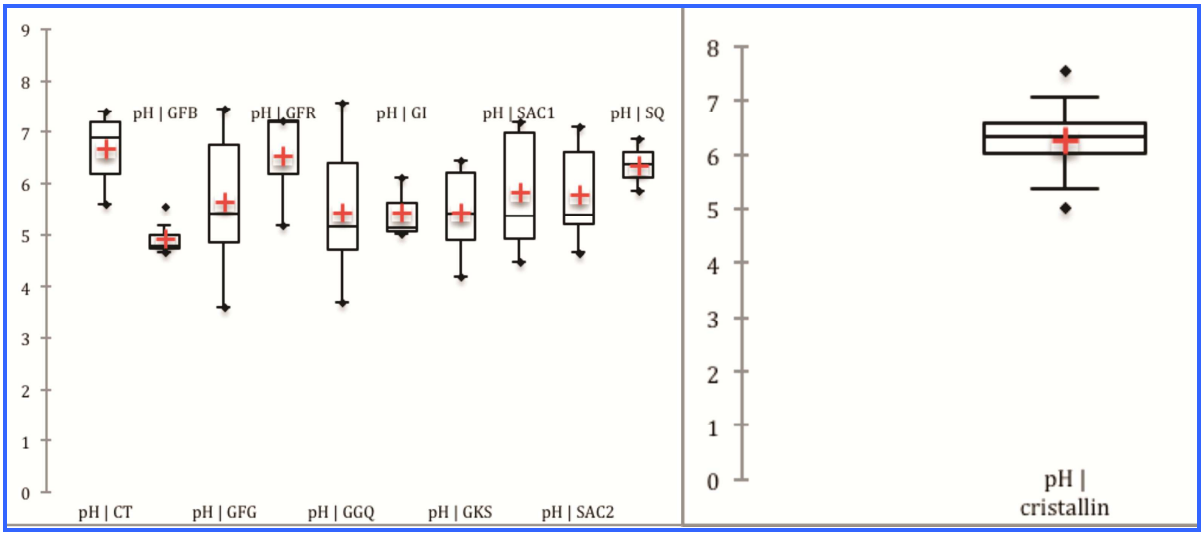

Figure 69: Variability and distribution of pH in the different geological formations.

- Cations

Calcium (Fig. 70) in crystalline formations shows an average value of 23 mg/l, it is a higher level than limestone lithology in Infra Cambrian in spite of it would be less abundant. If we compare calcium and sulfate for the highest content in calcium, we can see a close relationship (r^2=0.85), in fact it is due to a contamination process (Fig. 71). The CT formation shows an average value of 21 mg/l one of higher content with a great variability (1-56 mg/l), hydrolysis of limestones and dolomitic limestones dominate in the levels CT. It is similar for Infra Cambrian lithology composed by limestones and dolomitic limestones, SAC1, GFR with an average of 22 mg/l and to a lesser extent GKS and GFG. GFB, GGQ and GI show lower values, on average smaller than 5 mg/l, in accordance with lithology being more siliceous. This result agrees with those from Malian ICT and CTQ formations.

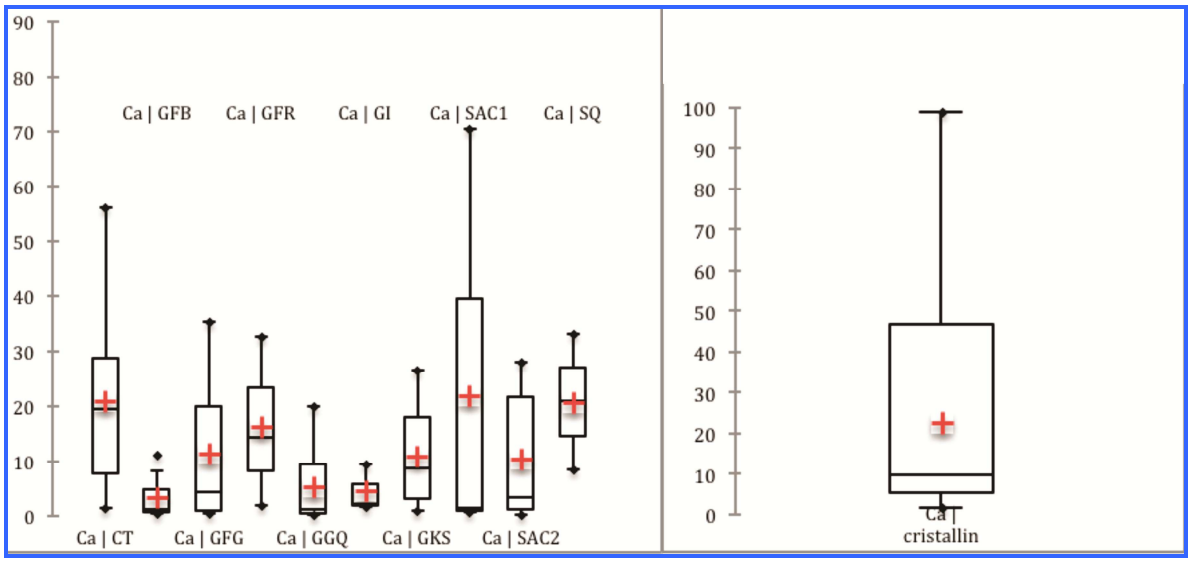

Figure 70: Variability and distribution of Ca in the different geological formations.

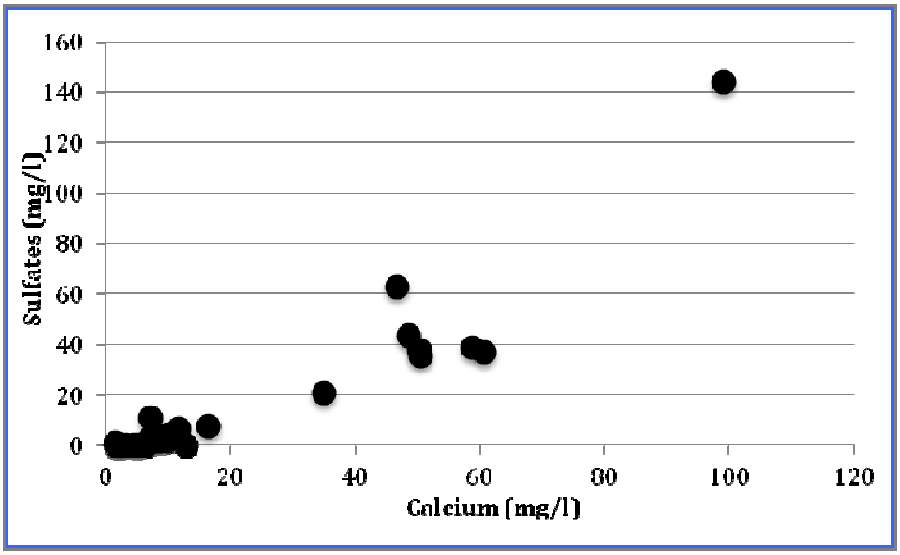

Figure 71: Relationship between calcium and sulfate contents in the crystalline formations.

Magnesium (Fig. 72) in the samples from crystalline formations have a similar behavior than calcium, an average of 44 mg/l but some points show higher values (> 100 mg/l) with respect to a basic level of 15-20 mg/l and they match with nitrate (r^2=0.82), also due to an anthropogenic influence (Fig. 73). For the CT and Infra Cambrian formations, magnesium follows calcium according to the lithology, with mean values of 35 mg/l (SAC1, GFR, and GKS). GFB, GGQ and GI show lower values again. In the Malian zone the magnesium content as a mean value of 10 mg/l in ICT formation lower than the global Infra Cambrian in BKS, the lithology could be more siliceous or without dolomitic profile. In CTQ formation the values are similar.

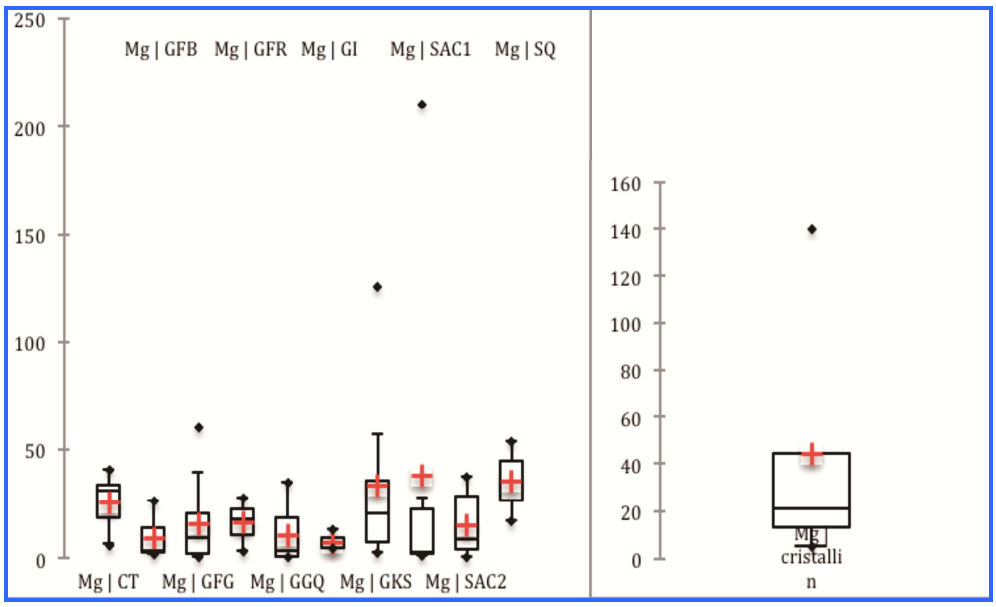

Figure 72: Variability and distribution of Mg in the different geological formations.

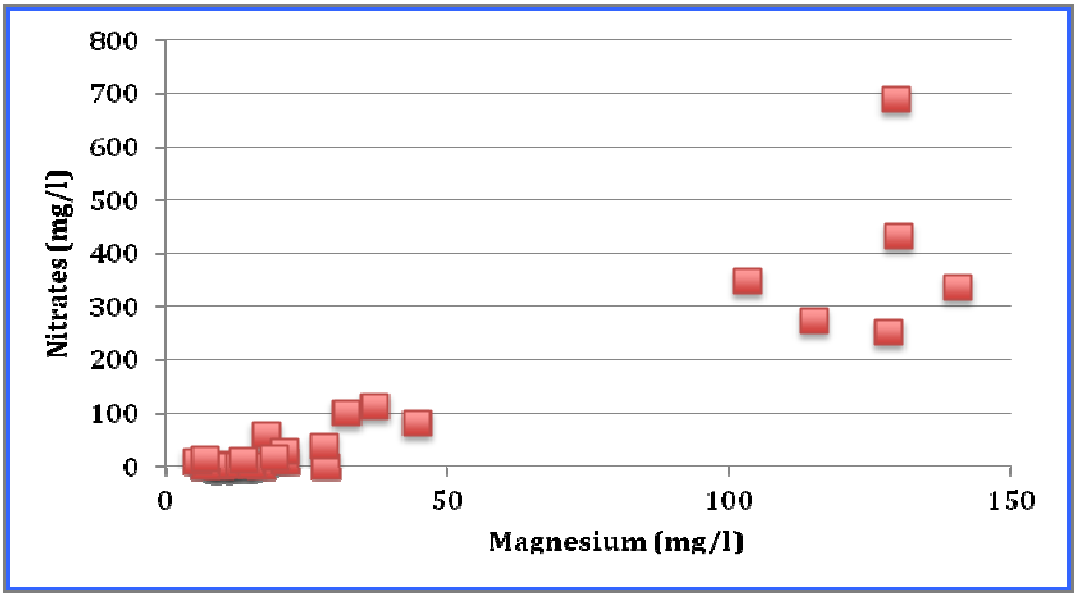

Figure 73: Relationship between magnesium and sulfate contents in the CT formation.

Sodium (Fig. 74) shows the highest contents in crystalline formations. In CT formation the level is low (mean of 7 mg/l) as well as the Infra Cambrian formations (2-10 mg/l) with higher content in GFR and GKS (15 mg/l) and a high variability. In GKS the samples with higher contents show higher chloride contents, due to anthropogenic influences (Valenza et al., 2000; Celle-Jeanton et al., 2009). Sodium contents show the same range of values in Malian zone for ICT and CTQ.

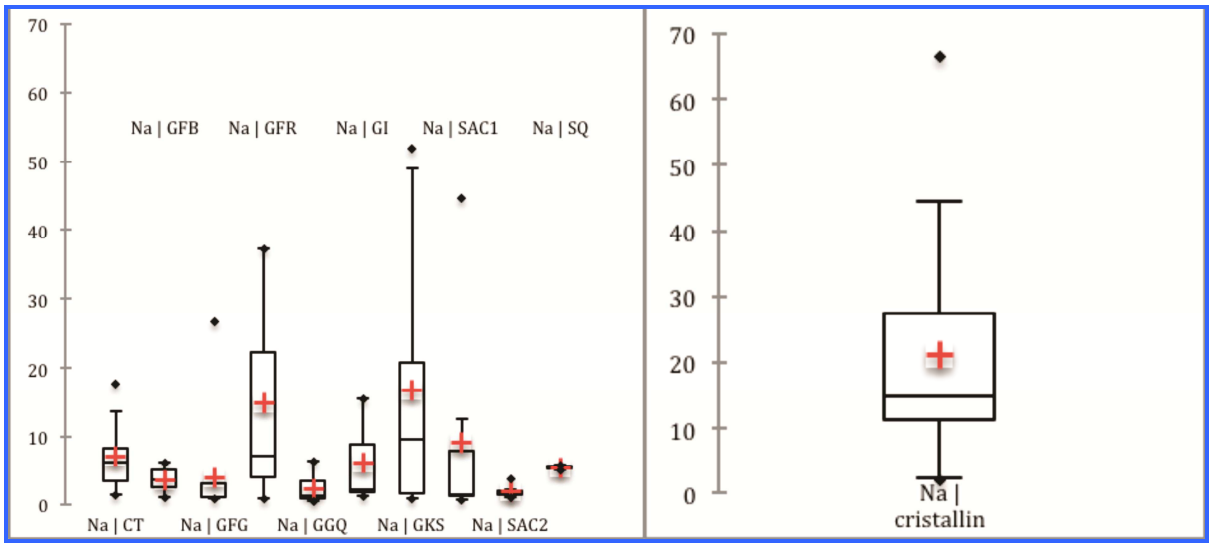

Figure 74: Variability and distribution of Na in the different geological formations.

-Potassium (Fig. 75) shows a general low level (median values smaller than 6.5 mg/l) in the whole formation with some samples (crystalline, GKS, GFG, SAC1, GFB) with content values between 25 and 190 mg/l and high values in nitrate and chloride which is the signature of anthropogenic influence. Potassium contents show the same range of values in Malian zone for ICT and CTQ.

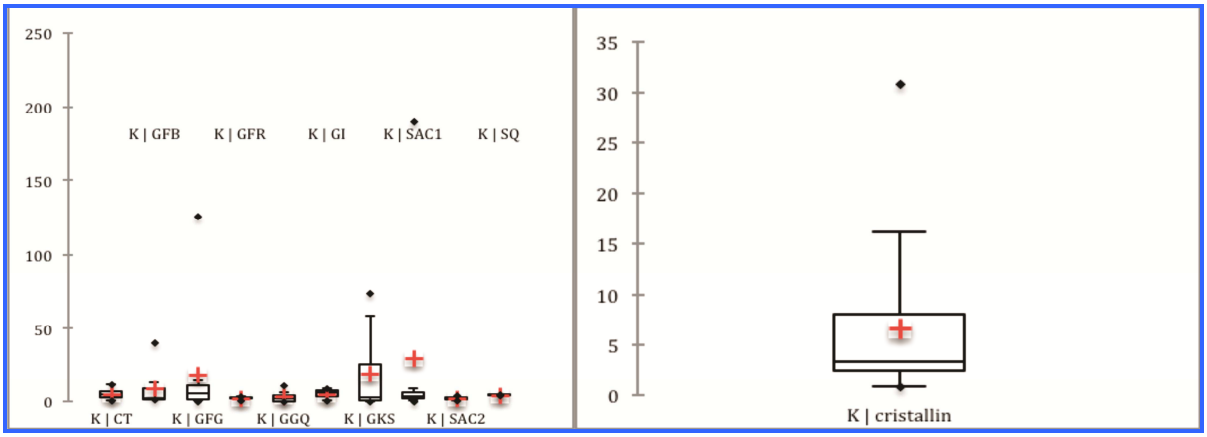

Figure 75: Variability and distribution of K in the different geological formations.

- Anions

Bicarbonate (Fig. 76) is the predominant anion in the ground waters with content exceeding 50 mg/l for 56% of samples and a high global variability (6 to 293 mg/l). In the same way that calcium and magnesium, the lowest values are in crystalline, GI and GFB formations. The values are similar in Malian zone in CT formation and lower than in Infra Cambrian formation (58 mg/l instead of 78 mg/l).

Chloride contents (Fig. 77) show low values (< 5 mg/l) as natural level, as shown. Above this limit, a strong correlation exists between chloride, nitrate, sodium and potassium linked mainly to an anthropogenic input. The crystalline formations are more affected and show 25% of samples with a level of chloride from anthropogenic origin (max. 111 mg/l).

-Sulfate excess in crystalline formations is an anthropogenic input as we have shown, CT formation is also impacted (Fig.78). In contrast, in the IC formation, only GKS, GFG, SAC1 and GFB are impacted with high content in sulfate and other anthropogenic inputs (nitrate, potassium, chloride), may be linked to a water level close to surface. Such pollutions are generally closely restricted around the well or borehole and are related to the very poor protection established around the pumping places (lack of any kind of protection area). In these spots it is common to find cattle watering places and latrines in boreholes vicinity. A few boreholes exhibit high concentrations of nitrate or sulfate (Figs. 79 and80). These concentrations are often related to the bad casing conditions of village wells and to contaminations via the infiltration and mixing with surface waters influenced by manure and wastewaters, since most of the sampled boreholes are located in villages and are used mainly for drinking water supply.

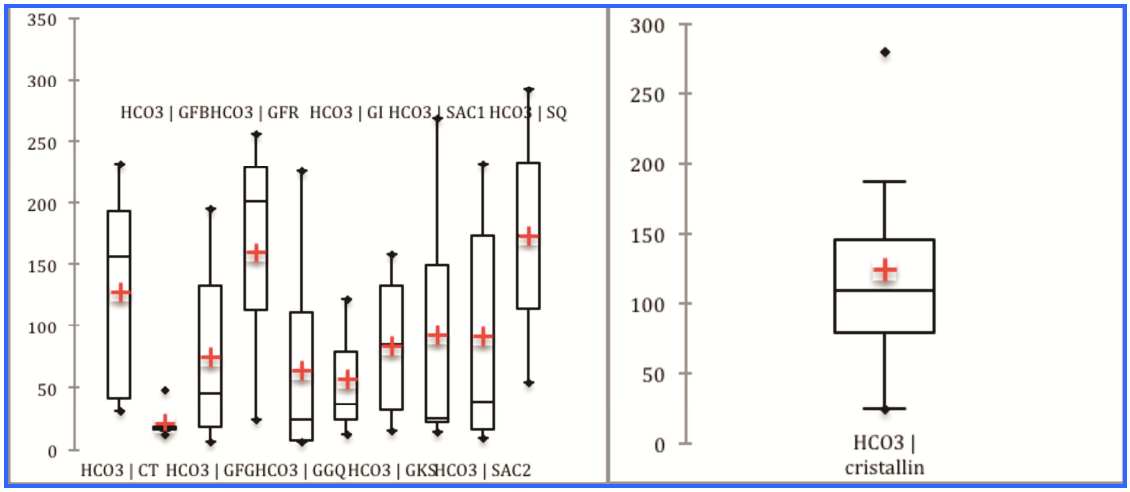

Figure 76: Variability and distribution of HCO_3 in the different geological formations.

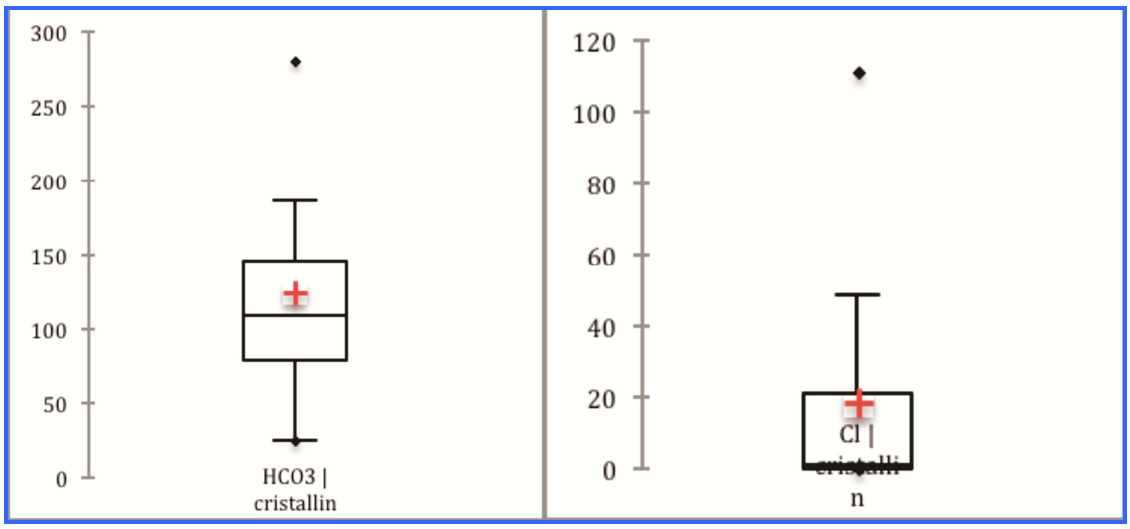

Figure 77: Variability and distribution of Cl in the different geological formations.

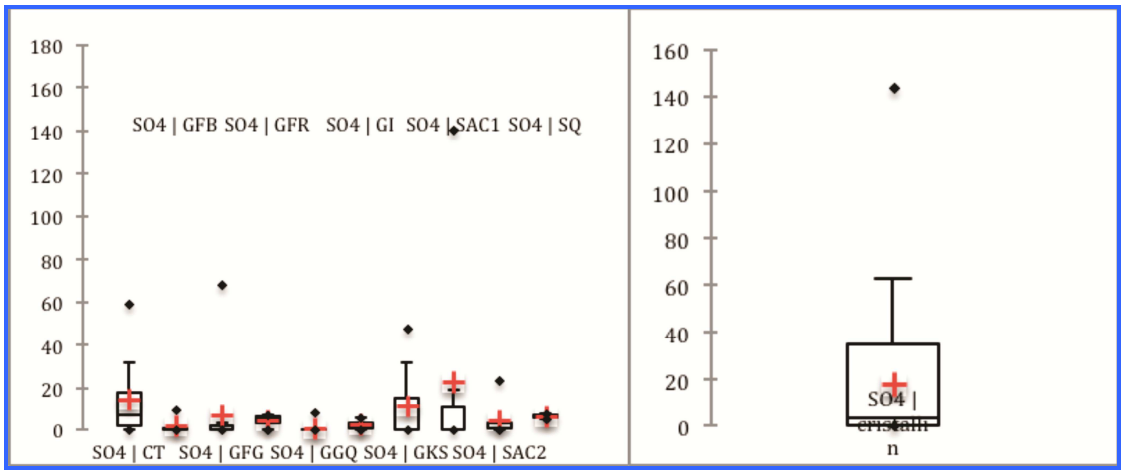

Figure 78: Variability and distribution of SO_4 in the different geological formations.

Nitrate contents in the study zone (Fig. 79) show a high variability, 43% of samples have nitrate content smaller than 10 mg/l, and 28% have values greater than 25 mg/l, with a maximum of 860 mg/l in SAC1 formation where it represents the major anion. GGQ, GFR and SAC2 formations do not show any nitrate contamination. Data from Huneau et al. (2011)

show high contents in nitrate for few samples, but the maximum value registered is only 160 mg/l.

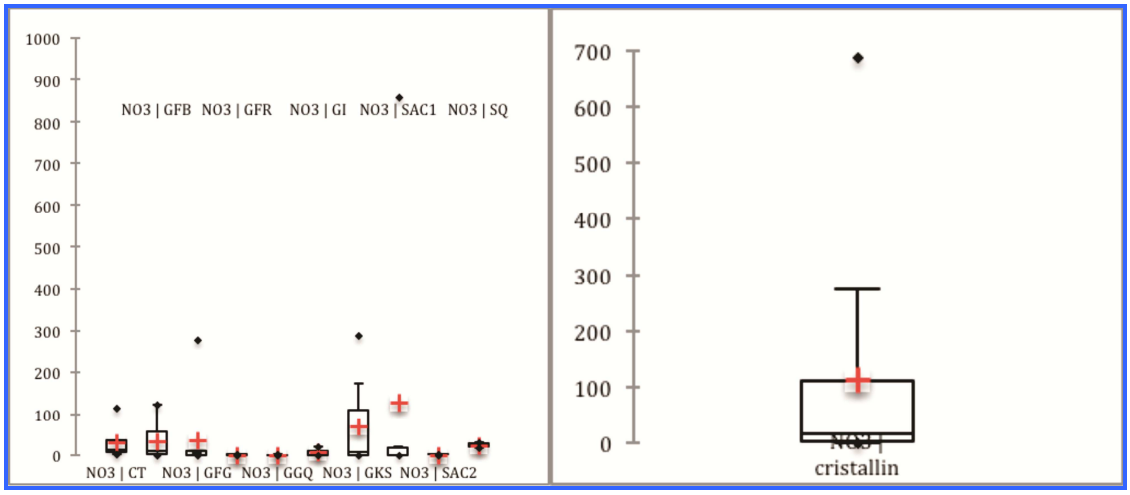

Figure 79: Variability and distribution of nitrate in the different geological formations.

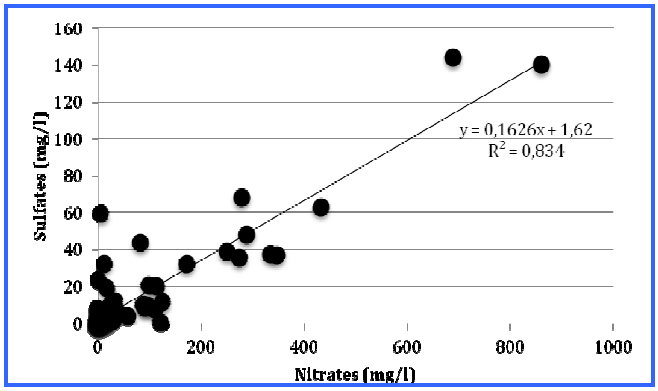

Figure 80: Relationship between NO_3 and SO_4 contents – all samples.

The silica content shows values between 2 and 51 mg/l, the highest values are found in the CT ground water but on average the crystalline ground waters show higher content s consistent with teir chemical composition (Fig. 81). In Infra Cambrian formation there is few variability between the various lithology. Silica content shows the same range of values in Malian zone for ICT and CTQ.

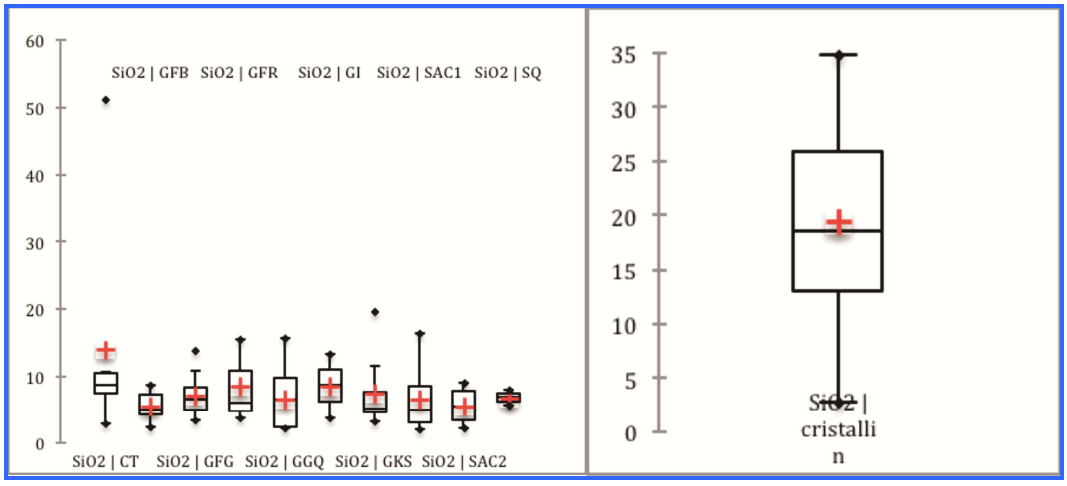

Figure 81: Variability and distribution of SiO_2 in the different geological formations.

- Water isotopes

The range of values in the whole aquifers is between -5.2 and -2.2 ‰ for oxygen-18 and -37.7 and -18.8‰ for deuterium (Fig. 82). In the same zone Huneau et al. (2011) reported values between -3.1 and -7.2‰ for oxygen-18 and -20.3 and -48.8‰ for deuterium.

The comparison of mean value for each group shows a low variability 1.0‰ (^{18}O) and 6‰ (^{2}H) and this value is consistent with the weighted isotopic value of annual rainfall. The variability observed for crystalline formations is low (-3.4/-5‰ in oxygen 18 and -20.1/-31.2‰ in deuterium) and is close to the current annual isotopic signal in rainfall, estimated around -4.4‰ ($\delta^{18}O$) and -26‰ ($\delta^{2}H$). The recharge process seems mainly not having sudden an evaporation process. The CT formation shows the highest variability but in the range of normal values found in superficial aquifer (-2.2/-5.3 ‰ in oxygen-18 and -18.8/-36.5‰ in deuterium). In Infra Cambrian formations values are very homogeneous, -4.5/-5.1‰ in oxygen-18 and -27.3/-32.6‰ in deuterium. By comparing with isotope contents in the Malian ICT part of the south eastern edge of Taoudeni basin, Malian values are more depleted with 73% of samples smaller than -5‰ (Annexes II), 4.5/-6.1‰ in oxygen-18 and -26.1/-40.8‰ in deuterium. The CTQ formation (closer part of BKF) shows a higher range with more depleted contents (max -6.0‰ in $\delta^{18}O$ and -38.0‰ in $\delta^{2}H$) and enriched contents (min -0.8‰ in $\delta^{18}O$ and -14.1‰ in $\delta^{2}H$). The enrichment is due to a shallow wells depth.

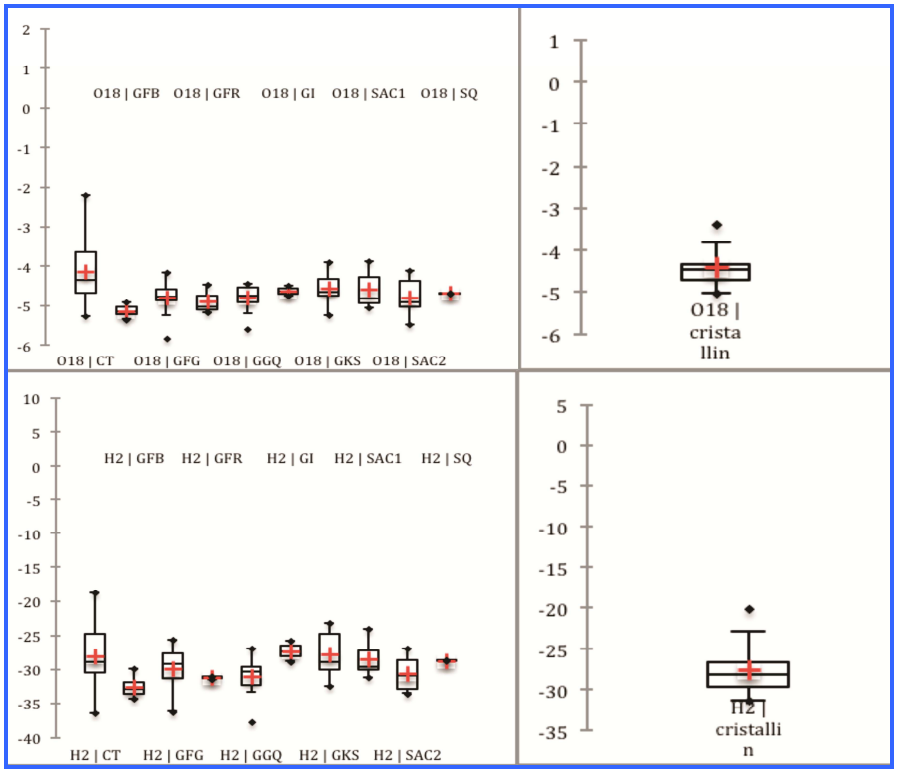

Figure 82: Distribution of ^{18}O and ^{2}H in the different geological formations.

The extensive study of Huneau et *al.*, (2011) used data (110 points) from previous IAEA projects carried out in the same zone between 1996 and 2003 (Fig. 83). Except GPS which show values more enriched (2‰ in $\delta^{18}O$), the distribution of isotope content is more or less similar in Infra Cambrian formations a few depleted in Huneau study. In CT formation samples are a little more depleted (1‰ in $\delta^{18}O$).

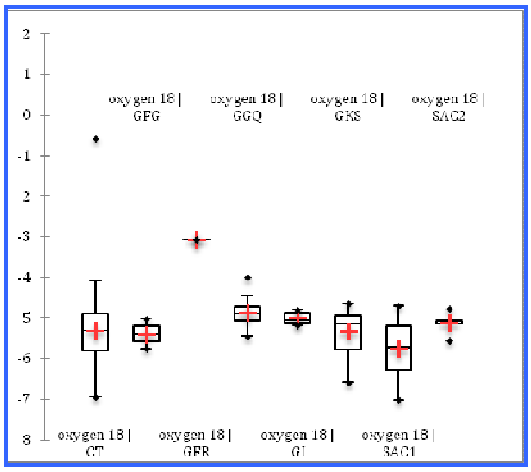

Figure 83: Distribution of $\delta^{18}O$ values in the different geological formations (Huneau et *al.*, 2011)

- Deuterium excess (d)

Water in the crystalline formations show 70% of samples (d > 8.0‰) without mark of evaporation, the others points show a slightly evaporation process, except one (d = 0.1‰) which seems questionable (Fig. 84). In CT formation all waters show an evaporation signature (d between 3.6 and 7.2‰) except one (d = -1.3‰), the well is 67 m depth and this data seems also questionable. In IC formations, deuterium excess are in the same range, 54 % of samples do not show an evaporation process, the others points show a very slightly evaporation (6<d<8‰), only 9 points (total number of samples: 59) show lower values between 4.3 and 6‰. In comparison with Malian zone, ICP and CTQ waters in BKF are less marked by evaporation process, due probably to a well depth higher.

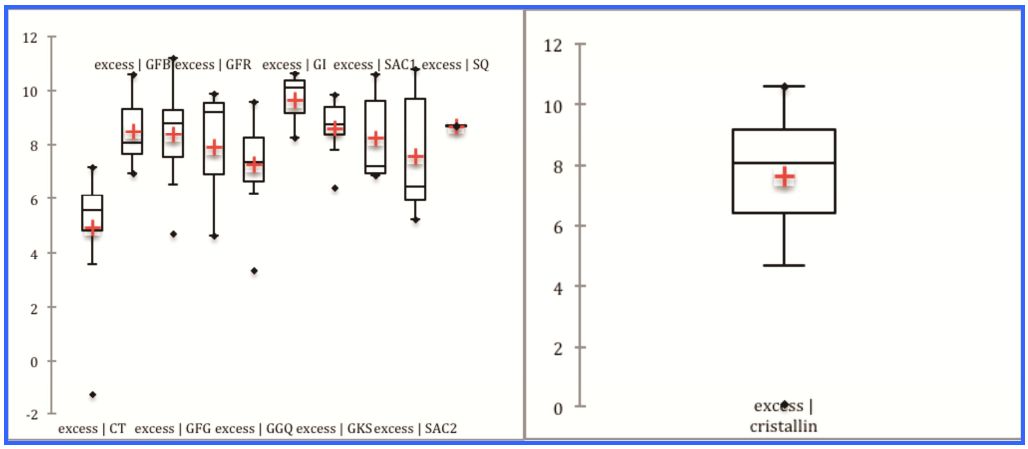

Figure 84: Distribution of deuterium excess values in the different geological formations.

- Tritium

Some tritium data are available (first campaign), 18 sites were sampled in crystalline formations, 28 in Infra Cambrian and 7 in the CT. Except one with value in the error measurements (B248-GGK) all samples show a tritium content. In crystalline formations, the Tritium contents vary between 0.6 and 4.9 UT; in CT formation between 1.2 and 4.9 TU and in Infra Cambrian formations between 0.5 and 8.7 UT, with some variations between them. GFR and SAC1 show lower and homogeneous values (Fig. 85). The samples in the others IC lithologies show a higher variation with values greater than 3 TU consistent with a significant current recharge as shown in discussion on data from Mali. With respect to data from Mali, CTQ shows a similar variation, ICT shows a higher variation (0.3-9.1 UT) in tritium and on average 1 TU higher. If we compare with data from old IAEA project used by Huneau et al. (2011), CT shows a higher variation with values greater than 6 TU (14 samples-max 13.3 TU) linked to recharge at the time of tritium peak period, the sampling is older than 10 years and to compare with our data it would be necessary to correct from radioactive decay (Fig. 86). In contrast the tritium values from Infra Cambrian show lower contents than our data of about 1 UT, in contradiction with a significant current recharge. The second campaign shows tritium values between 0 (8 samples) and 3.8 TU in groundwater samples, 4.5 TU (surface water) a variation smaller than the first campaign. A surface water (spring?) do not show tritium (C22).

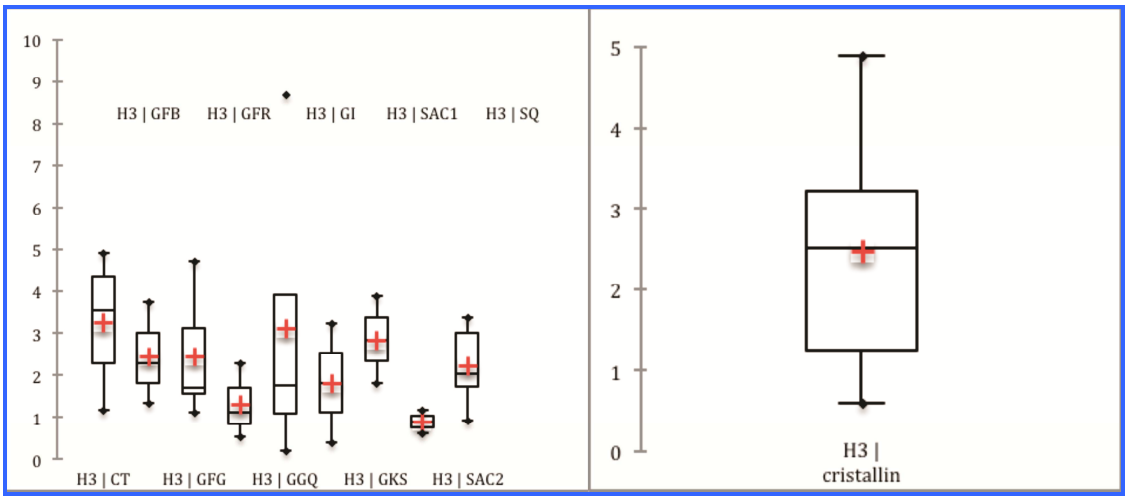

Figure 85: Distribution of tritium contents in the different geological formations.

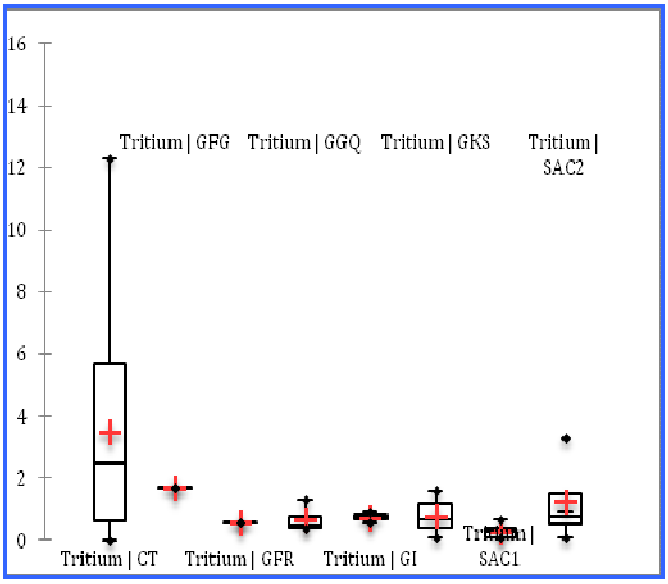

Figure 86: Distribution of tritium contents in the different geological formations (Huneau et al., 2011)

- Hydrochemical facies

The water chemistry expressed in meq/l is used to define chemical facies. Table 7 shows mainly HCO_3^- as the dominant anion and Mg^{2+} as the dominant cation for crystalline formations, all Infra Cambrian formations and Continental Terminal. In few samples, Ca^{2+} is dominant with HCO_3^- (Mg^{2+}) in IC and CT ground waters. When Na^+ and K^+ are dominant (2 samples) it is linked to a high anthropogenic contamination with high nitrate contents.

Table 7: Cation and anion contents expressed in meq/l.

	Ca^{2+}	Mg^{2+}	Na^+	K^+	HCO_3^-	SO_4^{2-}	Cl^-	NO_3^-
CRIST		25			21			4
GI		3			2			1
GKS		8			5			3
GGQ		10	1		11			
GFR	1	2			3			
SAC2		6			6			
GFG	2	10			9			3
SAC1	1	5		1	6			1
GFB		6	1		4			3
SQ		2			2			
CT	1	9			9			1

Nitrate is the dominant anion in some samples and mainly the second most abundant anion. These highest nitrate contents seem questionable, it is necessary to verify the sampling protocol (good sampling conditions, strictly observe cold chain integrity between the field and laboratory, sampling conservation in freezer or cold storage and chemical analysis within a reasonable time). The main risk with these climatic conditions (hot dry or hot humid) is the development of the algae or bacteria and the increasing of nitrate contents in water.

The Piper diagram with all the samples (Fig. 87) allows showing the main chemical facies characteristics. In contrast with Mali data, the water samples in BKS are gathered in a mainly chemical type HCO_3^- -Mg^{2+} and few points with a chemical type HCO_3^- -Ca^{2+}/Mg^{2+}. It is noted that there is a light evolution to waters more alkaline type. The diamond shape shows a high dispersion of ground water samples, but it is not due to particular mineral dissolution but due to the influx of nitrate and should be ignored to identify the geological dissolution processes. The waters in crystalline formations have a facies HCO_3^- -Mg^{2+}/Ca^{2+}/Na^+ showing the diversity of crystalline rocks more or less alkaline in the study zone. The facies in CT formation shows probably two components one HCO_3^- -Mg^{2+}/Ca^{2+} and the other HCO_3^- -Ca^{2+}/Mg^{2+} related to more or less dolomitic or calcic facies. The waters from Infra Cambrian (GKS, GFG, GGQ, SAC2, SAC1, and GFB) show an evolution from magnesium to magnesium-sodium/potassium. The main process is not the cation exchange but an anthropogenic evolution. For GKS (2 samples B221, B222) Na^+ , K^+, Cl^- and NO_3^-increasing, for SGFG (B249) Na^+, K^+, Cl^-, NO_3^- and SO_4^{2-} increasing, for SAC1 (B285) is similar, for GFB (B259, B261) increasing K^+, Cl^- and NO_3^-.

The samples from the 2nd campaign show more a mixing facies HCO_3^- -Ca^{2+}/Mg^{2+}, which can evaluate to more alkaline facies. We can note that nitrate can be reaching high level (311 mg/l) but lesser than the first campaign (sample problem in the first campaign?) and only 4 groundwater samples show high level. The surface waters show EC between 28-565 µS/cm (mean 140 µS/cm) and no obvious anthropogenic input (no or few nitrate, sulfate or chloride except A8 with a nitrate as dominant anion (16.5 mg/l).

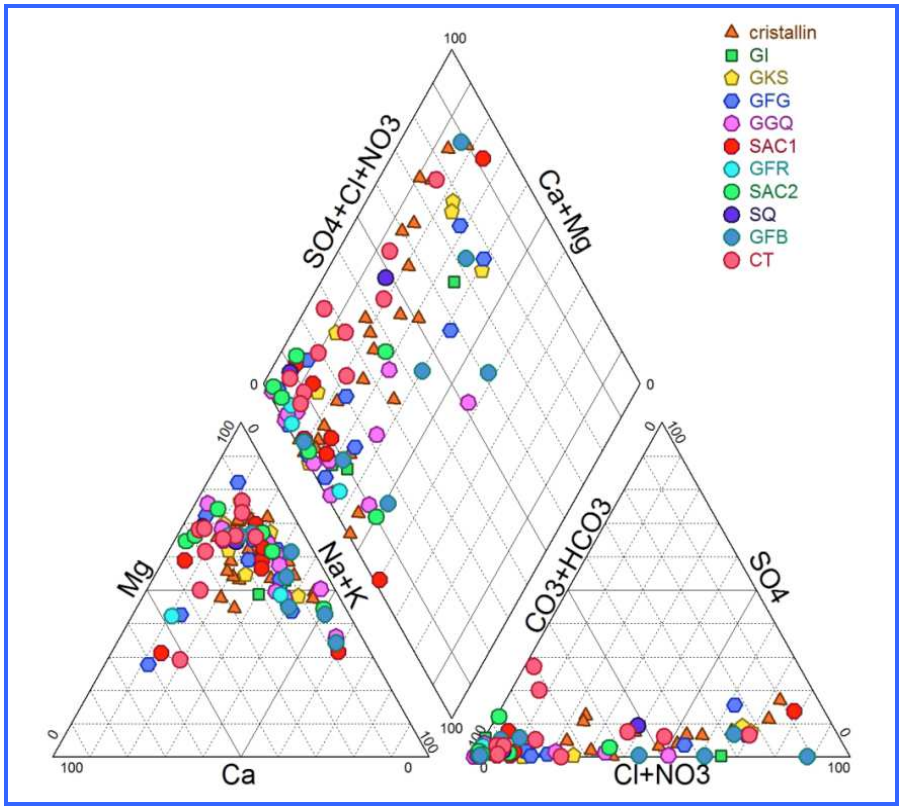

Figure 87: Piper diagram- all groundwater sampled

- Equilibrium between groundwater and minerals

With the software PHREEQC, it has been calculated the Saturation Index (SI) of water with respect to various classical minerals. It can be noted in the IAEA database there are total iron measurements with as result a systematic value of 0.01 mg/l. It is necessary to validate these measurements which seem questionable. With this value, waters show mainly an over saturation with respect to hematite and goethite. The others major minerals, which could interact in our geochemical environment, are calcite, dolomite and quartz.

The crystalline, ICT and CIT formations show ground waters mainly under saturated with respect to calcite and few samples show equilibrium (Fig. 88). In Infra Cambrian formation, the facies more siliceous show mainly lower values of SI with on average of -4.3 (GI, GKS, GGQ, GFB). It can be noted that the sample in equilibrium belongs to GGQ formation that shows there is no homogeneous lithology. With respect to dolomite (Fig. 89), more samples are in equilibrium, and the distribution is similar than calcite.

With respect to quartz most samples are in the stability zone, the main rocks in the study zone are composed by sandstones with quartz mineral inside or silica cement. Crystalline rocks and CT formations show some water over saturated with respect to dolomite. Inside Infra Cambrian formations more siliceous GI, GGQ and GFG show a higher SI (Fig. 90).

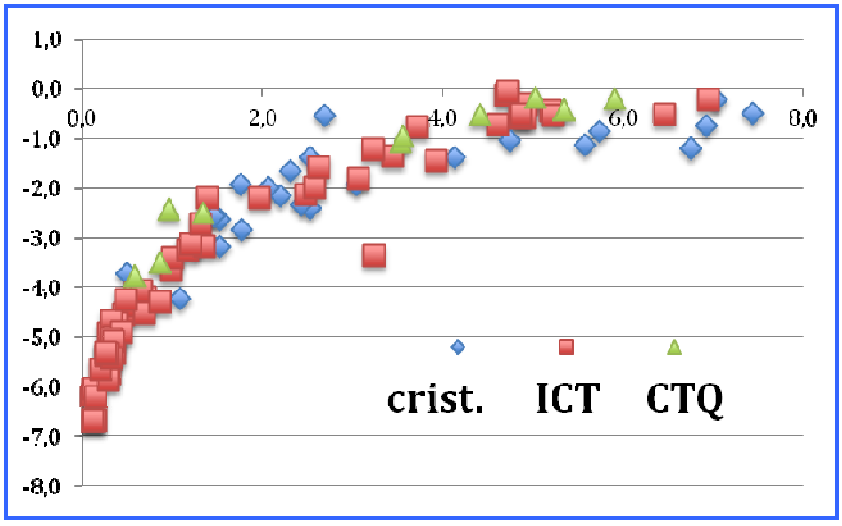

Figure 88: Saturation index of groundwater samples with respect to calcite

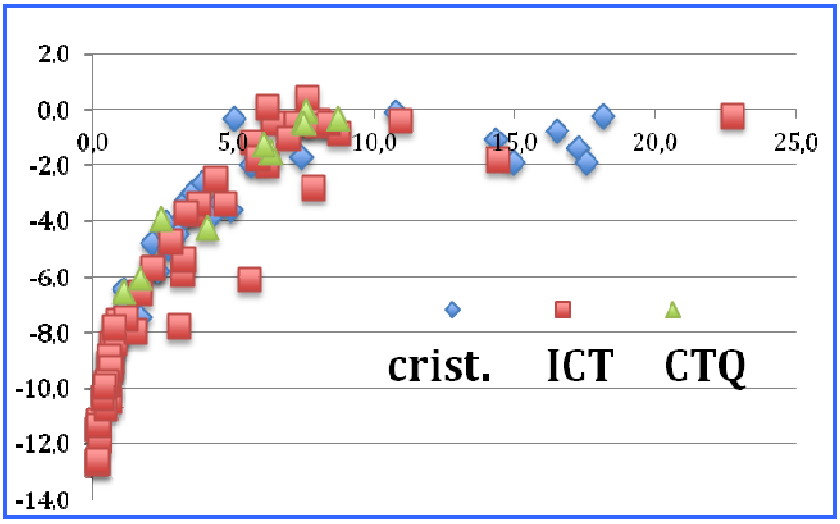

Figure 89: Saturation index of groundwater samples with respect to dolomite

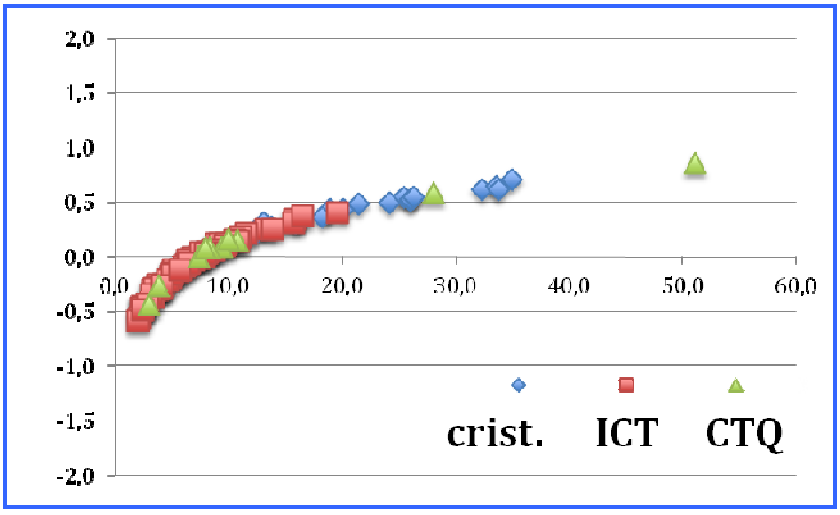

Figure 90: Saturation index of groundwater samples with respect to quartz.

Figure 91 shows the equilibrium state of waters with respect to silicate minerals. The water mainly is in equilibrium with kaolinite towards an evolution to smectite clays domain or feldspar. This evolution is shown mainly for waters from CT and crystalline formations. The

waters from Infra Cambrian are distributed in the graphic, inside it is not so obvious to separate groups with respect to lithology.

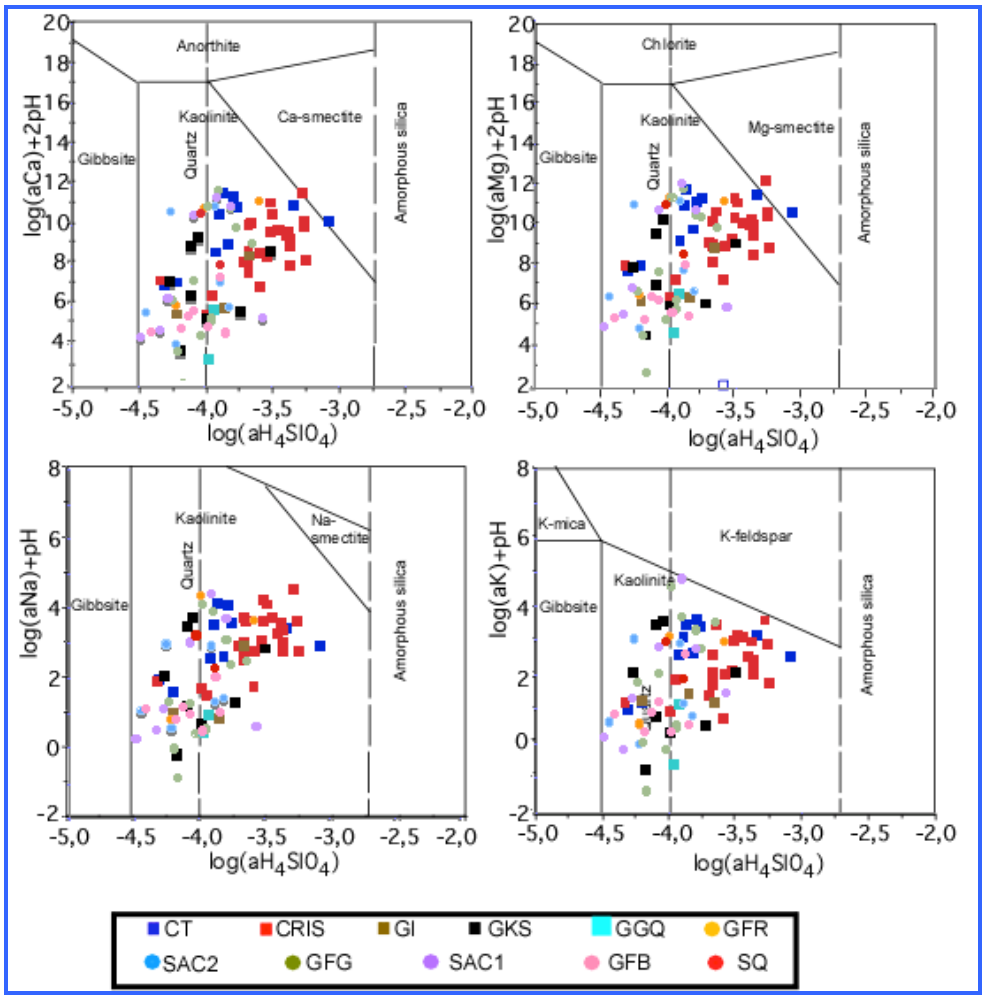

Figure 91: Korjinsky diagram, stability field diagram of silicate minerals.

- Multi correlation analysis

The results are presented in Table 8 and Figs 92 and 93 (complete analysis on 49 observations).

Table 8: Total variance measured by axis

	F1	F2	F3	F4	F5
Value	7,049	2,755	1,601	1,355	1,187
Variability (%)	44,056	14,758	11,078	6,702	5,776
Cumulative percentage	44,056	58,804	69,882	76,583	82,359

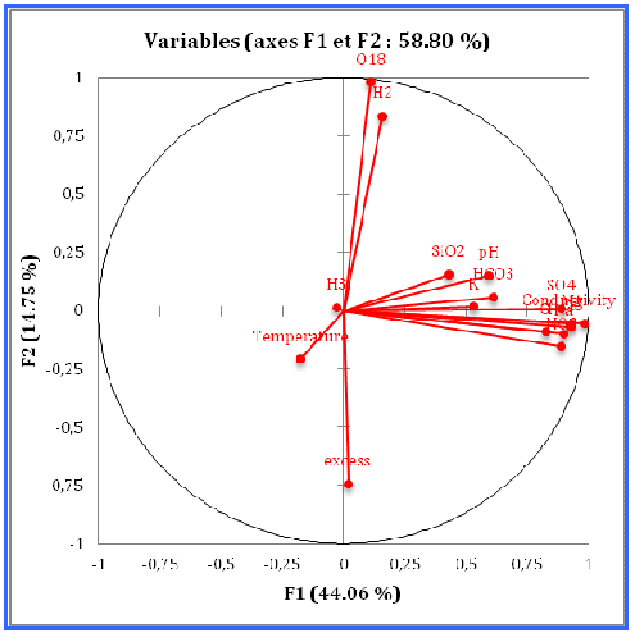

Figure 92: Principal component analysis of groundwaters (parameters).

F1 represents the mineralization but in relationship with contamination nitrate and sulfate in ground water and F2 the water stable isotopes and in opposite correlation the deuterium excess. F3 does not add new information.

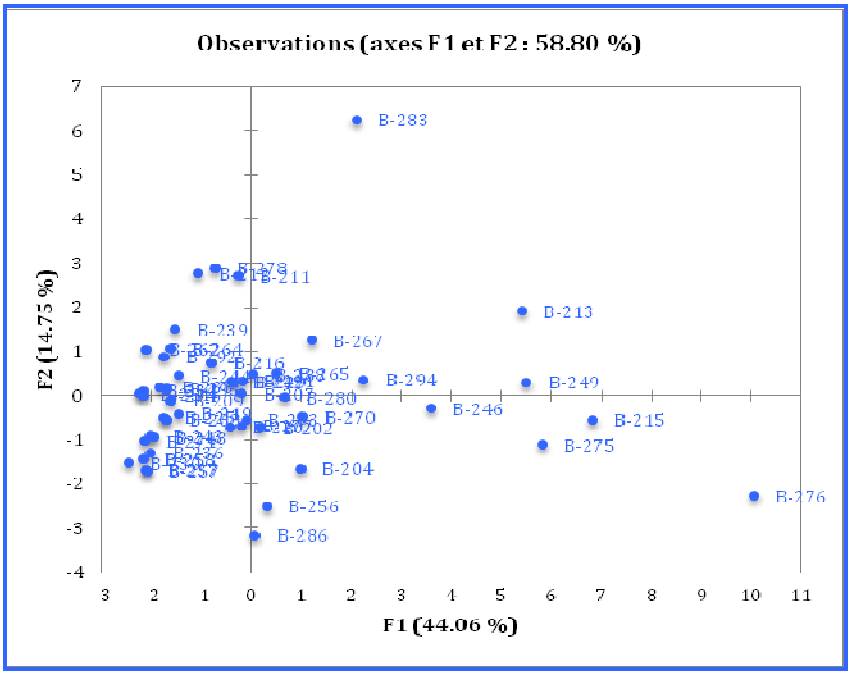

Figure 93: Principal component analysis of groundwaters (samples).

Two groups of samples can be identified separately for each axis depending on F1, F2 parameters. F1 shows the samples more mineralized and F2 the samples which show the most enriched isotopic values and as a result a deuterium excess lower. PCA does not make distinction with respect to the geological formations which are mainly similar in term of geochemistry.

-Spatial distribution of parameters in groundwaters (preliminary work)

Maps are presented according to geological formation, crystalline formations, Infra Cambrian formation and CT formation and detailed maps for all lithology of Infra Cambrian. There are no spatial pattern observed in crystalline aquifers, it seems obvious that due to the variety of mineralogy, structure, faults in the zone, the aquifers are discontinuous and the variability of chemical parameters depends on local conditions especially with the contamination process. However the impact of contamination seems higher in northern part with chloride, sulfate and nitrate higher than in southern part where 65% of points do not show any contamination. Isotope data in northern part samples are somewhat more depleted and deuterium excess slightly greater, wells depth is similar in northern and southern part, may be the slightly evaporation process observed in southern zone is due to infiltration conditions less favorable. It is noted that tritium follows the same pattern, in northern zone tritium contents have a mean value higher (3.5 UT) than in southern part (1.8 UT). Stable isotopes and tritium are showing a similar trend toward hydrodynamic conditions allowing a more efficient recharge in the northern part. Obvious it is a preliminary interpretation, but with carbon 14 analysis could be confirm this hypothesis.

The 10 samples of CT do not show any pattern with chemistry or isotope data, the number of points is not enough for trends. Comparing with Malian data from CT, it is noted differences surprising, on both side of the border. EC is higher in Malian zone with 60% of values greater than 500 µS/cm (500-2000 µS/cm), in BKF zone 30% (500-900 µS/cm), pH neutral in BKF and mainly basic in Mali (>8-11), nitrate higher in BKF, more depleted in oxygen 18 in Mali and more Tritium in BKF (mean 3.3 UT), in Mali 25% of sample do not have tritium. At that time no interpretation seems possible to explain these high differences.

The water from the Infra Cambrian formation shows a spatial structuration SW-NE, consistent with the direction flow established by Dakouré (2003) with potentiometric map. EC is higher in northern part, pH more basic in northern part. If the spatial pattern of stable isotope does not show clearly a trend, the deuterium excess clearly shows values lower from west southern zone to east northern zone, there is no correlation with wells depth. Tritium does not show any particular pattern. The spatial maps of chloride, sulfate and nitrate show the same structuration as a result of a unique contamination process. Comparing with Malian data from ICT, EC is higher in BKS 300-2000 µS/cm (in Mali 0-200 µS/cm), pH is similar, stables isotopes and deuterium excess are similar. Tritium shows in Mali on average higher values.

- Isotopic results and discussion

• Isotope contents in groundwaters

To complete and finalize the discussion about isotope contents in groundwater, we have compared isotope contents in current rainfall (see Mali discussion) and isotope contents in the different geological formations (Fig. 94).

With an estimated inter annual isotope content of -4.4 ‰ ($\delta^{18}O$) and -25.8‰ ($\delta^{2}H$) in rainfall, rainfall isotopes are enriched with respect to 73 % of groundwater samples (min -5.84 ‰/-36.2‰) for the first campaign and 63/% for the second campaign (min -6.48 ‰/-38.0‰). With respect to Malian data, they are less depleted but more depleted that the reference rainfall isotopes values. The data used by Huneau et al. (2011) in the same zone show more depleted values with 92% of the samples presenting < - 4.4‰ and a min of -7.2‰, The isotope problem between current rainfall and groundwater is therefore similar, it does not seem consistent. Regarding with deuterium excess, the same conclusion than Mali data can be done, with an excess too low. In the second campaign some samples the more enriched > -2‰ (^{18}O) correspond to surface sampling with maximum isotopic values (2.91 ‰/6.5‰).

Other aquifer multilayers CT in the same latitude located in Niger shows waters from shallow aquifer (CT3) right aligned on the Local Meteoric Line (LML close to GMWL) with a dispersion about 1.5‰ around the inter annual isotope rainfall value (-4.5‰ $\delta^{18}O$ and -28‰ $\delta^{2}H$) and a groundwater range between -5.8‰ and -2.9‰ in ^{18}O and -39‰ and -21‰ in ^{2}H, mean values are -4.7‰ and -30‰, respectively (Favreau et al., 2000). This aquifer shows in 1993 values between 0.8 and 20 TU (Leduc et al., 1997) and ^{14}C activities of DIC from 60.4 to 97.1 pmc, for a mean value of 83.4 (Favreau et al., 2002). In confined aquifer (CT2 and CT1) the mean value in oxygen 18 is -7.5‰ ± 0.2% and deuterium-58 ± 1‰ with low values in carbon 14 < 5pmc (recharge during LGM) and a deuterium excess of 2.6‰ (Le gal La Salle et al., 1994). A mixing between the superficial aquifer and the deeper aquifer could explain then the isotopic context of groundwater. However data used by Huneau et al. (2011) show carbon 14 values from 1 to 122 pmc (mean value of 83.4 pmc) and in a graph oxygen 18 *vs* ^{14}C, there is an opposite trend, with values more depleted currently (Fig. 95).

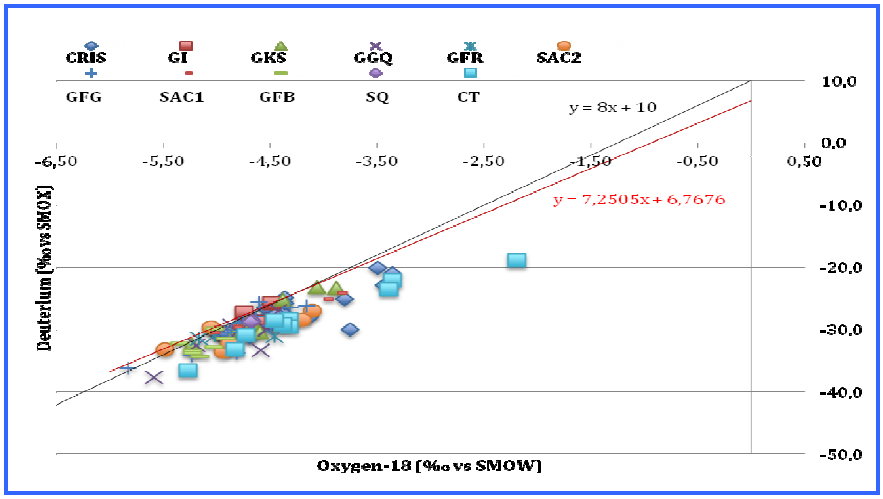

Figure 94: Relationship between oxygen-18 and deuterium in ground water samples (campaign 1).

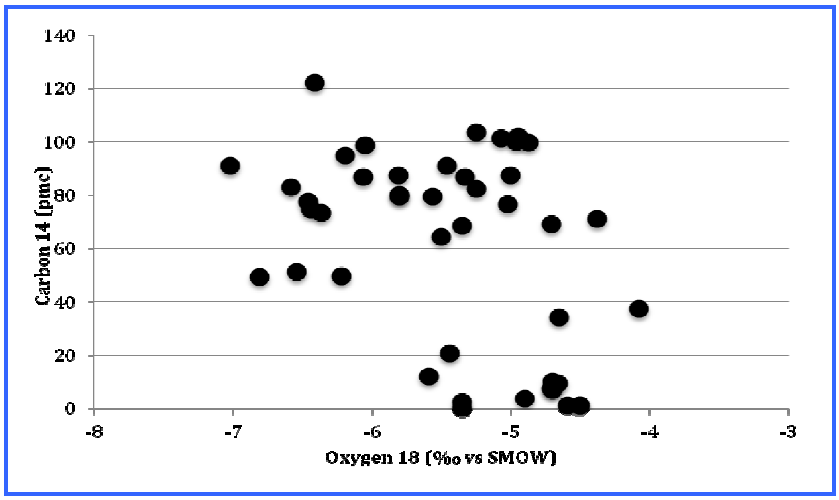

Figure 95: Relationship between oxygen-18 contents and carbon-14 activities in groundwater samples (Huneau et *al.*, 2011).

- **Isotope contents in surface waters**

The isotope values vary from -5.34/2.91‰ for oxygen-18 and -31.4/6.6‰ for deuterium. In the oxygen 18 vs deuterium graph the different points are in line which shows an evaporation process (marked in particular with points > -4‰ for oxygen-18 (Fig.96).

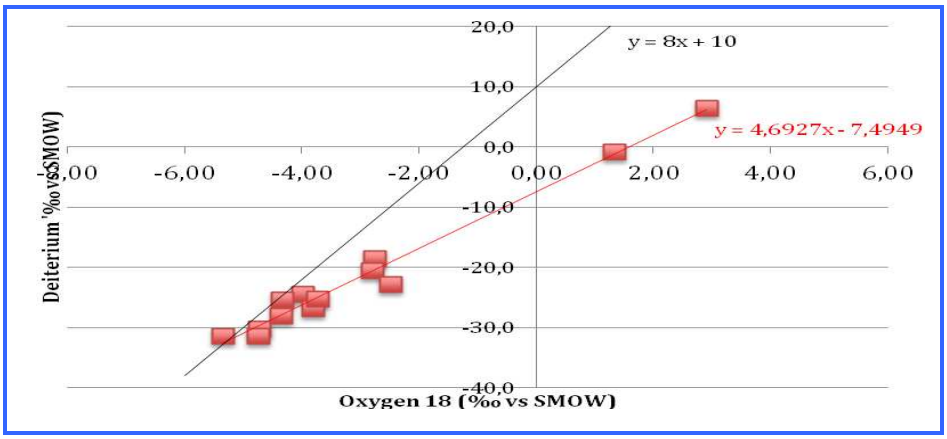

Figure 96: Relationship between $\delta^{18}O$ and $\delta^{2}H$ contents in surface waters (campaign 2).

5. CONCLUSIONS

This report is a first synthesis of the IAEA-supported project RAF/7/011 to improve the knowledge of this shared groundwater. It is the main water reservoir available in the western and northern part of this basin where climatic conditions are arid and rainfall and surface flow are low and very temporary. Three countries (Mauritania, Mali and Burkina Faso) take part in this project with objectives and involvements different due to other zone investigation inside the RAF/7/011 project.

In Mauritania, the results are preliminary and incomplete. There is no chemical data besides the field measurements but some results are available from the first campaign related to stable isotopes and tritium analysis. The methodology used in the two campaigns was a sampling according to the theoretical flow direction in two adjacent zones. Unfortunately no geological interpretation is available which could allow comparing the two campaigns which show a difference of pH very high. It is probably due to a geological layer different with possibly two aquifers system. Further, it is unfortunate that no detailed information is available about the potentiometric surface of the aquifer. Nevertheless, this project is new, with a new knowledge in this zone on mineralization and recharge condition. Isotope results have given some interesting results on the possibility of local current recharge, possibly weak but in terms of water resources management it is an important fact.

In Mali, the sampling was very extensive with 4 different geological formations studied (Continental terminal, Continental Intercalaire, Cambrian, and Infra Cambrian). The key output of project was to do a first investigation in the western part of Mali and a more detailed in eastern part where the known context is better because many studies were done at a high level. Geological, chemical, isotopic and hydrodynamic data are available with some first local model proposed. Some interesting results were obtained about groundwater chemistry. It is mainly HCO_3-Ca in ICT, ICP and CTQ waters. Concerning, CAM and CIT formations, it is noted a higher chemical variation with some facies as HCO_3-Na and SO_4-Na. A cation exchange process has been identified in the most aquifers. The other result is the generalized contamination with nitrate, only few points present a low natural level.

The isotope results show a significant Tritium content, in the most wells, suggesting a recent recharge. The water stable isotopes are more depleted with lower deuterium excess comparing the current isotope content of rainfall.

In Burkina Faso, the study zone is smaller (eastern edge of Taoudeni basin). The main results present a homogeneous groundwater chemical facies HCO_3-Mg with a small evolution to HCO_3-alcaline facies, which is not linked to a cation exchange process but to a high level of contamination by nitrate and also by potassium, chloride, sulfate and sodium.

Isotope results show the similar stable isotopes signature of groundwater as in Mali, with more depleted values and a lower deuterium excess than present day rainfall. Previous studies demonstrate the existence of high to very low recharge depending on the Infra Cambrian lithology with carbon 14 activities ranging between 1 to 122 pmc.

Recommendations

One of the final goal of this project is to optimise management of groundwater, to avoid a decreasing water level in the use of this resource in climatic change context and all problems associated like contamination and salinization.

The following recommendations are suggested:

- The implementation of public policy in national and regional levels to ensure a better management of groundwater resources (extracted quantity and quality of water) about reforestation, new farming techniques, decrease of irrigated crops, optimal use of surface and ground waters, protection zone around wells and boreholes, wastewater treatment plants...

- To improve surveys from hydrogeological public institutes with capacity (GIS, numerical tool, analytical apparatus...), field material acquisition (DGPS, continuous measurements of water level..) in order to improve the geological knowledge of the studied formation, to homogenize the lithology classification (a common geology and its continuity) and to define shared aquifer in space and depth.

- Implementation of piezometers and monitoring of long term network. This will allow a better comprehension of local and regional hydrodynamic; identify possible interaction between aquifers, determine flow direction and hydrodynamic parameters.

All this information is necessary to elaborate a common hydrogeologic model and forward a numerical model for each reservoir.

- Dating groundwater (^{14}C, ^{36}Cl) in order to better evaluate the residence time.

- Comparison of recent results with previous studies which will strengthen the hydrodynamic interpretation, allow to highlight any geochemistry evolution of groundwater (increase of anthropogenic contribution for instance) and to detect any anomalies in sampling or analysis. It is necessary to integrate the old chemical and isotopic results in common database.

- To enhance synergy between counterparts in particular in areas where the shared aquifer is over exploited (case of eastern part of Taoudeni Basin between Mali and Burkina Faso).

6. REFERENCES

Note: Some references above are not in the text and concern general environmental parameters at the country scale

Alpha A., Traoré A.Z., Mariko A., Banton O., Villeneuve J.P., Ait-Ssi L., 1991. Hydrogéologie et contamination de la nappe phréatique alimentant la ville de Bamako. Rapport des des travaux réalisés dans le cadre d'une subvention du Centre de Recherches pour le Développement International du Canada (CRDI) Ottawa, Canada.

Antea Group and JMB-Consult, 2012.GEstion intégrée et concertée des ressources en eau des systèmes aquifers d'Iullemeden, de Taoudeni/Tanezrouft, et du fleuve Niger. Rapport de synthèse hydrogéologique. Rapport OSS-GICRSAIT n°12.

Antea Group and JMB-Consult, 2012. GEstion intégrée et concertée des ressources en eau des systèmes aquifers d'Iullemeden, de Taoudeni/Tanezrouft, et du fleuve Niger. Rapport de synthèse hydro-climatologique. Rapport OSS-GICRSAIT n°12.

Antea Group and JMB-Consult, 2013. Gestion intégrée et concertée des ressources en eau des systèmes aquifers d'Iullemeden, de Taoudeni/Tanezrouft, et du fleuve Niger. Rapport de synthèse Télédetection. Rapport OSS-GICRSAIT n°13.

Auvray C., 1960. Monographie du Niger,B: la cuvette lacustre. Paris, Orstom, 12-45.

BEATH, 1995. Gestion des ressources en eau en Mauritanie. Gestion des Ressources en Eau en Mauritanie (Ministère de l'Hydraulique et de l'Energie - OMVS - UNDP, 1995, 56 p.

Bertone F., Ph. Renard, J. Kerrou, P. Moix2 & P., 2007. Perrochet, An assessment of the groundwater resources in the western margin of the Taoudeni basin, Mauritania Aquifer systems management Garcy's legacy in a world of impending water shortage. Hydrogeology, 10, 149-160.

Beyerle, U., Rueedi, J., Leuenberger, M., Aeschbach-Hertig, W., Peeters, F., Kipfer, R., Dodo, A., 2003. Evidence for periods of wetter and cooler climate in the Sahel between 6 and 40 kyr BP derived from groundwater. Geophys. Res. Lett. 30, 1173.

Boulet R,1976. Notice des cartes de ressources en sols de la Haute-Volta. ORSTOM, Paris. 97 p.

British Geological Survey, 2002. Groundwater Quality: Burkina Faso. NERC 2002.

British Geological Survey, 2002.Groundwater Quality: Mali. NERC 2002.

Bureau hydrologie ORSTOM, 1981.Atlas hydrologique de la Mauritanie, ORSTOM.

Carl Bro – DHI – IWACO, 2001. État des lieux des ressources en eau du Burkina Faso et de leur cadre de gestion. Ministère de l'Environnement et de l'Eau, Secrétariat Général, Direction Générale de l'Hydraulique.

Celle-Jeanton, H., Travi, Y., Loye-Pilot, M.D., Huneau, F., Bertrand, G., 2009. Rainwater chemistry at a Mediterranean inland station (Avignon, France): local contribution versus long range supply. Atmos. Res. 91, 118–126. doi:10.1016/j.atmosres.2008.06.003.

Coulibaly A., 2003.Profil fourragerMALI. Rapport FAO.

Dakouré, D., 2003. Etude hydrogéologique et géochimique de la bordure sud-est du bassin sédimentaire de Taoudeni (Burkina-Faso, Mali), essai de modélisation. Thèse de Doctorat, Université Pierre et Marie Curie UPMC, 222p.

Dakouré D., 2010.Multi-disciplinary approch to improve the knowledge of southeastern border of Taoudeni sedimentary basin.International Conference "Transboundary Aquifers: Challenges and New Directions" (ISARM2010).

Dhaoui Z., Zouari K, Taupin J-D., Farouni R., 2016. Hydrochemical and isotopic investigations as indicators of recharge processes of the Continental Intercalaire aquifer (Eastern piedmont of Dahar, southern Tunisia). Env. Earth Sc., 75, DOI 10.1007/s12665-016-5990-x.

FAO, 2014.Stratégie et Plan d'Action de mise en oeuvre de l'Initiative de la Grande Muraille Verte. Rapport.

Friedel M.J. and Finn C., 2008.Hydrogeology of the Islamic Republic of Mauritania.Open-File Report 2008–1136, U.S. Geological Survey.

Favreau G., Leduc C., Marlin C., Dray M., Taupin J.D., Massault M., Le Gal La Salle C. and Babic M., 2002. Estimate of recharge of a Rising Water-Table in Semiarid Niger from ^{3}H and ^{14}C Modeling. Groundwater, vol. 40, nº2, 144-151.

Fews Net, 2012. A Climate Trend Analysis of Burkina Faso. Fact Sheet 2012–3084 USGS.

Fontes, J.-C., Andrews, J.N., Edmunds, W.M., Guerre, A. and Travi, Y., 1991. Paleorecharge by the Niger River (Mali) deduced from groundwater geochemistry. Water Resources Research 27: doi: 10.1029/90WR01703. issn: 0043-1397.

Fontès J. and Guinko **S.** (1995).*Carte de la végétation et de l'occupation du sol du Burkina Faso. Notice explicative.* Toulouse, Institut de la Carte Internationale de la Végétation ; Ouagadougou, Institut du Développement Rural - Faculté des Sciences et Techniques, 67 p

Garcia M G, De Hidalgo M, Blesa M A (2001) Geochemistry of groundwater in the alluvial plain of Tucuman province Argentina. J Hydrol, 9, 597-610.

Gasse, F, 2000. Hydrological changes in the African tropics since the Last Glacial Maximum. Quat. Sci. Rev. 19, 189–211.

Gombert, P., 1998. Synthèse sur la géologie et l'hydrogéologie de la série sédimentaire du sud-est du Burkina Faso. Rapport technique, Programme RESO, ATG, IWACO, Ouagadougou.

Gourcy, L., Aranyossy, J.F., Olivry, J.C., Zuppi, G.M., 2000. Space and time variations in the isotopic composition ($\delta^{2}H$–$\delta^{18}O$) of Niger inland delta water (Mali). C. R. Acad. Sci. Paris, Earth Planet Sci., 331, 701–707.

Groen, J., Schuchmann, J.B. and Geirnaert, W. 1988. The occurrence of high nitrate concentration in groundwater in villages in northwestern Burkina Faso.Journal of African Earth Sciences, 7, 999-1009.

Guiguen N ; 1985. Etudes hydrologiques complémentaires de la cuvette lacustre du Niger, Rapport final. Autorité du bassin du Niger, projet Hydroniger, Orstom, Bamako, 71 p.

Hoerling, M., J. Hurrell, J. Eischeid, *and* A. Phillips *(*2006*),* Detection and attribution of twentieth-century northern and southern African rainfall change, J. Clim., 19, 3989–4008.

Hottin G. and O F. Ouédraogo,1976. Map Upper Volta. Direction de la géologie et des mines. France, BRGM.

Kagone I. H., 2001.BURKINA FASO FAO, Country Pasture/Forage Resource Profiles.FAO report.

Huneau F., D. Dakoure, H. Celle-Jeanton, T. Vitvar, M. Ito, S. Traore, N.F. Compaore, H. Jirakova, P. Le Coustumer, 2011.Flow pattern and residence time of groundwater within the south-eastern Taoudeni sedimentary basin (Burkina Faso, Mali). Journal of Hydrology, 409, 423–439.

IWACO, 1989. Etude du bilan d'eau du Burkina Faso - Tome 2 : Inventaire des ressources en eau, Ministère de l'Eau.

Jerzykiewicz T., 2011. Geology of the southern margin of the Taoudeni basin (Bamako area Progress Report (Mali), June-July 2011 (Geoclastica Consulting Ltd).

Koussoubé Y., 2010. Hydrogéologie des series sédimentaires de la depression piézométrique du Gondo (Bassin du Gourou)- Burkina Faso / Mali. These UPMC.

Koussobé, Y, Upton, K, and Ó Dochartaigh, B É. 2016. Africa Groundwater Atlas: Hydrogeology of Burkina Faso. British Geological Survey.
http://earthwise.bgs.ac.uk/index.php/Hydrogeology_of_Burkina_Faso.

Lebel, T. and Ali, A., 2009. Recent trends in the Central and Western Sahel rainfall regime (1990 - 2007). J. Hydr., 375(1-2) p. 52-64.

Leduc C., Taupin J.D. et Le Gal La Salle C., 1996. Estimation de la recharge de la nappe phréatique du Continental Terminal (Niamey, Niger) à partir des teneurs en tritium. C. R. Acad. Sci. Paris, t.323, série IIa, p. 599-605.
Leduc C., G. Favreau, P. Schroeter, 2001. Long-term rise in a Sahelian water-table: the Continental Terminal in South-West Niger. J. Hydr., 243, 43-54.

Le Gal La Salle C. & J-C. Fontes, J. N. Andrews, P. Schroeter & Atahiro Karbo, K. L. Futeld, 1995. Old groundwater circulation in the lullemeden basin (Niger): preliminary results of an isotopic study. Application of Tracers in Arid Zone Hydrology (Proceedings of the Vienna Symposium, August 1994. IAHS Publ. n°.232, 129-139.

Lepretre R., 2015.Evolution phanérozoïque du Craton Ouest Africain et de ses bordures Nord et Ouest. Thèse Université. Paris Sud.

Mahé, 2009.Surface/groundwater interactions in the Bani and Nakambé tributarie of the Niger and Volta basins, West Africa. Hydrological Sciences Journal-, 54 (4 Special issue: Groundwater and Climate in Afric), p. 704-712. ISSN 0262-6667.

Mc Sweeney C., M. and G. Lizcano1, 2006.Climate Change Country Profiles Mali. UNDP.

Moussu H, Trompette R (1966a) Notice explicative de la carte hydrogéologique au 1/200.000, Atar – BRGM pour le compte de la direction des services techniques du Ministère de la construction, des travaux publics et des transports. RIM.

Moussu H, Trompette R (1966b) Notice explicative de la carte hydrogéologique au 1/200.000, Chinguetti. BRGM pour le compte de la direction des services techniques du Ministère de la construction, des travaux publics et des transports. RIM.

Ngugi DK, Brune A., 2012. Nitrate reduction, nitrous oxide formation, and anaerobic ammonia oxidation to nitrite in the gut of soil-feeding termites (Cubitermes and Ophiotermes spp.). Environ Microbiol. 2012 Apr;14(4):860-71. doi: 10.1111/j.1462-2920.2011.02648.x.

Nouaceur Z., 2009. Evolution des précipitations depuis plus d'un demi-siècle en Mauritanie. Geographia Technica. Numéro spécial, 2009, 361-366.

Obuobie, E, and Barry, B. 2012.Burkina Faso, in Groundwater Availability and Use in Sub-Saharan Africa; a review of fifteen countries. Pavelic, P, et al. (Eds). International Water Management Institute, Sri Lanka.

OSS, 2015. Burkina Faso, Atlas des Cartes d'Occupation du So l. ISBN: 978-9973-856-83-3.

OSS, 2014.Mali, Atlas des Cartes d'Occupation du Sol. ISBN: 978-9973-856-78-4.

OSS, 2015. Mauritanie, Atlas des Cartes d'Occupation du So l. ISBN: 978-9973-856-81-4.

Ouédraogo, I. 1994. Géologie et hydrogéologie des formations sédimentaires de la boucle du Mouhoun (Burkina Faso). Thèse de Doctorat, Université Cheikh Anta Diop, Dakar, 116p

Ouédraogo, C., 1998. Cartographie géologique de la region Sud-Ouest du Burkina Faso au 1/200 000 – synthèse géologique. AQUATER/BUMIGEB.

Ozer P. , Houtondji Y. C., Gassani J., Djaby B.,De Longueville F., 2014. Evolution récente des extrèmes pluviométriques en Mauritanie (1933-2010). XXVIIe Colloque de l'Association Internationale de Climatologie, 2-5 juillet 2014 – Dijon (France).

Pana, 2007. Programme d'Action National d'Adaptationaux Changements Climatiques au Mali. UNDP.

Rooney A.D, D. Selby, J.-P. Houzay, P. R. Renne, 2010.Re–Os geochronology of a Mesoproterozoic sedimentary succession, Taoudeni basin, Mauritania: Implications for basin-wide correlations and Re–Os organic-rich sediments systematics. Earth and Planetary Science Letters, 289, 486-496.

Sea, F., Tanguay, M.G., Trudel, P. and Perrault, G. 1990.Preliminary results of a study on gold dispersion in the laterite deposits of a gold zone in Misseni, Mali. Canadian Journal of Earth Sciences, 27, 1686-1698.

Shahin M., 2006. Water Resources and Hydrometeorology of the Arab Region.Springer.
Smedley, P. L., Edmunds, W. M., West, J. M., Gardner, S. J. and Pelig-Ba, K. B. 1995. 2: Health problems related to groundwater in theObuasi and Bolgatanga areas, Ghana. British Geological Survey Technical Report, WC/95/43, 122 pp.

SOGREAH, 1988. Projet Mali Sud II - Sous projet hydraulique villageoise - Rapport final, Ministère de l'Agriculture - CMDT.

SOGREAH, 1994. Etude des ressources en eau souterraine de la zone sédimentaire de la région de Bobo-Dioulasso - Modélisation des nappes des grès GKS, GFG, GGQ et SAC – Utilisation des modèles MONA, ESTRA, TRAFT et SIMUTRA., DRH-HB.

Soule A. O., 2003. Profil fourrager MAURITANIE. Rapport FAO.

Taupin, J.D., Gaultier, G., Favreau, G., Leduc, C., Marlin, C., 2002. Isotopic variability of Sahelian rainfall at different time steps in Niamey (Niger, 1992–1999): climatic implications. C. R. Geosci., 334, 43-50.

Taupin JD, Coudrain-Ribstein A, Gallaire R, Zuppi GM and Filly A, 2000. Rainfall characteristics ($\delta^{18}O$, $\delta^{2}H$, T and H_r) in Western Africa, regional scale and influence of irrigated areas.. J. Geophy. Res., 2000, Vol (105) (D9), p.11911-11924.

Traore, A.Z., Bokar, H., Sidibe, A., Upton, K. & Ó Dochartaigh, B.É. 2016. Africa Groundwater Atlas: Hydrogeology of Mali. British Geological Survey.http://earthwise.bgs.ac.uk/index.php/Hydrogeology_of_Mali.

Travi Y., Gac J.Y., Fontes J. Ch., Fritz B., 1987. Reconnaissance chimique et isotopique des eaux de pluie au Sénégal. Géodynamique 2 (1), 43-53.

Trompette, R., 1973. Le Précambrien supérieur et le Paléozoïque inférieur de l'Adrar de Mauritanie, bordure occidentale du bassin de Taoudeni, Afrique de l'Ouest : un exemple de sédimentation de craton. Thèse Université de Provence, Marseille, France.

Upton, K. & Ó Dochartaigh, B.É. 2016. Africa Groundwater Atlas: Hydrogeology of Mauritania. British Geological Survey.]. http://earthwise.bgs.ac.uk/index.php/Hydrogeology_of_Mauritania.

Valenza, A., Grillot, J.C., Dazy, J., 2000. Influence of groundwater on the degradation of irrigated soils in a semi-arid region, the inner delta of the Niger River, Mali. Hydrogeol. J. 8, 417–429.

UN, 1983.Ground Water in West Africa. Natural Resources/Water Series No. 18, United Nations, pp 53-65.

UNEP, 2009. Actualisation du Projet de démonstration 1 (PD1) : Mécanisme d'alerte précoce d'annonce des crues fondé sur une meilleure connaissance du milieu physique du complexe MOUHOUN-SOUROU (Burkina – Mali) Projet PNUE-FEM Volta Numéro du projet: 53885.

United States Agency for International Development, 2012.Climate vulnerabilities and development in Burkina Faso and Niger Background paper. Global Climate Change Office, Climate Change Resilient Development Project, technical report, Washington.

Venema, H. D., E. J. Schiller, K. Adamowski et J-M. Thizy.« A Water Resources Planning Response to Climate Change in the Senegal River Basin », *Journal of Environmental Management*, 1997, vol. 49, no 1, p. 125–155.

Villeneuve M., Paleozoic basins in West Africa and the Mauritanide thrust belt. Journal of African Earth Sciences, 43, 166-195

Whycos, 2006. Niger – Hycos. Système d'information hydrologique au service d'une gestion intégrée des ressources en eau pour le bassin du Niger.

ACRONYMS

Ba: Bakoye group

Bg&Bs: Lower Proterozoic Birrimian sediments

BKF: Burkina Faso

CAM : Cambrian

CI: Continental Intercalaire

Crist : Crystalline

CT : Continental Terminal

DO : Dissout oxygen

CTQ: Continental Terminal Quaternaire

EC: Electrical Conductivity

GB: Sandstone of Bandiagara

GFB: Fo-Bandiagara Sandstones

GFG: Fine Grained Sandstones with Glauconite

GFR: Fine Grained Sandstones

GGQ: Quartz Granulates Sandstones

GI: lower sandstones

GK: Sadstone of Koutiala

GKS: The Kawara-Sindou sandstones

GMWL: Global Meteoric Water line

GNIP: Global Network of Isotopes in Precipitation

GSD : Sandstone and silt-dolomitic

GW: Ground-Water

IAEA: International Atomic Energy Agency

ICP: Infra-Cambrian Plisse

ICT : Infra-Cambrian Tabulaire

IRD: Institut de recherche pour le développement

ITCZ: Intertropical convergence zone

ITF: Inter Tropical Front

LGM: Last Glacial Maximum

LML: Local Meteoric Line

LMWL: Local Meteoric Water Line

LRAE: Laboratory of Radio-Analysis and Environment

P: precipitation

PCA: Principal Component Analysis

SAC1: The siltstones, argillites and carbonates of Guena-Souroukoundinga (sandstones, schist, dolomite)

SAC2: siltstones, argillites and carbonates of Samandeni-Kiébani

SAI: Iullemeden Aquifer System

SI: Saturation Index

So: Souroukoto

SQ: sandstones of Koutiala

St: Sotuba

ST: Schists of Toun

T: Temperature

TDS: Total dissolved salts

TU: Tritium Unit

ANNEXES

ANNEX I-OLD DATA

Burkina-Faso / Mali (Huneau et al., 2011)

Sample ID	Strat.	X (UMT)	Y (UMT)	Sampling date	T (°C)	EC (µS/cm)	pH	HCO_3^- (mg/L)	$\delta^{18}O$ (‰)	$\delta^{2}H$ (‰)	^{3}H* (TU)	$\delta^{13}C$ (‰)	$a^{14}C$ (pmC)
1	CT	465 668	1 444 439	30/08/00	31.6	99	7.20	-	-4.84	-37.8	1.3	-	-
2	CT	455 022	1 434 779	30/08/00	33.2	160	6.60	165	-4.91	-39.8	1.9	-16.0	91.0 ± 3.5
3	CT	477 994	1 416 782	30/08/00	31.3	24	5.20	-	-4.88	-38.3	1.1	-	-
4	CT	410 950	1 407 945	31/08/00	33.2	246	6.80	207	-5.25	-38.0	3.8	-12.8	49.1 ± 2.5
5	CT	493 000	1 606 000	01/09/00	-	-	-	-	-4.90	-38.7	0.7		-
6	CT	455 000	1 570 000	30/08/00	-	-	-	-	-5.15	-35.8	0.0	-13.6	82.9 ± 0.8
7	CT	519 000	1 565 000	31/08/00	-	-	-	-	-5.40	-38.8	0.6	-8.4	51.3 ± 0.5
8	CT	490 000	1 592 000	01/09/00	-	-	-	-	-5.16	-34.5	0.7	-	-
9	CT	479 000	1 588 000	30/08/00	-	-	-	-	-5.80	-36.6	3.8	-10.3	54.9 ± 0.7
10	CT	491 000	1 592 000	30/08/00	-	-	-	-	-5.35	-34.4	1.9	-10.7	77.6 ± 0.7
11	CT	493 000	1 606 000	30/08/00	-	-	-	-	-6.19	-41.7	1.4	-11.8	74.7 ± 0.4
12	CT	492 000	1 612 000	31/08/00	-	-	-	-	-0.57	-6.7	3.6	-11.2	122.1 ± 0.9
13	CT	520 000	1 605 000	01/09/00	-	-	-	-	-5.33	-40.5	1.5	-9.4	73.2 ± 0.7
14	GFG	356 224	1 232 794	24/05/97	-	16	-	6	-5.77	-29.8	1.7	-	-
15	GFG	354 468	1 247 561	23/05/00	31.0	23	4.70	-	-5.02	-36.1	-	-	-
16	GFR	369 914	1 300 534	09/04/99	29.7	738	8.48	363	-3.06	-	0.6	-7.4	49.7 ± 0.5
17	GGQ	342 471	1 237 005	23/05/97	28.0	29	7.30	15	-5.05	-	0.5	-18.2	94.9 ± 0.9
18	GGQ	341 670	1 234 705	23/06/84	-	-	-	-	-5.00	-29.1	0.5	-	-
19	GGQ	345 294	1 231 001	23/06/84	-	-	-	-	-4.00	-23.9	1.1	-	-
20	GGQ	362 436	1 252 243	31/01/98	31.7	70	7.38	35	-4.83	-	1.3	-17.1	86.7 ± 0.9
21	GGQ	266 435	1 211 742	25/05/97	26.7	10	6.20	6	-4.90	-	0.4	-17.1	98.7 ± 0.9
22	GGQ	372 791	1 278 803	28/05/97	30.4	122	6.50	65	-5.35	-34.0	0.4	-	-
23	GGQ	343 473	1 231 009	23/06/84	-	-	-	-	-4.70	-27.7	0.7	-	-
24	GGQ	342 715	1 237 433	26/05/97	29.1	46	6.20	32	-5.10	-29.7	0.4	-17.6	87.3 ± 0.8
25	GGQ	342 715	1 237 433	23/03/99	30.3	97	6.30	35	-5.46	-29.6	0.8	-15.2	79.3 ± 0.8
26	GGQ	419 064	1 310 054	22/05/00	31.4	456	6.10	160	-4.73	-34.6	-	-13.7	80.0 ± 0.8
27	GGQ	386 762	1 264 602	23/05/00	31.5	178	5.90	-	-4.45	-34.2	-	-	-
28	GI	310 040	1 179 107	19/03/99	30.5	42	5.00	15	-4.80	-27.8	0.9	-	-
29	GI	310 680	1 179 468	03/03/01	29.7	25	6.00	4	-4.87	-34.5	-	-	-
30	GI	310 796	1 178 515	03/03/01	29.9	30	6.00	6	-5.06	-35.7	-	-	-
31	GI	310 250	1 189 874	25/05/00	29.5	26	7.00	-	-5.18	-38.1	-	-	-
32	GI	306 821	1 190 661	25/05/00	28.1	20	6.90	-	-5.12	-37.5	0.6	-	-
33	GKS	426 785	1 337 034	22/05/00	31.9	17	7.90	-	-5.11	-37.3	1.6	-	-

Sample ID	Strat.	X (UMT)	Y (UMT)	Sampling date	T (°C)	EC (µS/cm)	pH	HCO_3^- (mg/L)	$\delta^{18}O$ (‰)	$\delta^{2}H$ (‰)	^{3}H* (TU)	$\delta^{13}C$ (‰)	$a^{14}C$ (pmC)
34	GKS	334 335	1 316 099	09/04/99	31.1	475	6.85	325	-6.58	-	1.4	-9.9	12.1 ± 0.2
35	GKS	381 870	1 347 163	23/05/00	32.9	435	7.20	202	-4.95	-37.7	0.7	-16.9	79.4 ± 3.2
36	GKS	374 773	1 451 032	31/08/00	33.8	198	5.90	-	-6.06	-44.9	0.1	-	-
37	GKS	411 233	1 372 679	29/08/00	32.2	67	5.50	-	-4.66	-37.8	0.3	-	-
38	GKS	351 257	1 221 388	24/05/97	29.3	150	6.62	102	-5.25	-28.4	0.4	-15.0	64.4 ± 0.7
39	GKS	355 904	1 194 210	04/02/98	29.7	123	6.32	60	-4.65	-	0.5	-15.8	91.0 ± 0.9
40	GKS	372 650	1 243 784	04/02/98	30.0	455	7.30	323	-5.88	-	0.4	-9.4	20.6 ± 0.2
41	GKS	402 500	1 287 003	22/05/00	30.6	71	5.30	16	-5.16	-35.3	-	-	-
42	GKS	386 700	1 264 233	22/05/00	31.5	364	5.40	33	-4.78	-37.7	-	-	-
43	GKS	208 897	1 252 245	24/03/99	28.9	430	7.30	43	-4.95	-	0.9	-14.7	68.4 ± 0.7
44	GKS	208 897	1 252 245	24/03/99	29.0	430	7.40	43	-5.79	-	0.9	-11.2	0.3 ± 0.1
45	GKS	245 246	1 244 556	25/03/99	29.2	392	7.20	250	-5.44	-	1.4	-8.7	2.3 ± 0.1
46	CT	345 085	1 529 662	22/05/80	-	80	7.00	24	-4.50	-27.3	7.2	-	-
47	CT	228 979	1 454 979	04/03/80	30.0	39	5.00	11	-5.80	-38.0	0.4	-19.0	86.9 ± 0.7
48	CT	234 402	1 454 926	06/03/80	-	-	-	16	-6.95	-38.6	0.2	-	-
49	CT	234 402	1 454 926	06/03/80	-	128	-	41	-6.15	-37.9	0.1	-	-
50	CT	324 581	1 424 697	24/05/80	-	240	8.00	66	-5.00	-30.5	10.4	-	-
51	CT	199 809	1 433 142	05/03/80	29.0	136	6.20	40	-5.40	-32.3	12.3	-17.3	103.6 ± 0.1
52	CT	321 276	1 472 656	07/03/80	31.0	185	6.00	84	-5.35	-36.3	0.8	-16.3	82.2 ± 0.3
53	CT	288 699	1 463 672	23/05/80	-	485	8.00	137	-4.70	-27.4	7.2	-	-
54	CT	288 627	1 454 452	20/05/80	-	56	6.00	12	-5.34	-36.0	3.1	-	-
55	CT	324 792	1 457 883	21/05/80	-	210	7.00	132	-5.90	-40.0	0.8	-	-
56	CT	230 732	1 449 427	04/03/82	28.0	140	5.00	4	-5.20	-33.0	5.4	-	-
57	CT	339 455	1 492 822	22/05/80	-	183	7.00	20	-4.50	-39.7	4.5	-	-
58	CT	319 131	1 421 044	24/05/80	-	24	7.00	20	-5.00	-32.3	1.5	-	-
59	CT	292 074	1 432 297	24/05/80	-	30	7.00	11	-5.30	-33.1	7.0	-	-
60	CT	312 171	1 461 655	20/05/80	-	250	8.00	146	-4.71	-32.4	0.5	-	-
61	CT	291 978	1 419 389	07/03/80	-	78	-	16	-5.30	-33.7	4.5	-	-
62	CT	319 582	1 489 262	22/05/80	-	44	7.00	7	-4.70	-27.4	8.6	-	-
63	CT	319 582	1 489 262	22/05/80	-	21	6.00	3	-4.90	-31.2	4.5	-	-
64	CT	230 606	1 436 515	06/03/80	-	-	-	524	-5.72	-39.0	0.2	-	-
65	CT	230 606	1 436 515	05/03/80	29.0	-	6.40	22	-5.05	-33.7	4.7	-13.1	101.2 ± 1.0
66	CT	230 606	1 436 515	05/03/80	-	133	-	30	-4.95	-33.3	5.2	-	-
67	CT	230 606	1 436 515	06/03/80	-	-	-	35	-4.59	-35.8	7.2	-	-
68	CT	227 024	1 440 240	20/05/80	-	110	6.00	22	-5.62	-36.8	6.8	-	-
69	CT	231 787	1 370 096	08/03/80	-	-	-	11	-6.54	-42.6	0.2	-	-
70	CT	231 787	1 370 096	08/03/80	30.0	-	6.50	10	-6.49	-41.5	0.0	-19.4	76.6 ± 0.7

Sample ID	Strat.	X (UMT)	Y (UMT)	Sampling date	T (°C)	EC (µS/cm)	pH	HCO_3^- (mg/L)	$\delta^{18}O$ (‰)	$\delta^{2}H$ (‰)	^{3}H* (TU)	$\delta^{13}C$ (‰)	$a^{14}C$ (pmC)
71	CT	231 787	1 370 096	08/03/80	29.0	51	5.00	23	-6.81	-44.3	0.2	-	-
72	CT	231 787	1 370 096	08/03/80	30.0	28	5.00	12	-5.74	-36.8	0.0	-18.8	87.3 ± 0.3
73	CT	339 511	1 502 040	22/05/80	-	110	7.00	29	-3.10	-20.8	9.7	-	-
74	CT	228 906	1 447 601	06/03/80	-	-	-	7	-6.06	-36.3	8.7	-	-
75	CT	290 336	1 441 530	20/05/80	-	-	6.00	18	-5.50	-20.3	5.2	-	-
76	CT	294 175	1 471 006	07/03/80	29.0	38	5.00	7	-5.56	-39.5	0.3	-20.0	99.9 ± 1.0
77	CT	294 175	1 471 006	06/03/80	-	213	-	25	-4.38	-24.9	9.6	-	-
78	CT	294 175	1 471 006	06/03/80	30.0	85	6.30	17	-5.24	-35.0	3.1	-18.4	101.9 ± 0.9
79	CT	328 325	1 444 954	21/05/80	-	41	5.00	1	-4.60	-28.4	7.4	-	-
80	CT	293 979	1 445 191	07/03/80	-	130	-	12	-4.96	-30.1	6.0	-	-
81	CT	313 927	1 454 267	21/05/80	30.0	130	6.00	52	-6.05	-41.9	0.4	-	-
82	CT	230 624	1 438 360	20/05/80	-	48	6.00	12	-5.50	-37.6	2.5	-	-
83	CT	229 071	1 464 202	04/03/82	29.0	430	9.00	286	-	-	0.1	-11.5	3.6 ± 0.1
84	CT	336 100	1 533 405	22/05/80	-	44	7.00	107	-4.78	-31.3	2.5	-	-
85	CT	326 801	1 489 214	07/03/80	29.0	-	6.50	23	-4.08	-25.3	8.2	-18.4	99.7 ± 0.9
86	CT	192 776	1 451 672	05/03/80	-	122	-	21	-6.47	-42.5	-	-	-
87	CT	192 776	1 451 672	05/03/80	-	122	-	17	-6.36	-43.2	3.7	-	-
88	CT	192 776	1 451 672	05/03/80	-	65	-	10	-6.80	-43.9	0.3	-	-
89	CT	192 776	1 451 672	05/03/80	-	40	-	7	-6.46	-42.4	0.8	-	-
90	CT	292 227	1 452 580	24/05/80	-	155	8.00	55	-5.30	-35.5	1.4	-	-
91	CT	250 587	1 445 550	06/03/80	-	125	-	6	-6.44	-33.7	2.8	-	-
92	CT	284 868	1 436 040	24/05/80	-	21	6.00	6	-5.00	-30.8	8.3	-	-
93	SAC1	342 654	1 237 311	23/05/97	28.7	137	6.35	84	-5.20	-	0.3	-15.3	69.2 ± 0.7
94	SAC1	308 001	1 236 147	27/05/97	28.5	532	7.84	330	-5.81	-36.6	0.4	-10.1	7.6 ± 0.1
95	SAC1	273 379	1 240 612	03/02/98	28.6	437	7.64	225	-6.22	-	-	-9.1	7.0 ± 0.1
96	SAC1	322 902	1 259 242	04/02/98	-	624	7.20	51	-5.04	-32.7	0.4	-	-
97	SAC1	215 605	1 265 606	20/03/99	28.9	440	7.20	293	-6.28	-40.0	0.7	-9.8	10.1 ± 0.1
98	SAC1	283 578	1 245 797	23/06/00	29.9	235	6.90	244	-6.33	-47.0	0.1	-12.5	9.6 ± 1.7
99	SAC1	295 851	1 239 431	23/06/00	31.1	294	7.00	310	-7.02	-48.8	0.4	-14.0	34.2 ± 2.1
100	SAC1	296 221	1 239 845	23/06/00	30.4	267	7.30	329	-5.59	-45.3	0.1	-	-
101	SAC1	299 525	1 244 280	24/06/00	30.4	290	7.50	256	-5.74	-42.8	0.1	-8.9	1.0 ± 0.1
102	SAC1	299 684	1 245 508	24/06/00	31.1	538	7.50	311	-5.65	-41.5	0.1	-9.2	1.0 ± 0.1
103	SAC1	296 716	1 227 319	19/06/00	29.3	388	7.60	147	-6.41	-45.8	0.2	-10.7	1.1 ± 1.0
104	SAC1	416 492	1 310 000	22/05/00	31.6	37	4.90	-	-4.71	-32.5	-	-	-
105	SAC1	320 136	1 241 775	24/06/00	31.4	222	8.50	168	-5.00	-36.0	0.6	-11.1	71.2 ± 3.0
106	SAC2	302 156	1 300 558	20/04/99	30.0	386	8.40	286	-5.55	-	0.9	-10.2	37.4 ± 0.4
107	SAC2	449 918	1 376 917	29/08/00	-	-	-	-	-5.07	-37.2	3.3	-	-

Sample ID	Strat.	X (UMT)	Y (UMT)	Sampling date	T (°C)	EC (µS/cm)	pH	HCO_3^- (mg/L)	$\delta^{18}O$ (‰)	$\delta^{2}H$ (‰)	^{3}H* (TU)	$\delta^{13}C$ (‰)	$a^{14}C$ (pmC)
108	SAC2	367 058	1 333 247	23/05/00	31.2	675	7.10	-	-5.07	-39.2	-	-	-
109	SAC2	395 561	1 437 950	31/08/00	34.8	31	5.10	-	-5.16	-38.5	0.7	-	-
110	SAC2	304 390	1 285 501	19/06/00	31.5	317	7.40	276	-4.77	-40.0	0.1	-12.2	53.4 ± 2.6

ANNEX II-DATA FROM THE IAEA-SUPPORTED PROJECT RAF/7/011

Tritium measurements : Mauritania

Sample Number	Sample code	Lab code	Sample type	Date	Tritium TU	Tritium error
1	406/A561/1	333	GWB	2015.09.07	<0.4	
2	407/A561/2	344	GWB	2015.09.09	2.8	±0.3
3	408/A561/3	270	GWB	2015.09.09	2.3	±0.3
4	409/A561/4	273	GWB	2015.09.12	1.1	±0.2
5	410/A561/5	274	GWB	2015.09.12	1.4	±0.2
6	411/A561/6	275	GWD	2015.09.12	<0.4	
7	412/A561/7	277	GWB	2015.09.12	1.0	±0.2
8	413/A561/8	281	GWB	2015.09.11	3.0	±0.3
9	414/A561/9	282	GWD	2015.09.11	<0.4	
10	415/C575/1	283	GWD	2015.09.11	<0.4	
11	416/C575/2	284	GWB	2015.09.11	<0.4	
12	417/C575/3	334	GWB	2015.09.12	2.0	±0.3
13	418/C575/5	335	GWB	2015.09.15	1.6	±0.2
14	419/C575/6	336	GWB	2015.09.14	0.7	±0.2
15	420/C575/7	337	GWB	2015.09.15	1.9	±0.3
16	421/C575/8	338	GWB	2015.09.16	0.8	±0.2
17	422/C575/9	339	GWB	2015.09.16	1.3	±0.2
18	423/F581/1	340	GWB	2015.09.16	2.0	±0.3
19	424/F581/2	341	GWB	2015.09.16	2.8	±0.3

First campaign : Mauritania

OurLabID	Sample ID	SampleSite Name	Campaign	Longitude	Latitude	Elevation	EC	pH	T°C	Alkalinity	$\delta^{18}O$, in ‰	$\delta^{2}H$, in ‰	d-excess ‰	Tritium (TU)
W-21535	333	F13 Atar	sept.-19	-13,11538	20,62127	297	1230	8,5	31,0	226,0	-4,85	-33,31	5,5	0,0
W-21536	344	Tawaz solaire	sept.-19	-12,9408	20,57	267	865	8,4	29,9	160,0	-3,16	-22,67	2,6	2,8
W-21537	270	JREIF F1	sept.-19	-12,4542	20,8517	300	540	9,5	35,0	200,0	-3,06	-22,14	2,3	2,3
W-21538	273	TIRBANE	sept.-19	-13,0291	19,9586	233	1490	8,5	33,0	233,0	-4,3	-28,7	5,7	1,1
W-21539	274	F1 AOUJEFT	sept.-19	-13,0603	20,0272	228	510	9,9	32,0	194,0	-4,43	-27,98	7,5	1,4
W-21540	275	Lemoilih P007	sept.-19	-13,1954	20,2085	173	866	9,1	35,0	220,0	-4,65	-34,2	3,0	0,0
W-21541	277	CHINGUETTI F3	sept.-19	-12,36677	20,45861	496	461	7,6	31,0	171,0	-5,42	-37,14	6,2	1,0
W-21542	281	OUADANE F2014	sept.-19	-11,6401	20,942	434	395	8,7	32,0	126,0	-4,1	-27,92	4,9	3,0
W-21543	282	N'Tomadi	sept.-19	-11,9304	20,9584	535	1332	7,6	31,0	374,0	-4,9	-37,51	1,7	0,0
W-21544	283	Oued Amlellek P012	sept.-19	-12,0886	20,8895	517	3331	8,3	30,0	219,0	-3,92	-31,85	-0,5	0,0
W-21545	284	AD63	sept.-19	-11,62153	20,93929	431	1090	9,1	34,0	114,0	-5,72	-37,25	8,5	0,0
W-21546	334	Terjit F saoudien	sept.-19	-13,10592	20,27456	284	549	9,2	36,0	126,0	-4,03	-26,85	5,4	2,0
W-21547	335	Terjit F1 goudron	sept.-19	-13,1117	20,2704	297	860	9,4	34,0	286,0	-4,04	-27,22	5,1	1,6
W-21548	336	Aoujeft	sept.-19	-13,05259	20,00952	226	378	9,2	34,0	140,0	-3,91	-26,38	4,9	0,7
W-21549	337	Timnit F1	sept.-19	-12,89944	19,91414	212	1398	9,5	32,5	226,0	-3,61	-22,68	6,2	1,9
W-21550	338	Timnit F2	sept.-19	-12,90462	19,89334	212	917	8,4	31,6	228,0	-5,33	-38,15	4,5	0,8
W-21551	339	Daaji F1	sept.-19	-12,7601	19,84757	279	1375	8,8	31,9	126,0	-3,3	-24,5	1,9	1,3
W-21552	340	Daaji F2	sept.-19	-12,7608	19,84667	279	1591	8,5	31,5	160,0	-4,22	-28,16	5,6	2,0
W-21553	341	Tenwamen F1	sept.-19	-12,7045	19,74281	315	574	9,0	32,0	166,0	-5,15	-35,41	5,8	2,8

2nd campaign Mauritania **Taoudeni** Basin

Sample Code	SampleSite Name	Sampling date	Sample type	Latitude	Longitude	Elevation (m)/sol	EC (µS/cm)	pH	Temp. (ºC)	Alcalinity as CaCO3, mg/L
348	NIMLANE	22/07/16	GWD	18,352	-11,67	309	1478	6,84	32,1	160
351	Titemlel	20/07/16	GWB	18,5583	-11,0731	502	1085	7,51	30	140
352	D'Boulgui	22/07/16	GWD	18,3995	-11,5966	407	994	6,96	30,4	239
359	SALA	22/07/16	GWD	18,2563	-11,8168	282	397	6,12	32,9	208
363	BIR ZIK 1	19/07/16	GWD	18,5808	-9,80667	280	516	7,38	31,4	99
364	TICHITT F5DH	19/07/16	GWB	18,4206	-9,4989	171	952	7,14	32,9	155
365	Gawya AEP11	15/07/16	GWB	18,4569	-10,8183	502	1608	6,7	30,3	70
366	BIR LEKCHEB 1	15/07/16	GWD	18,5125	-10,3461	223	178	5,9	39,4	63
367	BIR KHAT EL WAHCHIYA	15/07/16	GWD	18,4067	-10,5608	466	1906	7,5	30,6	271
370	Lehouetat	21/07/16	GWB	18,657	-11,579	343	620	7,15	30	83
371	Rachid F3	21/07/16	GWB	18,784	-11,686	265	798	6,67	31,9	138
372	Agnane	21/07/16	GWD	18,8103	-11,7718	225	1549	8,85	30,6	240
373	F1 Tidjikja	20/07/16	GWB	18,5328	-11,41137	390	1005	7,02	30,7	170
384	Nbeika F Solaire	22/07/16	GWB	17,9817	-12,2603	122	384	6,65	31,6	180

Mali 3rd campaign

SampleSiteName	Site_Code	Latitude	Longitude	Altitude	SampleName	SampleDate	SampleType	MaxDepth	AquiferName
Kourounde	B-501	14,050278	-3,522500	300	Kourounde	2013/06/18	GWB	56	CTQ
Dounde	B-502	13,961111	-3,712500	318	Dounde	2013/06/19	GWB	54	CTQ
Koboho	B-503	13,975000	-3,693333	466	Koboho	2013/06/19	GWB	50	CTQ
Bankass	B-504	14,076111	-3,526667	234	Bankass	2013/06/19	GWB	65	CTQ
Dimbal	D-501	14,028333	-3,591667	296	Dimbal	2013/06/19	GWD	37	CTQ
Koyentombo	D-502	14,085833	-3,533056	293	Koyentombo	2013/06/19	GWD	27	CTQ
Segue	B-505	13,845278	-3,750833	464	Segue	2013/06/20	GWB	96	ICT
Yolo	D-503	13,899444	-3,746667	376	Yolo	2013/06/20	GWD	30	ICT
Tissagou	D-504	13,656944	-3,820000	400	Tissagou	2013/06/20	GWD	50	ICT
Tanga	D-505	13,614722	-3,849444	314	Tanga	2013/06/20	GWD	65	ICT
Toun	D-506	13,546944	-3,909722	334	Toun	2013/06/20	GWD	39	ICT
Bobosso	D-507	13,662222	-3,672778	271	Bobosso	2013/06/20	GWD	38	CTQ
Songore	B-506	13,555000	-3,470000	253	Songore	2013/06/21	GWB	44	CTQ
Sirakele	D-508	13,438889	-3,813056	153	Sirakele	2013/06/21	GWD	30	CTQ
Thiondougou	D-509	13,235556	-3,583889	258	Thiondougou	2013/06/21	GWD	52	CTQ
Souhe	D-510	13,230556	-3,486389	264	Souhe	2013/06/21	GWD	42	CTQ
Poura - fitini	D-511	13,595000	-3,624722	262	Poura - fitini	2013/06/21	GWD	60	CTQ
Diallassagou	B-507	13,737500	-3,629444	255	Diallassagou	2013/06/22	GWB	25	CTQ
Pissa	B-508	13,728333	-3,404167	256	Pissa	2013/06/22	GWB	32	CTQ
Baye	B-509	13,625556	-3,368333	251	Baye	2013/06/22	GWB	33	CTQ
Koulogon- peulh	B-510	13,817500	-3,441667	259	Koulogon-peulh	2013/06/22	GWB	46	CTQ
Koporo-na	B-511	13,130556	-3,357500	259	Koporo-na	2013/06/23	GWB	40	ICP
Wol - konsangou	B-512	14,195278	-3,429167	320	Wol - konsangou	2013/06/23	GWB	60	ICP
Koporo-pen	B-513	14,225556	-3,300556	259	Koporo-pen	2013/06/23	GWB	40	ICP

SampleSiteName	Site_Code	Latitude	Longitude	Altitude	SampleName	SampleDate	SampleType	MaxDepth	AquiferName
Tendjerli	B-514	14,369444	-3,195556	286	Tendjerli	2013/06/23	GWB	48	ICP
Madoudougou	B-515	14,396111	-3,075556	273	Madoudougou	2013/06/23	GWB	45	ICP
Yoro	B-516	14,278611	-2,133889	300	Yoro	2013/06/24	GWB	45	CTQ
Dioungani	B-517	14,316389	-2,740556	257	Dioungani	2013/06/24	GWB	80	CTQ
Yandiaga	B-518	14,071111	-3,190556	255	Yandiaga	2013/06/24	GWB	35	CTQ
Gangafani	D-512	14,381667	-2,397500	257	Gangafani	2013/06/24	GWD	60	CTQ
Fleuve niger	R-502	12,630010	-7,998378	316	Fleuve niger	2013/06/24	SRI		
Tene	B-519	13,411667	-4,582222	293	Tene	2014/05/22	GWB	60	CTQ
Tominian	B-520	13,285556	-4,401389	298	Tominian	2014/05/23	GWB	58	ICT
Messo	B-521	13,263889	-4,465556	305	Messo	2014/05/23	GWB	70	ICT
Hanekuy	B-522	13,237222	-4,502222	308	Hanekuy	2014/05/23	GWB	60	ICT
Bodwo	B-523	13,235833	-4,593333	316	Bodwo	2014/05/23	GWB	52	ICT
Benena	B-524	13,123056	-4,364600	320	Benena	2014/05/23	GWB	42	ICT
Mandiakuy	B-525	13,018889	-4,464360	299	Mandiakuy	2014/05/23	GWB	48	ICT
Bokuy	B-526	12,972500	-4,536944	400	Bokuy	2014/05/23	GWB	92	ICT
Kona	B-527	12,905278	-4,569444	340	Kona	2014/05/23	GWB	80	ICT
Makoina	B-528	12,870278	-4,569722	360	Makoina	2014/05/23	GWB	68	ICT
Marena	B-529	12,725278	-4,440556	310	Marena	2014/05/23	GWB	68	ICT
Minamba	B-530	12,393333	-4,396640	434	Minamba	2014/05/23	GWB	60	ICT
Mouni	D-513	12,856111	-4,605000	364	Mouni	2014/05/23	GWD	76	ICT
Mafoune	D-514	12,790833	-4,638056	424	Mafoune	2014/05/23	GWD	54	ICT
Goutchina	B-531	12,299167	-4,562778	398	Goutchina	2014/05/24	GWB	65,59	ICT
Sorobasso	B-532	12,523611	-5,747500	299	Sorobasso	2014/05/24	GWB	60	ICT
Koumbi	B-533	12,452222	-5,646111	314	Koumbi	2014/05/24	GWB	57	ICT
Yorosso	D-515	12,359722	-4,729440	417	Yorosso	2014/05/24	GWD	52	ICT
Kouri	D-516	12,185000	-4,813920	310	Kouri	2014/05/24	GWD	104	ICT
Karangana	D-517	12,224444	-5,965000	390	Karangana	2014/05/24	GWD	90	ICT
Tandio	D-518	12,165833	-4,959240	341	Tandio	2014/05/24	GWD	81	ICT

SampleSiteName	Site_Code	Latitude	Longitude	Altitude	SampleName	SampleDate	SampleType	MaxDepth	AquiferName
Sougoumba	D-519	12,175000	-5,808611	356	Sougoumba	2014/05/24	GWD	58	ICT
Molobala	D-520	12,180000	-5,667778	326	Molobala	2014/05/24	GWD	70	ICT
Farakoro	D-521	12,245000	-5,634167	402	Farakoro	2014/05/24	GWD	51	ICT
Farakala	D-522	12,263333	-5,554444	317	Farakala	2014/05/24	GWD	60	ICT
Sincina	D-523	12,356667	-5,563889	380	Sincina	2014/05/24	GWD	60	ICT
Koutiala	B-534	12,362222	-5,527778	360	Koutiala	2014/05/25	GWB	92	ICT
Niessoumana	B-535	12,580556	-5,388056	297	Niessoumana	2014/05/25	GWB	70	ICT
CAA M'Pessoba	B-536	12,619167	-5,311667	319	CAA M’Pessoba	2014/05/25	GWB	55	ICT
M'Pessoba Ville	B-537	12,556667	-5,274444	319	M’Pessoba ville	2014/05/25	GWB	61,8	ICT
Kentieri	B-538	12,738333	-5,298889	299	Kentieri	25/05/2014	GWB	55	ICT
Niguena	B-539	13,077500	-5,813830	300	Niguena	25/05/2014	GWB	60	ICT
Douna PMH	B-540	13,212600	-5,922571	388	Douna PMH	25/05/2014	GWB	46	CTQ
Banankoroni	B-541	13,349167	-6,349360	290	Banankoroni	25/05/2014	GWB	70,5	CTQ
Tingoni	B-542	12,753690	-7,145250	271	Tingoni	25/05/2014	GWB	45	ICT
Djebougou	B-543	12,887500	-6,838910	336	Djebougou	2014/05/25	GWB	41	ICT
Fana AEP	B-544	12,772778	-6,958870	318	Fana AEP	2014/05/25	GWB	100	ICT
Marcakoungo	B-545	12,736900	-7,286768	340	Marcakoungou	25/05/2014	GWB	75,71	ICT
Diallabougou	D-524	13,415738	-6,230220	289	Diallabougou	25/05/2014	GWD	45	CTQ
Douna fleuve Bani	R-501	13,207231	-5,919385	277	Douna fleuve Bani	25/05/2014	SRI		
Gadougou Puits	D-525	14,871056	-6,766306	265	Gadougou Puits	2015/03/10	GWD	52	ICT
N'Galamankoura	B-546	14,143306	-6,013694	226	N'Galamankoura	2015/03/18	GWB	30	CTQ
Bagadadji	B-547	14,330917	-6,004250	270	Bagadadji	2015/03/18	GWB	25	CTQ
Kourouma	B-548	14,654222	-6,001250	274	Kourouma	2015/03/18	GWB	2	CTQ
Kogoni Bozo	B-549	14,731083	-6,023528	273	Kogoni Bozo	2015/03/18	GWB	2	CTQ
Kogoni ferme	B-550	14,718278	-6,029306	273	Kogoni ferme	2015/03/18	GWB	2	CTQ
Rattenga	B-551	14,687111	-6,024806	273	Rattenga	2015/03/18	GWB	2	CTQ
Sika	B-552	14,674944	-6,018167	273	Sika	2015/03/18	GWB	15	CTQ

SampleSiteName	Site_Code	Latitude	Longitude	Altitude	SampleName	SampleDate	SampleType	MaxDepth	AquiferName
Markala Fleuve	R-503	13,289947	-4,587370	305	Markala Fleuve	2015/03/18	SRI		
Diabaly Koura	B-553	14,700722	-6,062333	273	Diabaly Koura	2015/03/19	GWB	20	CTQ
Guiré	B-554	14,650028	-6,695944	262	Guiré	2015/03/19	GWB	60	ICT
Gadougou Forage	B-555	14,869722	-6,765222	265	Gadougou Forage	2015/03/19	GWB	50	ICT
Famabougou	D-526	14,785500	-6,228028	267	Famabougou	2015/03/19	GWD	60	CTQ
Aboité	D-527	14,827056	-6,473639	267	Aboité	2015/03/19	GWD	85	ICT
Bougoudjiiré	D-528	14,881167	-6,848194	267	Bougoudjiiré	2015/03/19	GWD	55	CIT
Sikéré	D-529	14,901472	-7,030861	260	Sikéré	2015/03/19	GWD	65	CIT
Karonga	B-556	15,333194	-7,606111	256	Karonga	2015/03/20	GWB	21	CAM
Dilly	B-557	15,026667	-7,685000	256	Dilly	2015/03/20	GWB	60,0	CAM
Dembassalla	B-558	14,996722	-7,519667	271	Dembassalla	2015/03/20	GWB	15,0	CAM
Goumbou	B-559	14,990833	-7,453889	257	Goumbou	2015/03/20	GWB	60,0	ICT
Mourdiah	B-560	14,486444	-7,470306	306	Mourdiah	2015/03/20	GWB	25,0	ICT
Wolokoro	B-561	14,432583	-7,567361	304	Wolokoro	2015/03/20	GWB	27,0	ICT
Medina Kagoro	B-562	14,375500	-7,669389	299	Medina Kagoro	2015/03/20	GWB	60,0	ICT
N'Gai	B-563	14,323444	-7,857250	300	N'Gai	2015/03/20	GWB	21,0	ICT
Diadiebougou	B-564	14,279139	-7,988639	350	Diadiebougou	2015/03/20	GWB	25,0	ICT
Segué	B-565	14,103528	-8,036111	388	Segué	2015/03/20	GWB	25,0	ICT
Nara	D-530	15,063611	-7,161389	260	Nara	2015/03/20	GWD	60	CIT
Koumara	D-531	15,196444	-7,383444	260	Koumara	2015/03/20	GWD	19	CIT
Moussawelli	D-532	15,180861	-7,428833	267	Moussawelli	2015/03/20	GWD	30	CAM
Terrou	D-533	15,220139	-7,407361	266	Terrou	2015/03/20	GWD	30	CAM
Zida Touré	D-534	15,263306	-7,503111	272	Zida Touré	2015/03/20	GWD	30	CAM
Boullol	D-535	15,189417	-7,721250	300	Boullol	2015/03/20	GWD	25,0	CAM
Galafouga	B-566	13,657833	-8,036528	390	Galafouga	2015/03/21	GWB	40,0	ICT
Kolokani	B-567	13,584917	-8,038000	400	Kolokani	2015/03/21	GWB	35,0	ICT
Tioribougou	B-568	13,384056	-7,994972	442	Tioribougou	2015/03/21	GWB	30,0	ICT

SampleSiteName	Site_Code	Latitude	Longitude	Altitude	SampleName	SampleDate	SampleType	MaxDepth	AquiferName
N'Golobougou	B-569	13,156028	-7,952667	390	N'Golobougou	2015/03/21	GWB	30,0	ICT
Niossombougou	B-570	13,095750	-7,939028	380	Niossombougou	2015/03/21	GWB	35,0	ICT
Djidieni	D-536	13,885806	-8,095250	392	Djidieni	2015/03/21	GWD	40,0	ICT
Sokolo	B-571	14,736083	-6,122472	270	Sokolo	2016/03/19	GWB	35	CTQ
Birou	B-572	14,565056	-7,451278	297	Birou	2025/03/20	GWB	30,0	ICT

Site_Code	Ca	Mg	Na	K	Cl	SO4	HCO3	NO3	SiO2	CO3	Fe_tot	EC	T	pH	Alkalinity	DO
B-501	0,31	2	1,29	1,1	2,29	0,62	7,06	1,02			0,0001	29	33,0	6,3	6	8
B-502	14,46	4,4	3,27	3	6,48	0,78	11,1	13,56			0,0002	145	31,9	5,9	9	4
B-503	16,22	4,98	0,7	4	4,93	1,56	50,4	5,5			1,3007	154	33,2	7,0	41	11
B-504	10,98	6,94	5,25	3,5	4,48	3,14	38,41	8,17			0,0001	153	33,3	7,5	32	13
D-501	20,87	10,66	0,7	1,5	3,01	5,73	80,97	6,7			0	220	30,3	8,6	66	13
D-502	8,26	2,03	1,89	2,4	3,93	1,62	24,49	2,72			0,3505	80	32,0	7,1	20	10
B-505	32,96	18,14	1,89	11	3,85	32,82	160,56	1,74			0,0001	444	30,5	8,3	132	15
D-503	16,46	4,39	4,06	3,6	13,11	1,1	13,66	13,67			0,1192	172	31,3	6,8	11	16
D-504	5,16	2,46	4,06	1,6	5,87	1,05	14,5	3,56			0,0001	73	32,5	7,8	12	11
D-505	29,57	14,61	3,67	3,7	5,7	5,5	137,17	5,72			0,0001	320	30,2	8,2	112	10
D-506	12,47	6,23	6,83	2,4	9,8	10,61	36,26	5,53			0,0527	157	30,2	8,4	30	11
D-507	30,12	11,85	8,02	2,8	4,86	10,5	132	5,37			0,0001	327	31,8	8,6	108	8
B-506	77,61	90,24	74,2	11,6	7,65	196,01	545,95	17,08			0,0001	1236	31,0	8,7	448	6
D-508	8,06	3,86	3,67	2,9	7,62	1,38	15,25	6,48			0,0001	105	31,0	6,8	13	3
D-509	130,48	51,04	253,6	4,8	11,74	521,77	510,99	49,42			0,0001	2580	31,0	8,1	419	5
D-510	137,31	30,3	94	9,2	41,79	433,38	346,48	100,09			0,0001	2570	35,0	8,1	284	7
D-511	79,68	41,69	11,97	4,4	6,27	34,72	388,23	10,52			0,0002	713	34,8	8,7	318	4
B-507	127,07	5,51	209	6	23,25	571,21	171,41	9,11			0,0001	1751	31,0	8,7	141	5
B-508	66,43	66,81	32,15	15,5	6,052	34,89	518,5	15,588			0,0003	898	32,0	8,0	425	9
B-509	68,96	40,02	40,4	30	6,219	80,431	405,61	10,601			0,0002	1047	33,0	8,9	333	7
B-510	52,19	33,92	5,05	2,6	5,034	4,466	294,99	8,576			0	638	35,0	9,2	242	11
B-511	26,3	13,84	1,89	2,3	14,41	1,784	137,13	234,007			0	251	31,0	9,8	112	4
B-512	47,19	22,88	5,25	2,7	5,718	5,204	46,36	9,424			0,0002	531	34,0	8,5	38	3
B-513	35,55	19,5	2,68	2,1	5,437	2,337	185,56	6,789			0,0001	342	32,0	10,1	155	4
B-514	28,99	13,77	1,29	2,1	6,108	16,511	100,69	6,816			0,0199	260	33,0	10,4	83	4
B-515	38,25	21,25	2,28	1,9	8,527	5,844	148,41	14,113			0,0001	400	28,0	10,2	122	4
B-516	35,23	19,92	16,82	11	10,909	37,363	150,28	10,483			0,0001	518	31,0	10,3	123	4

Site_Code	Ca	Mg	Na	K	Cl	SO4	HCO3	NO3	SiO2	CO3	Fe_tot	EC	T	pH	Alkalinity	DO
B-517	32,8	13,8	12,17	4,6	4,12	2,56	197,03	0,2			0,2151	491	31,6	9,1	162	3
B-518	17,18	9,01	18	2,5	4	2,54	135,24	0,4			0,0001	928	35,0	9,5	111	4
D-512	2,4	2,24	116,9	2,8	28,81	25,69	230,74	0,27			0,0418	494	32,0	9,2	189	3
R-502																
B-519	1,0	0,3	4,7	0,9	2,5	0,2		7,3	8,5		0,0	24	36,6	5,6	6	6
B-520	5,6	1,8	3,7	1,9	2,0	1,6		7,9	10,6		0,0	59	35,3	5,6	24	6
B-521	2,7	0,9	3,7	1,6	1,3	0,2		17,3	5,2		0,0	45	31,5	4,6	6	6
B-522	8,9	2,9	3,9	3,4	3,8	0,1		46,4	7,8		0,0	98	36,6	5,1	6	6
B-523	2,2	0,8	7,4	5,7	4,9	0,2		19,5	11,5		0,0	64	31,5	4,9	12	3
B-524	4,3	1,8	3,9	5,4	1,4	1,8		0,0	12,6		0,0	54	34,4	6,1	37	7
B-525	9,9	2,9	8,6	2,8	3,9	0,0		49,2	15,1		0,0	105	35,3	5,2	18	5
B-526	2,1	0,8	4,5	2,3	1,2	0,7		10,7	9,5		0,0	41	32,3	5,3	12	4
B-527	3,0	0,8	4,0	1,5	1,7	0,0		17,8	8,7		0,0	131	32,5	5,8	6	4
B-528	5,3	1,8	3,7	9,8	5,1	0,0		28,2	9,3		0,0	81	31,0	5,4	12	5
B-529	9,9	2,7	3,5	8,3	6,5	2,0		31,9	10,3		0,0	100	35,8	5,9	24	6
B-530	3,9	1,0	1,6	1,7	0,9	0,2		2,7	8,1		0,0	21	34,1	5,1	19	5
D-513	4,8	1,4	1,9	1,7	2,2	0,8		11,4	9,2		0,0	52	31,5	5,2	14	4
D-514	2,0	0,6	1,8	1,7	1,0	0,0		3,2	7,2		0,0	36	36,4	7,5	12	6
B-531	1,7	0,5	2,6	1,1	3,3	0,0		2,6	5,9		0,0	26	31,2	5,0	8	5
B-532	3,1	0,6	1,4	1,5	1,8	0,0		3,4	6,3		0,0	28	31,7	5,0	12	5
B-533	4,6	1,7	2,9	9,0	0,2	2,0		0,0	10,9		0,0	72	30,5	5,5	42	4
D-515	2,3	0,5	0,9	0,6	0,5	0,4		1,2	8,4		0,0	13	32,7	5,4	10	7
D-516	32,7	11,1	8,6	10,1	0,9	6,1		0,3	25,4		0,0	331	34,7	7,7	189	6
D-517	9,0	1,8	3,4	7,1	10,1	0,3		20,6	7,9		0,0	104	30,7	5,2	18	3
D-518	2,0	0,8	2,2	1,4	1,2	0,2		3,8	10,9		0,0	18	34,2	4,5	12	4
D-519	3,7	0,9	2,3	1,5	1,2	0,0		3,9	10,2		0,0	29	31,5	5,2	18	5
D-520	2,8	0,9	2,2	2,0	0,3	0,2		0,5	9,2		0,0	22	34,4	5,6	20	7
D-521	3,7	0,8	1,5	0,9	1,2	0,0		4,2	10,1		0,0	32	33,0	5,1	16	5

Site_Code	Ca	Mg	Na	K	Cl	SO4	HCO3	NO3	SiO2	CO3	Fe_tot	EC	T	pH	Alkalinity	DO
D-522	4,4	1,6	1,9	1,2	0,5	0,0		0,9	14,4		0,0	29	30,5	5,6	26	4
D-523	3,3	1,0	1,1	0,9	0,3	0,0		1,0	7,7		0,0	23	33,7	5,3	18	5
B-534	3,0	0,8	2,9	1,0	2,1	1,0		9,0	7,3		0,0	28	30,0	5,0	9	4
B-535	4,6	1,4	2,7	1,8	0,5	0,6		3,4	9,2		0,0	33	29,3	5,2	24	4
B-536	3,9	1,3	3,0	1,6	0,6	0,4		1,9	7,9		0,0	26	29,0	5,1	25	4
B-537	3,0	1,2	2,6	1,5	2,6	1,9		0,6	7,7		0,0	24	35,0	5,6	16	6
B-538	3,9	1,0	2,9	3,1	1,2	0,4		4,9	6,3		0,0	35	32,2	6,1	23	
B-539	3,0	0,6	1,9	0,6	0,8	0,0		1,1	8,4		0,0	20	34,6	6,8	16	6
B-540	8,9	3,8	8,8	1,6	5,6	1,5		19,3	22,1		0,0	107	31,5	6,0	42	4
B-541	21,4	14,5	3,1	1,2	1,3	0,0		0,0	30,8		0,0	249	35,3	8,0	142	6
B-542	24,8	17,2	4,6	5,8	2,6	3,5		29,5	20,7		0,0	292	31,3	6,5	142	5
B-543	16,9	5,9	4,7	2,7	12,4	0,1		50,5	8,2		0,0	166	30,0	5,2	27	5
B-544	6,2	3,9	1,9	7,2	0,2	0,5		0,0	20,1		0,0	77	30,7	5,7	52	3
B-545	5,8	2,4	1,8	7,5	0,2	0,4		0,0	15,2		0,0	66	31,6	5,9	46	6
D-524	12,4	35,6	2,7	2,2	3,8	1,3		2,1	30,4		0,0	323	32,2	7,4	211	4
R-501	7,5	3,3	4,6	3,3	1,5	0,7		3,8	8,5		0,0	76	28,4	6,7	48	7
D-525	35,7	35,6	140,6	9,6	29,5	152,6	231,8	153,5	29,8	12,0		1489	30,8	7,4		5
B-546	11,3	4,6	7,8	3,3	2,7	0,6	79,3	2,3	5,4	0,0		59	29,3	6,6		6
B-547	13,0	6,2	18,3	3,6	2,3	0,7	85,4	0,0	11,2	12,0		45	29,8	6,5		3
B-548	5,8	2,6	10,0	3,3	3,2	0,0	57,9	4,8	6,5	0,0		98	31,0	6,1		4
B-549	6,5	2,4	7,4	3,1	2,5	0,4	54,9	0,0	5,0	0,0		97	30,0	6,5		3
B-550	7,0	3,4	13,4	3,1	4,1	0,9	67,1	7,6	10,3	0,0		136	30,0	6,2		3
B-551	16,4	7,2	22,2	4,2	11,1	13,0	91,5	32,9	12,9	0,0		304	30,0	6,2		5
B-552	3,7	1,7	6,2	2,1	0,9	0,0	36,6	0,2	3,2	0,0		63	29,7	6,6		4
R-503	3,4	1,6	4,9	3,8	3,1	0,4	30,5	0,3	5,2	0,0		49	23,8	7,5		8
B-553	14,6	4,3	6,6	3,2	1,4	0,2	91,5	0,0	7,3	0,0		159	29,5	7,1		4
B-554	81,2	73,2	207,3	22,2	53,7	430,7	317,2	105,2	33,9	36,0		213	30,7	7,3		6
B-555	49,8	60,9	89,6	10,5	45,2	211,0	183,0	82,4	27,9	24,0		1418	32,1	7,2		3

Site_Code	Ca	Mg	Na	K	Cl	SO4	HCO3	NO3	SiO2	CO3	Fe_tot	EC	T	pH	Alkalinity	DO
D-526	27,0	15,2	46,4	11,8	3,5	5,3	231,8	14,3	16,6	18,0		481	30,6	7,4		6
D-527	9,4	4,7	3,7	1,4	1,1	1,9	61,0	0,0	7,4	0,0		163	32,1	6,9		5
D-528	47,9	44,3	358,6	36,6	78,2	458,7	329,4	155,3	36,5	36,0		231	31,5	7,2		4
D-529	28,4	7,0	96,3	8,9	25,4	48,4	250,1	0,0	22,8	36,0		696	30,1	8,1		6
B-556	12,6	14,7	252,2	11,6	52,6	49,7	446,4	103,7	21,5	65,0		1640	29,7	8,6		6
B-557	28,0	12,2	70,7	4,5	20,4	14	146	96,4	14,3	24,0		801	32,4	7,49		8
B-558	22,1	20,8	112,9	3,0	36,2	88	183	86,1	18,2	24,0		1161	31,5	7,44		3
B-559	32,7	9,3	29,8	5,9	14,6	31	159	7,0	9,9	12,0		487	32,3	7,84		2
B-560	5,2	2,5	18,8	1,6	8,1	2	24	48,8	6,8	0,0		158	31,2	7,46		6
B-561	22,9	14,1	21,1	8,5	13,5	9	128	42,3	15,2	9,0		372	32,1	6,92		4
B-562	31,9	12,8	14,9	17,1	14,8	19	134	14,2	14,6	12,0		407	30,1	7,18		3
B-563	11,4	4,8	4,9	10,0	6,6	3	49	26,3	9,0	0,0		144	29,9	7,22		3
B-564	4,5	2,7	5,5	2,1	3,7	1	24	15,8	4,3	0,0		77	31,7	6,28		4
B-565	14,5	7,3	6,5	2,2	6,1	2	73	26,3	9,8	0,0		178	29,1	7,95		5
D-530	2,9	1,7	3,2	1,7	1,4	0,3	24,4	0,0	6,9	0,0		36	30,3	6,7		6
D-531	33,7	35,7	225,7	10,6	36,5	314,9	329,4	76,9	27,0	36,0		1847	30,8	7,2		4
D-532	18,0	27,4	234,8	10,7	80,7	120,2	278,2	227,9	22,5	48,0		1374	29,5	7,5		4
D-533	47,4	25,8	87,3	5,0	53,1	35,8	146,4	210,4	17,1	12,0		1118	31,3	7,2		4
D-534	251,0	86,8	167,2	53,8	209,2	98,3	195,2	926,6	33,6	0,0		2660	28,8	7,5		4
D-535	52,9	26,7	75,0	5,9	51,3	39	159	184,3	12,5	30,0		1024	29,8	7,42		5
B-566	7,9	4,5	6,2	7,5	1,3	3	61	2,7	7,9	0,0		121	30,1	6,22		4
B-567	13,6	14,5	22,0	10,5	5,8	6	134	0,0	12,5	12,0		278	31,1	7,08		4
B-568	9,2	9,2	5,7	5,7	5,0	0	49	51,4	9,9	0,0		188	29,5	7,43		5
B-569	4,7	0,0	41,0	1,7	13,7	6	92	3,3	9,5	6,0		356	29,5	10,64		5
B-570	23,8	24,4	6,1	2,8	0,4	2	183	15,1	13,7	12,0		393	29,1	7,84		3
D-536	19,1	7,5	23,9	10,0	29,0	2	31	82,1	11,5	0,0		300	30,1	5,98		5
B-571	53,3	15,8	38,4	130,8	44,1	25,1	268,4	81,3	28,5	24,0		953	29,9	7,8		7
B-572	18,8	7,6	19,3	5,8	5,8	4	122	12,4	7,9	9,0		256	31,5	7,18		4

Burkina Faso first campaign

SampleSiteName	SiteCode	Latitude	Longitude	Altitude	SampleName	SampleDate	SampleType	MaxDepth	Ca	Mg	Na	K	Cl	SO4	HCO3
Badara	B-201	11,418028	-4,350250	202	DGW01	2013/12/26	GWB	118	1,2	2,9	1,3	1,8	0,4	0,1	18,3
Koundougou	B-202	11,759333	-4,512472	211	DGW02	2013/12/26	GWB	65	27,9	33,9	1,6	2,5	0,1	3,6	231,8
Toécé	B-203	11,806167	-4,518028	207	DGW03	2013/12/26	GWB	64	33,1	53,8	5,2	4,6	2,6	5,0	292,8
Lanfiéra-Coura	B-204	11,538222	-4,519000	192	DGW04	2013/12/26	GWB	62	14,3	27,9	37,3	3,2	1,0	7,0	256,2
Dingasso	B-205	11,060778	-4,292306	211	DGW05	2013/12/26	GWB	68	35,0	32,1	33,4	3,8	21,1	20,6	183,0
Matourkou	B-206	11,069333	-4,348417	220	DGW06	2013/12/26	GWB	101	5,0	9,8	1,1	10,1	0,3	0,1	67,1
Péni	B-207	10,950472	-4,470444	219	DGW07	2013/12/26	GWB	61	7,9	26,3	8,8	15,0	15,8	9,9	36,6
Toussiana	B-208	10,834667	-4,615222	208	DGW08	2013/12/26	GWB	61	1,7	4,7	2,2	6,4	1,4	0,1	12,2
Bérégadougou	B-209	10,775694	-4,725389	214	DGW09	2013/12/27	GWB	72	2,3	5,1	1,3	8,9	0,9	1,4	36,6
Tiéfora	B-210	10,637444	-4,840167	203	DGW10	2013/12/27	GWB	65	9,6	13,5	15,6	0,5	0,2	5,9	122,0
Banagourou	B-211	10,514667	-3,970306	214	DGW11	2013/12/27	GWB	63	4,7	28,6	15,6	0,8	1,1	0,1	140,3
Toukoro	B-212	10,403611	-3,864528	195	DGW12	2013/12/27	GWB	82	6,4	9,8	5,2	0,8	0,4	0,1	73,2
Noumoutiédougou	B-213	9,917306	-4,276389	184	DGW13	2013/12/27	GWB	67	50,5	114,9	27,0	30,8	48,9	35,2	268,4
Mangodara	B-214	9,905611	-4,355611	196	DGW14	2013/12/27	GWB	61	58,8	128,4	53,1	9,2	111,5	38,7	274,5
Logognièngnè	B-215	9,902528	-4,520278	194	DGW15	2013/12/27	GWB	62	50,3	140,4	44,4	16,2	107,5	37,6	187,1
Timperba	B-216	10,156861	-4,903583	197	DGW16	2013/12/27	GWB	73	1,9	9,7	14,9	2,8	0,9	0,1	73,2
Ziédougou	B-217	10,404611	-5,060028	298	DGW17	2013/12/28	GWB	64	5,4	11,3	12,7	3,3	0,3	0,1	91,5
Dakoro	B-218	10,448778	-5,152667	241	DGW18	2013/12/28	GWB	74	9,9	13,3	10,1	1,5	1,3	2,1	103,7
Fourkoura	B-219	10,329722	-5,374139	217	DGW19	2013/12/28	GWB	66	1,8	7,3	11,2	3,4	0,1	0,1	61,0

SampleSiteName	SiteCode	Latitude	Longitude	Altitude	SampleName	SampleDate	SampleType	MaxDepth	Ca	Mg	Na	K	Cl	SO4	HCO3
Loumana	B-220	10,578694	-5,354750	280	DGW20	2013/12/28	GWB	68	16,8	28,1	11,5	3,2	5,5	0,2	146,4
Sindou	B-221	10,655556	-5,162917	260	DGW21	2013/12/28	GWB	82	21,3	57,3	49,0	73,8	89,4	31,9	122,0
Sindou	B-222	10,657000	-5,161722	270	DGW22	2013/12/28	GWB	76	26,6	126,0	52,1	58,8	88,9	47,7	158,6
Sindou	B-223	10,668972	-5,173250	236	DGW23	2013/12/28	GWB	40	1,0	4,0	0,9	0,4	0,2	0,1	15,0
Kolasso	B-224	10,732194	-5,263472	280	DGW24	2013/12/28	GWB	45	0,4	0,9	0,9	0,4	0,5	0,1	6,1
Kankalaba	B-225	10,757472	-5,284250	286	DGW25	2013/12/29	GWB	39	1,9	9,8	1,1	1,4	0,8	0,1	36,6
Tourny	B-226	10,721528	-5,118694	268	DGW26	2013/12/29	GWB	40	0,6	2,5	1,1	2,1	0,1	0,1	15,5
Douna	B-227	10,621389	-5,089417	279	DGW27	2013/12/29	GWB	62	9,5	14,7	10,5	2,9	0,1	0,1	128,1
Wolonkoto	B-228	10,677139	-4,988000	278	DGW28	2013/12/29	GWB	37	3,9	8,3	1,8	1,1	0,1	0,1	48,8
Toumousseni	B-229	10,581556	-4,927194	263	DGW29	2013/12/29	GWB	51	12,9	16,9	10,6	3,1	0,2	0,1	146,4
Moussodougou	B-230	10,830389	-4,940528	250	DGW30	2013/12/29	GWB	72	0,4	0,8	0,8	0,7	0,3	0,1	6,1
Bendougou	B-231	10,977278	-4,867250	246	DGW31	2013/12/29	GWB	85	0,8	2,5	5,7	3,3	8,0	0,1	15,0
Potan	B-232	10,938056	-4,796833	235	DGW32	2013/12/29	GWB	76	0,3	1,0	0,6	0,5	0,1	0,1	6,1
Kotoudéni	B-233	10,950972	-5,020750	190	DGW33	2013/12/30	GWB	54	10,6	21,1	5,0	2,7	0,1	0,1	128,1
Kotoura	B-234	10,969944	-5,277639	191	DGW34	2013/12/30	GWB	44	0,4	1,4	1,0	0,6	0,1	0,1	6,1
Ou0lonkoto	B-235	11,099167	-5,147778	171	DGW35	2013/12/30	GWB	58	19,9	35,1	6,4	11,6	0,5	8,0	225,7
Soungalobougou	B-236	11,298611	-5,105556	161	DGW36	2013/12/30	GWB	45	1,9	3,7	0,9	0,9	0,1	0,1	24,4
Fanfiéla	B-237	11,633333	-5,283333	220	DGW37	2013/12/30	GWB	51	0,9	3,5	1,6	1,0	0,1	0,1	21,0
Banzon	B-238	11,325528	-4,796806	200	DGW38	2013/12/30	GWB	26	1,6	3,4	1,2	3,2	0,1	0,1	24,4
Djigouèra	B-239	11,158889	-4,875833	241	DGW39	2013/12/30	GWB	56	0,7	1,6	0,7	9,0	0,1	0,1	24,4

SampleSiteName	SiteCode	Latitude	Longitude	Altitude	SampleName	SampleDate	SampleType	MaxDepth	Ca	Mg	Na	K	Cl	SO4	HCO3
Koumi	B-240	11,133583	-4,428944	183	DGW40	2013/12/30	GWB	61	3,6	6,5	3,2	14,5	4,2	2,0	29,0
Kokorowé	B-241	11,179306	-4,443333	231	DGW41	2014/01/06	GWB	86	1,9	3,6	0,8	6,7	0,1	0,1	30,5
Satiri	B-242	11,420778	-4,103222	254	DGW42	2014/01/06	GWB	65	15,1	33,2	1,3	2,4	0,1	0,8	164,7
Bobo Dioulasso	B-243	11,177528	-4,296278	261	DGW43	2014/01/06	GWB	118	1,1	3,0	0,9	1,6	0,1	0,1	18,3
Sirakélé	B-244	12,248083	-3,136444	300	BGW01	2014/01/06	GWB	58	1,5	5,7	2,2	8,8	2,9	0,7	30,5
Kongosso	B-245	12,156722	-3,164500	295	BGW02	2014/01/06	GWB	62	8,6	21,2	13,1	2,2	1,2	1,9	122,0
tounou	B-246	11,995944	-3,349611	260	BGW03	2014/01/06	GWB	64	48,6	44,8	35,2	3,3	13,1	43,5	280,6
fakéna	B-247	12,021833	-3,628111	310	BGW04	2014/01/06	GWB	56	8,2	16,3	1,4	6,0	0,1	0,1	95,0
ouarkoye	B-248	12,088028	-3,668750	255	BGW05	2014/01/06	GWB	61	1,2	4,2	1,3	3,1	0,1	0,1	24,4
dampan	B-249	11,853528	-3,749778	240	BGW06	2014/01/07	GWB	68	32,3	60,5	26,7	125,4	39,7	68,3	128,1
pié	B-250	12,175194	-3,445889	257	BGW07	2014/01/07	GWB	58	0,9	2,9	1,1	0,8	0,1	0,1	18,3
koukatenga	B-251	12,348417	-3,539556	270	BGW08	2014/01/07	GWB	50	0,1	1,2	2,0	0,3	0,1	0,1	8,5
dédougou	B-252	12,452861	-3,429778	265	BGW09	2014/01/07	GWB	100	35,4	9,8	3,1	7,9	0,1	1,8	189,1
bagala	B-253	12,512556	-3,555389	284	BGW10	2014/01/07	GWB	47	51,0	17,4	12,5	2,3	0,2	19,1	268,5
bendougou	B-254	12,471528	-3,606806	276	BGW11	2014/01/07	GWB	85	28,2	28,1	3,2	3,3	0,2	2,6	195,2
sanaba	B-255	12,403528	-3,814528	245	BGW12	2014/01/07	GWB	94	0,7	2,6	1,2	0,4	0,1	0,1	14,0
yasso	B-256	12,364333	-4,032667	260	BGW13	2014/01/07	GWB	53	27,0	37,4	2,3	4,4	0,2	23,4	213,5
balavé	B-257	12,378306	-4,158056	248	BGW14	2014/01/08	GWB	49	0,5	3,3	2,2	1,9	0,1	0,8	18,3
tansila	B-258	12,421056	-4,384722	255	BGW15	2014/01/08	GWB	79	1,1	3,3	1,1	1,3	0,1	0,1	18,3
toula	B-259	12,616972	-4,320000	283	BGW16	2014/01/08	GWB	67	11,2	26,4	4,5	13,5	14,2	0,2	18,3

SampleSiteName	SiteCode	Latitude	Longitude	Altitude	SampleName	SampleDate	SampleType	MaxDepth	Ca	Mg	Na	K	Cl	SO4	HCO3
féléwé	B-260	12,666611	-4,252444	275	BGW17	2014/01/08	GWB	59	0,5	2,1	3,6	2,1	0,5	1,0	18,3
ben	B-261	12,700028	-4,351556	264	BGW18	2014/01/08	GWB	62	8,3	24,4	6,2	40,5	12,6	9,6	48,8
mollé	B-262	11,932583	-4,318889	292	BGW19	08/01/2014	GWB	57	0,2	0,9	1,6	0,7	0,1	0,1	9,0
kouka	B-263	11,901889	-4,341528	244	BGW20	08/01/2014	GWB	57	4,8	11,3	1,2	1,4	0,1	0,4	57,0
dissankuy	B-264	12,205028	-4,043361	282	BGW21	08/01/2014	GWB	56	1,6	5,6	3,8	1,5	3,3	0,5	15,0
bourasso	B-265	12,633944	-3,709389	263	BGW22	09/01/2014	GWB	40	32,6	17,7	7,1	2,2	0,1	5,6	201,3
dokuy	B-266	12,930111	-4,178556	246	BGW23	09/01/2014	GWB	91	1,0	2,8	5,8	5,2	3,6	0,1	15,0
kononiba	B-267	12,825861	-4,015917	251	BGW24	09/01/2014	GWB	58	22,1	33,5	3,2	2,2	1,6	32,1	148,0
teni	B-268	12,939917	-4,086417	238	BGW25	09/01/2014	GWB	49	22,4	36,5	4,0	3,6	0,5	6,0	201,3
niankouini	B-269	12,970500	-3,958306	275	BGW26	2014/01/09	GWB	56	1,6	6,4	1,4	0,9	0,1	0,9	30,5
bomborokuy	B-270	13,006972	-3,961889	262	BGW27	2014/01/09	GWB	67	31,0	40,7	7,8	7,8	4,1	12,1	231,8
kolokan	B-271	13,081167	-4,271222	249	BGW28	09/01/2014	GWB	55	1,2	2,3	2,9	1,6	0,4	0,1	12,2
soyé	B-272	13,307278	-4,029000	280	BGW29	2014/01/09	GWB	86	8,5	17,2	6,0	4,0	6,1	7,8	54,9
kolokan goure diallo	B-273	13,283472	-3,872306	267	BGW30	2014/01/09	GWB	78	14,9	32,6	7,3	11,9	11,0	8,3	36,6
gassan	B-274	12,809278	-3,205500	248	BGW31	2014/01/10	GWB	84	0,6	2,2	1,2	0,5	0,1	0,1	10,5
touaré	B-275	13,058111	-2,757611	239	BGW32	2014/01/10	GWB	54	46,8	130,1	39,2	15,3	45,5	62,8	109,8
tourouba	B-276	13,261694	-2,544750	277	BGW33	2014/01/10	GWB	62	99,1	129,6	66,7	25,3	63,1	143,9	109,8
bangasso	B-277	13,314222	-2,910250	261	BGW34	2014/01/10	GWB	68	8,5	18,0	17,1	5,0	4,3	3,6	67,1
sinzié	B-278	13,601944	-2,993833	250	BGW35	2014/01/10	GWB	65	5,4	18,0	3,2	5,3	3,7	4,3	42,2
toungaré	B-279	13,271111	-3,099639	286	BGW36	2014/01/10	GWB	64	9,9	39,9	3,0	53,9	19,9	11,4	54,9

SampleSiteName	SiteCode	Latitude	Longitude	Altitude	SampleName	SampleDate	SampleType	MaxDepth	Ca	Mg	Na	K	Cl	SO4	HCO3
daka	B-280	13,163222	-3,038083	248	BGW37	2014/01/10	GWB	59	11,8	28,2	20,9	3,8	0,8	6,8	128,1
diouroum	B-281	12,992667	-3,115444	255	BGW38	2014/01/10	GWB	68	60,8	103,2	27,3	8,1	25,4	36,9	164,7
kassoum	B-282	13,072722	-3,305583	274	BGW39	2014/01/20	GWB	61	16,6	31,6	1,2	4,6	0,1	3,6	146,4
niassan	B-283	13,093778	-3,428611	244	BGW40	2014/01/20	GWB	67	36,5	30,8	13,7	4,6	0,8	59,3	195,2
débé	B-284	13,068833	-3,428944	253	BGW41	2014/01/20	GWB	85	17,1	30,6	8,3	4,9	1,1	1,3	164,7
yaran	B-285	12,976611	-3,444500	262	BGW42	2014/01/20	GWB	74	70,5	210,6	44,7	189,9	96,8	140,5	103,7
toroba	B-286	12,461278	-3,235778	284	BGW43	2014/01/20	GWB	68	30,5	17,6	6,2	6,3	0,2	0,2	195,2
siguinvoussé	B-287	12,516750	-3,080917	289	BGW44	2014/01/20	GWB	70	7,3	15,3	10,0	2,6	0,1	2,9	103,7
gossina	B-288	12,523806	-2,874083	290	BGW45	2014/01/20	GWB	65	7,2	21,2	13,9	2,6	2,6	10,9	85,4
toma	B-289	12,760389	-2,895250	247	BGW46	2014/01/20	GWB	61	16,6	37,2	20,2	6,2	8,0	7,3	103,7
yaba	B-290	12,864778	-2,836944	261	BGW47	2014/01/20	GWB	64	3,2	14,0	13,7	2,5	0,1	0,1	79,3
bagnotenga	B-291	12,864028	-2,745833	255	BGW48	2014/01/20	GWB	67	10,1	19,4	11,7	3,4	0,1	4,5	109,8
doubaré	B-292	13,861528	-1,862750	236	BGW49	2014/01/20	GWB	88	2,0	7,3	2,8	0,9	0,1	0,1	24,4
yensé	B-293	13,898000	-2,843806	242	BGW50	2014/01/20	GWB	68	3,2	9,7	5,3	0,9	0,5	0,1	42,7
niongono	B-294	14,088667	-2,584806	280	BGW51	2014/01/20	GWB	73	56,2	19,2	17,8	10,8	8,0	20,2	189,1

Site_Code	NO3	SiO2	CO3	Fe_tot	EC	T	pH	Alkalinity	TDS	O18	H2	H3	H3_ERR
B-201	1,3	2,0	ND	<0.02	30	30,9	4,5	90	27	-4,84	-29,6		
B-202	1,0	7,4	ND	<0.02	426	30,6	7,1	222	302	-4,94	-33,5	2,1	0,3
B-203	17,7	5,7	ND	<0.02	564	30,3	6,9	275	415	-4,67	-28,7		
B-204	0,2	6,1	ND	<0.02	457	30,5	7,2	242	347	-5,17	-31,5	0,5	0,3
B-205	99,2	13,1	ND	<0.02	555	26,4	6,6	144	428	-4,55	-26,6		
B-206	0,1	5,1	ND	<0.02	111	27,2	5,6	51	94	-4,79	-29,0		
B-207	88,4	3,3	ND	<0.02	304	26,4	5,5	22	209	-4,60	-30,4	3,9	0,2
B-208	21,4	3,8	ND	<0.02	69	27,5	5,0	1	50	-4,74	-27,3	3,2	0,3
B-209	0,7	8,6	ND	<0.02	67	30,3	5,1	3	57	-4,49	-25,8	0,4	0,3
B-210	0,1	13,3	ND	<0.02	195	29,8	6,1	90	167	-4,63	-28,8		
B-211	0,1	12,3	ND	<0.02	220	30,5	6,1	114	191	-3,44	-22,8	0,6	0,2
B-212	0,1	15,9	ND	<0.02	110	31,1	5,4	52	96	-3,36	-21,0	1,3	0,3
B-213	274,5	13,7	ND	<0.02	1192	29,5	6,6	284	850	-3,50	-20,1	3,1	0,3
B-214	251,1	20,0	ND	<0.02	1332	29,7	6,8	263	925	-3,75	-30,0		
B-215	335,0	18,7	ND	<0.02	1364	29,7	6,4	185	918	-4,45	-29,2	2,4	0,3
B-216	2,9	13,1	ND	<0.02	118	28,4	6,2		106	-4,33	-27,9	0,8	0,3
B-217	1,1	13,1	ND	<0.02	137	26,8	5,8	64	126	-3,81	-25,1		
B-218	2,1	13,1	ND	<0.02	190	25,1	6,2	93	144	-4,39	-28,1		
B-219	0,1	6,3	ND	<0.02	88	29,2	5,0	43	85	-4,69	-29,2	1,3	0,2
B-220	12,6	11,5	12,0	<0.02	307	28,7	4,6	139	236	-4,81	-29,8	1,8	0,3
B-221	173,5	4,9	12,0	<0.02	910	29,2	6,2	128	630	-3,88	-23,3		
B-222	288,5	5,5	12,0	<0.02	1168	30,0	6,4	149	859	-4,07	-23,2		
B-223	5,1	4,1	ND	<0.02	26	31,7	4,2	4	27	-4,38	-25,2		
B-224	0,1	4,2	ND	<0.02	19	30,5	3,6	2	9	-4,61	-25,6		
B-225	5,3	6,9	ND	<0.02	56	28,2	4,9	19	57	-4,75	-28,7	4,7	0,3
B-226	0,1	3,9	ND	<0.02	19	30,4	4,3	6	22	-4,86	-30,1		
B-227	0,1	19,6	ND	<0.02	189	31,6	6,2	89	166	-4,68	-28,9		

Site_Code	NO3	SiO2	CO3	Fe_tot	EC	T	pH	Alkalinity	TDS	O18	H2	H3	H3_ERR
B-228	0,1	4,9	ND	<0.02	69	30,7	5,3	30	64	-4,72	-28,8		
B-229	0,1	16,2	ND	<0.02	214	30,2	6,1	108	190	-4,37	-24,8	2,0	0,3
B-230	1,1	2,3	ND	<0.02	18	27,3	3,7		10	-5,19	-32,6	8,7	0,3
B-231	2,3	2,4	ND	<0.02	58	27,2	4,8	5	38	-4,86	-29,3		
B-232	0,1	2,4	ND	<0.02	12	28,0	4,7		9	-4,47	-28,2		
B-233	0,1	15,8	ND	<0.02	205	29,2	6,6	11	168	-4,80	-30,4		
B-234	3,1	2,4	ND	<0.02	21	29,6	4,7	2	13	-4,43	-26,9	3,9	0,3
B-235	0,5	11,1	ND	<0.02	376	29,6	7,6	174	308	-5,59	-37,7		
B-236	0,1	3,7	ND	<0.02	28	30,0	5,2	11	32	-5,03	-31,0	1,1	0,2
B-237	0,1	2,2	ND	<0.02	28	31,9	5,2	7	28	-5,06	-29,6	0,9	0,3
B-238	1,4	3,2	ND	<0.02	33	28,4	5,4		35	-4,51	-29,2	1,2	0,2
B-239	0,1	16,5	ND	<0.02	40	28,4	5,1	14	37	-4,00	-25,1	0,6	0,3
B-240	30,4	3,5	ND	<0.02	124	27,6	5,2	13	93	-4,63	-28,0		
B-241	0,1	8,9	ND	<0.02	47	26,9	5,4	18	44	-4,74	-30,6		
B-242	1,0	3,5	ND	<0.02	286	28,5	6,6	143	219	-4,53	-30,0	1,7	0,3
B-243	0,1	6,9	ND	<0.02	22	29,6	4,9	5	25	-4,90	-30,4	1,1	0,2
B-244	8,8	6,9	ND	<0.02	74	28,3	5,5	15	61	-4,40	-27,2	4,1	0,3
B-245	9,0	34,9	ND	<0.02	242	27,3	6,0	92	179	-4,91	-31,3		
B-246	82,1	18,9	ND	<0.02	1101	28,1	7,1	396	551	-4,66	-28,2	3,4	0,3
B-247	1,6	10,6	ND	<0.02	156	30,2	6,2	67	129	-4,54	-30,0		
B-248	0,1	7,3	ND	<0.02	34	30,4	5,2	11	35	-4,93	-32,1	0,2	0,2
B-249	279,1	6,4	ND	<0.02	1317	27,7	7,1	219	760	-4,32	-26,6	3,1	0,3
B-250	0,1	6,3	ND	<0.02	21	30,3	5,0	3	24	-5,24	-32,5		
B-251	0,7	6,6	ND	<0.02	15	30,1	4,5		13	-4,59	-33,4	1,1	0,2
B-252	0,1	9,8	12,0	<0.02	589	29,6	7,0	297	259	-4,81	-33,8		
B-253	16,5	9,7	6,0	<0.02	795	30,9	7,0	397	394	-5,02	-29,6		
B-254	22,1	5,1	ND	<0.02	451	29,5	6,9	197	283	-5,06	-30,4		
B-255	0,1	2,8	ND	<0.02	18	30,8	4,8		19	-4,80	-31,2		

Site_Code	NO3	SiO2	CO3	Fe_tot	EC	T	pH	Alkalinity	TDS	O18	H2	H3	H3_ERR
B-256	1,6	3,4	ND	<0.02	469	32,1	7,0	195	310	-5,48	-33,3	1,8	0,3
B-257	0,8	4,6	ND	<0.02	24	30,3	5,2	74	28	-5,23	-33,5	2,3	0,3
B-258	0,1	6,5	ND	<0.02	25	29,9	4,8	5	25	-5,16	-34,3	1,3	0,3
B-259	122,2	5,1	ND	<0.02	314	29,9	4,7	16	211	-5,35	-32,2		
B-260	1,2	8,7	ND	<0.02	24	30,6	4,8		29	-5,02	-29,9		
B-261	96,9	8,1	ND	<0.02	367	29,8	5,6	28	247	-5,23	-33,8		
B-262	0,7	3,7	ND	<0.02	14	29,3	4,7		13	-4,11	-26,9	3,0	0,3
B-263	1,0	8,0	ND	<0.02	87	29,5	5,6	34	77	-4,89	-32,2		
B-264	2,6	9,2	6,0	<0.02	38	28,2	5,2	11	40	-4,21	-28,4	3,4	0,3
B-265	1,8	15,7	6,0	<0.02	547	30,6	7,2	261	274	-4,47	-31,1	2,3	0,3
B-266	18,0	2,4	ND	<0.02	58	29,4	4,7		51	-5,03	-32,8		
B-267	12,6	51,1	ND	<0.02	414	28,7	6,8	150	255	-4,32	-28,3	2,8	0,3
B-268	8,9	28,0	ND	<0.02	394	29,6	7,2	189	283	-5,27	-36,5		
B-269	2,0	3,8	ND	<0.02	48	28,3	5,8	17	44	-4,32	-29,5		
B-270	32,8	10,7	ND	<0.02	594	30,2	7,1	242	368	-4,84	-33,2	1,2	0,3
B-271	8,9	4,1	ND	<0.02	35	30,3	4,7		30	-4,92	-31,5	3,7	0,3
B-272	31,3	8,0	ND	<0.02	205	30,4	5,9	34	136	-4,69	-28,8		
B-273	91,5	7,4	18,0	<0.02	368	30,2	6,1	36	232	-4,73	-30,8	4,0	0,3
B-274	2,4	5,8	ND	<0.02	18	30,7	4,7	2	18	-4,50	-29,5	1,6	0,3
B-275	432,7	25,4	ND	<0.02	1168	29,7	6,4	90	882	-4,72	-28,9	3,2	0,3
B-276	689,1	21,5	ND	<0.02	1856	28,9	6,3		1326	-4,98	-30,4	0,8	0,3
B-277	58,6	26,0	ND	<0.02	250	32,4	5,9		182	-4,71	-27,7	2,6	0,3
B-278	37,4	9,4	ND	<0.02	149	30,7	6,5		120	-3,36	-22,1	3,6	0,3
B-279	125,6	13,8	6,0	<0.02	470	31,3	6,4		325	-4,16	-26,2		
B-280	38,2	32,4	6,0	<0.02	311	31,2	7,6		245	-4,70	-31,2	4,9	0,3
B-281	346,9	33,6	24,0	<0.02	1045	30,6	6,6		797	-4,59	-28,6		
B-282	0,1	10,8	12,0	<0.02	265	31,7	6,7		216	-5,24	-34,2		
B-283	5,5	8,3	6,0	<0.02	632	27,7	7,4		352	-2,20	-18,8	1,8	0,2

Site_Code	NO3	SiO2	CO3	Fe_tot	EC	T	pH	Alkalinity	TDS	O18	H2	H3	H3_ERR
B-284	8,8	8,0	6,0	<0.02	356	26,4	7,0		243	-3,39	-23,6		
B-285	859,7	7,5	ND	<0.02	2000	27,8	7,2		1716	-3,86	-24,0		
B-286	0,2	7,8	12,0	<0.02	481	31,5	7,5		268	-5,84	-36,2	1,7	0,3
B-287	0,8	26,0	ND	<0.02	157	31,0	6,4		143	-5,03	-29,7		
B-288	27,1	26,3	ND	<0.02	226	30,1	6,6		171	-4,37	-25,8	1,3	0,3
B-289	111,1	33,8	ND	<0.02	445	32,8	6,7		310	-4,99	-30,5		
B-290	11,3	18,3	ND	<0.02	147	32,0	6,3		124	-4,93	-30,4		
B-291	16,7	24,2	ND	<0.02	233	31,0	6,6		176	-4,44	-27,5	3,2	0,3
B-292	14,2	2,9	ND	<0.02	58	32,0	5,8		52	-4,13	-28,0	4,7	0,3
B-293	12,3	3,0	ND	<0.02	91	32,9	5,6		75	-4,38	-29,3	4,7	0,3
B-294	114,9	10,0	12,0	<0.02	863	27,4	7,2		448	-4,46	-28,5	4,9	0,3

Site_Code	TDS	EC_in_Lab	pH_in_Lab	O18	H2	H3	H3_ERR
B-501				-4,85	-33,7	-0,2	0,0
B-502				-3,74	-24,7	2,1	0,1
B-503				-5,58	-38,2	-0,3	0,0
B-504				-5,17	-33,2	0,6	0,0
D-501				-5,49	-38,5	-0,5	0,0
D-502				-5,00	-35,3	-0,7	0,0
B-505				-5,52	-33,3	0,3	0,0
D-503				-5,15	-29,5	3,0	0,1
D-504				-6,13	-36,1	7,0	0,1
D-505				-5,59	-33,8	1,9	0,1
D-506				-5,81	-35,1	3,4	0,1
D-507				-6,03	-38,0	-0,9	0,1
B-506				-1,44	-18,7	0,3	0,1
D-508				-4,37	-29,5	2,7	0,1
D-509				-4,18	-27,7	3,0	0,6
D-510				-3,02	-25,9	0,7	0,1
D-511				-5,15	-35,1	1,6	0,3
B-507				-5,90	-39,4	0,1	0,1
B-508				-1,89	-23,1	0,1	0,4
B-509				-0,79	-14,1	1,8	0,4
B-510				-5,51	-36,4	0,6	0,1
B-511				-5,37	-35,2	-0,7	0,2
B-512				-4,53	-31,2	-1,1	0,2
B-513				-4,91	-32,8	0,1	0,0
B-514				-6,30	-41,5	1,6	0,3
B-515				-5,35	-35,7	1,4	0,3
B-516				-4,29	-27,2	4,3	0,9

Site_Code	TDS	EC_in_Lab	pH_in_Lab	O18	H2	H3	H3_ERR
B-517				-4,21	-25,7	2,1	0,4
B-518				-3,83	-25,6	4,7	0,9
D-512				-4,42	-30,7	2,6	0,5
R-502				-3,00	-18,3		
B-519	23	30,7	6,54	-5,02	-31,4	6,1	0,3
B-520	49	55,2	6,87	-4,80	-31,6	2,7	0,3
B-521	34	36,2	7,22	-4,79	-29,1	4,4	0,3
B-522	75	90,7	6,74	-4,73	-30,1	5,5	0,3
B-523	53	58,2	6,97	-4,52	-26,1	3,5	0,3
B-524	55	56,4	7,08	-5,26	-34,5	2,1	0,3
B-525	96	113,3	6,77	-5,21	-32,9	8,1	0,3
B-526	35	36,3	7,14	-5,54	-34,1	6,0	0,3
B-527	35	37,5	6,97	-4,49	-30,1	3,6	0,3
B-528	66	84,2	6,84	-5,14	-33,8	4,8	0,3
B-529	89	100,3	6,80	-5,26	-29,8	2,2	0,3
B-530	31	22	6,87	-5,14	-32,2	3,2	0,3
D-513	38	50,3	7,03	-5,76	-37,3	2,4	0,3
D-514	23	31,1	6,88	-4,98	-29,7	5,1	0,3
B-531	20	18	7,50	-4,88	-32,9	4,4	0,3
B-532	24	22	7,19	-4,27	-29,9	5,9	0,3
B-533	63	67	7,27	-5,68	-40,8	3,7	0,3
D-515	16	12	6,99	-5,30	-33,6	2,0	0,3
D-516	259	322	7,57	-6,04	-40,8	0,9	0,3
D-517	70	101	7,83	-4,40	-30,9	3,0	0,3
D-518	24	15	7,36	-5,47	-34,4	5,4	0,3
D-519	32	27	7,44	-5,17	-34,1	4,1	0,3
D-520	29	21	7,53	-6,03	-40,3	2,4	0,3
D-521	28	27	7,38	-4,18	-27,5	6,4	0,3

Site_Code	TDS	EC_in_Lab	pH_in_Lab	O18	H2	H3	H3_ERR
D-522	37	27	7,35	-5,27	-34,0	2,7	0,3
D-523	26	20	7,34	-4,83	-34,4	5,3	0,3
B-534	29	28	7,34	-4,56	-34,3	6,5	0,3
B-535	39	30	7,18	-5,08	-38,5	4,8	0,3
B-536	38	31	7,23	-5,24	-36,4	6,0	0,3
B-537	30	22	7,33	-4,89	-37,8	5,5	0,3
B-538	40			-5,10	-34,5	2,0	0,3
B-539	24	17	7,27	-5,82	-39,6	0,8	0,3
B-540	92	99	7,16	-5,38	-35,6	6,3	0,3
B-541	184	240	7,18	-5,00	-29,7	1,2	0,3
B-542	230	291	7,24	-6,24	-37,6	1,7	0,3
B-543	120	164	7,49	-6,35	-39,7	2,6	0,3
B-544	72	73	7,35	-6,32	-39,6	9,1	0,3
B-545	64	62	7,29	-6,64	-41,9	0,4	0,3
D-524	271	309	7,85	-6,72	-42,8	1,7	0,3
R-501	73	81	7,08	0,48	-8,5	6,7	0,3
D-525	801	1489	7,82	-4,68	-37,9	3,5	0,3
B-546	112	59	7,81	-3,50	-23,2	2,0	0,3
B-547	141	44,7	8,00	-1,21	-11,1	3,7	0,3
B-548	88	98,2	7,70	-0,40	-8,8	2,7	0,3
B-549	77	96,7	7,65	1,34	1,0	2,7	0,3
B-550	107	135,8	7,73	-0,03	-6,0	1,6	0,3
B-551	198	304	7,81	-1,11	-12,8	1,7	0,3
B-552	51	63	7,74	0,20	-5,0	3,0	0,3
R-503	48	49,1	7,11	-1,14	-11,7	3,5	0,3
B-553	122	159	7,78	-1,34	-11,5	3,2	0,3
B-554	1327	213	7,98	-3,85	-31,7	3,4	0,3
B-555	756	1418	7,90	-5,26	-42,2	1,0	0,3

Site_Code	TDS	EC_in_Lab	pH_in_Lab	O18	H2	H3	H3_ERR
D-526	373	481	8,01	-5,60	-40,6	0,9	0,3
D-527	83	163,4	7,62	-6,37	-48,4	0,5	0,2
D-528	1545	231	8,01	-4,32	-31,3	2,9	0,3
D-529	500	696	8,02	-1,91	-18,6	0,4	0,3
B-556	1008	1640	8,38	-4,15	-30,7	3,4	0,3
B-557	416,3	801	7,86	-5,26	-37,2	1,08	0,31
B-558	576,7	1161	8,05	-4,07	-30,7	2,22	0,34
B-559	300,675	487	8,08	-7,19	-51,5	-0,24	0,30
B-560	111,113	157,7	7,33	-5,24	-33,1	3,63	0,33
B-561	268,24	372	7,91	-5,75	-38,6	2,08	0,33
B-562	271,045	407	7,86	-6,39	-44,3	0,73	0,32
B-563	115,739	143,6	7,72	-5,30	-33,9	3,58	0,34
B-564	59,72	77,3	7,71	-5,19	-34,0	1,42	0,29
B-565	138,293	178	7,41	-5,94	-37,9	2,62	0,34
D-530	36	36,3	7,26	-5,40	-41,4	0,2	0,3
D-531	1099	1847	8,02	-4,83	-32,7	1,5	0,3
D-532	1046	1374	8,19	-5,88	-46,6	2,7	0,3
D-533	623	1118	7,77	-1,07	-16,8	3,6	0,3
D-534	1988	2660	7,76	-4,52	-32,5	2,0	0,3
D-535	624,19	1024	7,95	-4,78	-34,0	1,51	0,35
B-566	94,552	121,1	7,50	-5,61	-39,2	0,84	0,32
B-567	218,48	278	7,98	-6,04	-43,2	0,37	0,22
B-568	135,112	187,6	7,77	-5,46	-36,8	3,15	0,32
B-569	167,636	356	9,35	-5,89	-41,8	0,51	0,34
B-570	269,895	393	8,27	-3,32	-21,3	1,58	0,33
D-536	204,075	300	7,26	-5,51	-35,6	2,42	0,27
B-571	681	953	8,08	-2,59	-23,1	2,4	0,3
B-572	204,341	256	7,74	-6,09	-41,9	-0,14	0,31

Burkina Faso 2nd campaign

Sample name	(local name)	Aquifer	(a)	**Latitude** N/S DDMMSS.DD		**Longitude** W/E DDDMMSS.DD		Altitude (m)	Cond µS/cm	Temp. °C	pH units	Alk mg/l
Doubaré	A8	**Sédimentaire**	**0**	13°51'41,6''N	13,86138889	02°51'45,8''W	-2,8625	264	58,7	26	5,7	0,28
Yensé	A9	**Sédimentaire**	**68**	13°54'33,4''N	13,90916667	02°50'32,6''W	-2,84222222	268	426	31, 3	6,7	4,7
Ziédougou	A10	**Sédimentaire**	**64**	10°24' 16,4''N	10,40444444	05°03'36,1"W	-5,06	301	147	28,4	6,43	1,61
Badara	A11	**Sédimentaire**	**0**	10°27' 32,8''N	10,45888889	05°05'31,7"W	-5,09194444	289	64	20,5	7,33	0,34
Badara	A12	**Sédimentaire**	**71**	10°26' 55,7''N	10,44861111	05°09'09,8"W	-5,1525	313	221	28,3	6,92	2,11
Tébéna	A13	**Sédimentaire**	**66**	10°19' 47,0''N	10,32972222	05°22'26,9"W	-5,37388888	323	105,8	28,8	6,5	1,01
Loumana	A14	**Sédimentaire**	**68**	10°34' 43,4''N	10,57861111	05°21'17,0"W	-5,35472222	329	342	29,8	6,40	3,01
Kankalaba	A15	**Sédimentaire**	**39**	10°45' 27,0''N	10,7575	05°17'03,3"W	-5,28416666	513	60	29	6,92	0,45
Tourny	A16	**Sédimentaire**	**40**	10°46' 19,7''N	10,77194444	05°09'23,9"W	-5,15638888	477	39,9	23,5	7,20	0,39
Douna	A17	**Sédimentaire**	**62**	10°40' 40,7''N	10,67777778	05°06'08,2"W	-5,10222222	320	32,6	21,4	7,50	0,35
Sirifessora secteur 3	A18	**Sédimentaire**	**17**	10°39' 25,3''N	10,65694444	05°09'42,0"W	-5,16166666	346	1439	27,2	5,98	3,7
Sindou	A19	**Sédimentaire**	**21**	10°39' 20,2''N	10,65555556	05°09'46,3"W	-5,16277777	335	1109	27,5	7,22	2,6
Sabaribougou	A20	**Sédimentaire**	**40**	10°37' 16,9''N	10,62111111	05°05'21,8"W	-5,08916666	318	190.3	29,6	6,94	2
Niangoloko secteur 03	A21	**Sédimentaire**	**0**	10°17' 12,9''N	10,28666667	04°54'53,9"W	-4,91472222	341	180,4	28,7	7,17	1,12
Tounfadéni	A22	**Sédimentaire**	**60**	10°09' 24,7''N	10,15666667	04°54'12,9"W	-4,90333333	311	125,9	30	6,56	1,18
Timperba école	A23	**Sédimentaire**	**73**	10°09' 55,9''N	10,16527778	04°54'14,1"W	-4,90388888	328	166	30,5	6,80	1,58
Idoro	A24	**Sédimentaire**	**68**	10°15' 17,2''N	10,25472222	04°51'38,8"W	-4,86055555	346	601	29,6	7,8	1,61
Ouangolodougou	A25	**Sédimentaire**	**71**	10°06' 21,0''N	10,10583333	04°46'57,3"W	-4,7825	328	998	29,6	6,80	3,48
NASSO	C17	**Sédimentaire**	**0**	11°11'27,1"N	11,19083333	04°26'25,9"W	-4,44027777	349	80,1	26,9	5,816	0,95
NASSO F1	C18	**Sédimentaire**	**110**	11°11'26,4" N	11,19055556	04°26'03,7"W	-4,43416666	354	134,2	29,8	6,39	1,45
NASSO F3	C 19	**Sédimentaire**	**95**	11°11'43,7" N	11,19527778	04°26'03,6"W	-4,43416666	351	17,5	30,9	5,01	0,27
NASSO F4	C20	**Sédimentaire**	**86**	11°11'58,3"N	11,19944444	04°26'02,3"W	-4,43388888	350	15,2	31,5	4,9	0,21
NASSO F2	C21	**Sédimentaire**	**158**	11°11'16,5"N	11,18777778	04°26'11,4W	-4,43638889	355	98,7	32,4	5,92	0,92

Sample name	(local name)	Aquifer	(a)	**Latitude** N/S DDMMSS.DD		**Longitude** W/E DDDMMSS.DD		Altitude (m)	Cond µS/cm	Temp. °C	pH units	Alk mg/l
NASSO	C22	**Sédimentaire**	**0**	11°10'45,4"N	11,17916667	04°26'36,1"W	-4,44333333	359	46,9	30	5,25	0,61
TOUKORO-SAMBLA	C23	**Sédimentaire**	**0**	11°11'21,0"N	11,18916667	04°31'03,3"W	-4,5175	354	591	25,4	7,02	6,9
NOUMOUSSOBA	C24	**Sédimentaire**	**0**	11°08'53,1"N	11,14805556	05°16'47,2"W	-5,27972222	340	46,1	22,2	5,56	0,42
KARTASSO	C25	**Sédimentaire**	**65**	11°08'54,8"N	11,14833333	05°15'15,6"W	-5,25416666	472	96,6	29,1	5,68	1,33
OULONKOTO	C26	**Sédimentaire**	**49**	11°05'57,0"N	11,09916667	05°05'52,0"W	-5,09777777	447	406	29,9	7,53	4,1
DJAN	C27	**Sédimentaire**	**62**	11°09'43,1"N	11,16194444	04°52'38,6"W	-4,877222222	414	613	30,6	7,1	6,69
MONDON	C28	**Sédimentaire**	**0**	11°10'05,4"N	11,16805556	04°48'58,1"W	-4,816111111	379	208	27,1	6,99	2,26
BAZON	C29	**Sédimentaire**	**46**	11°19'31,9"N	11,32527778	04°47'48,6"W	-4,796666667	380	32,1	28,7	5,24	0,29
SAMANDENIE	C30	**Sédimentaire**	**0**	11°27'46,2"N	11,46277778	04°27'51,6"W	-4,464166667	340	105,5	20,8	6,85	1,08
DINGASSO	C31	**Sédimentaire**	**74**	11°42'28,5"N	11,70777778	04°49'01,1"W	-4,816944444	337.7	631	27,3	7,65	7,04
DINGASSO	C32	**Sédimentaire**	**76**	11°42'28,5"N	11,70777778	04°49'01,1"W	-4,816944444	350	386	28,1	6,7	4,5
KOSSARA	C33	**Sédimentaire**	**0**	11°10'39,6"N	11,1775	04°43'36,1"W	-4,726666667	782	56,5	23,7	7,13	0,7
NASSO	C34	**Sédimentaire**	**118**	11°11'55,4"N	11,19861111	04°26'04,8"W	-4,434444444	346	20	31,1	4,63	0,16
NASSO	C35	**Sédimentaire**	**98**	11°11'56,8"N	11,19888889	04°26'03,3W	-4,434166667	347	58,7	30,5	5,09	0,4
LERY	C36	Sédimentaire	0	12°45'04,2"N	12,75111111	03°26'10,0"W	-3,436111111	350	136,4	26,3	7,1	1,46
YARAN	C37	**Sédimentaire**	**63**	12°58'30,8"N	12,975	03°26'37,2"W	-3,443611111	264	730	30,04	7,2	5,87
DEBE	C38	**Sédimentaire**	**30**	13°04'07,9"N	13,06861111	03°25'44,6"W	-3,428888889	262	335	32,4	6,65	3,32
NIASSAN	C39	**Sédimentaire**	**75**	13°05'37,7"N	13,09361111	03°25'42,8"W	-3,42833333	261	626	31,8	7,1	6,03
DI	C40	**Cristallin**	**0**	13°12'24,9"N	13,20666667	03°24'09,8"W	-3,4025	263	162,1	27,2	7,55	1,76
KASSOUM	C41	**Cristallin**	**56**	13°04'21,8"N	13,0725	03°18'20,2W	-3,30555555	285	324	32,2	6,46	3,23
GASSAN CSPS	C42	**Cristallin**	**61**	12°48'43,4"N	12,81194444	03°12'19,9"W	-3,205277778	272	16	30,07	5,4	0,33
Nowkuy	C43	**Cristallin**	**0**	12°30'18,2"N	12,505	03°33'13,3"W	-3,553611111	265	222	22,1	7,39	2,4
KODOUGA-BADALA	C44	**Cristallin**	**30**	12°30'37,8"N	12,51027778	03°33'42,6"W	-3,56166666	263	43,1	27,8	5,5	0,3

Sample Name	Sampling date	CE (µS/cm) lab	pH lab	HCO_3^-	F^- (mg/l)	Cl^- (mg/l)	NO_3^- (mg/l)	SO_4^{2-} (mg/l)	Na^+ (mg/l)	K^+ (mg/l)	Mg^{2+} (mg/l)	Ca^{2+} (mg/l)	TDS (mg/l)	^2H	error	^{18}O	error	^3H	error
		Réf 20°C	Unité pH	(mg/l)										‰	^2H	‰	^{18}O	TU	^3H
A8	14 02 2016	53	7,05	15,1	<LD	1,43	16,53	<0,01	2,74	1,29	1,43	5,04	43,56	-24,39	0,91	-3,98	0,18	1,66	0,3
A9	14 02 2016	425	8,48	244	<LD	6,68	5,04	8,92	10,37	3,27	21,29	46,33	345,88	-34,24	0,90	-5,72	0,19	0,34	0,3
A10	04 02 2016	136	7,64	87	0,13	0,44	0,66	<0,01	11,97	3,13	4,76	9,29	117,24	-26,24	1,15	-4,92	0,17	3,97	0,3
A11	04 02 2016	28	7,01	18,3	<LD	0,84	<0,01	<0,01	1,44	1,33	1,07	2,19	25,18	-18,57	1,15	-2,75	0,15	2,46	0,3
A12	04 02 2016	188	7,72	115,9	<LD	1,55	1,27	<0,01	11,66	1,67	10,54	11,61	154,21	-25,00	1,06	-4,76	0,12	1,29	0,3
A13	04 02 2016	86	7,48	53,9	<LD	0,29	<0,01	<0,01	10,73	3,24	1,37	5,38	74,92	-24,59	0,48	-4,64	0,16	1,72	0,3
A14	04 02 2016	327	7,78	164,7	<LD	9,85	16,46	1,06	13,23	3,48	18,32	25,31	252,42	-26,88	1,14	-4,20	0,10	0,77	0,3
A15	04 02 2016	54	7,6	30,5	<LD	1,34	5,23	<0,01	1,18	1,13	1,49	7,38	48,25	-28,77	1,10	-4,46	0,12	3,43	0,3
A16	04 02 2016	31	7,2	23,1	<LD	0,62	<0,01	<0,01	1,87	2,15	1,32	2,93	31,98	-23,15	1,51	-3,78	0,15	2,69	0,3
A17	04 02 2016	30	7,01	18,3	<LD	1,02	2,22	<0,01	1,88	2,40	1,39	2,73	29,94	-15,60	1,00	-2,56	0,05	1,69	0,3
A18	04 02 2016	1381	8,02	201,3	<LD	108,91	311,25	61,85	66,60	77,69	30,21	123,31	981,12	-22,60	1,10	-3,78	0,12	2,80	0,3
A19	04 02 2016	1084	7,78	140,3	<LD	101,68	214,55	45,09	56,27	96,55	24,16	64,15	742,75	-22,35	0,77	-3,51	0,18	2,67	0,3
A20	04 02 2016	184	7,23	109,8	<LD	0,55	<0,01	<0,01	11,77	3,23	8,95	12,91	147,22	-28,38	1,06	-4,82	0,19	0,65	0,3
A21	05 02 2016	173	7,01	91,4	0,24	2,66	4,94	1,89	16,96	2,82	3,46	14,62	138,74	-25,38	1,14	-4,33	0,11	0,57	0,3
A22	05 02 2016	118	7,16	73	0,20	0,93	2,89	<0,01	14,66	2,44	1,85	7,86	103,63	-25,42	1,45	-4,26	0,11	-0,03	0,3
A23	05 02 2016	156	7,21	97,6	<LD	0,90	1,84	<0,01	18,08	3,27	2,05	11,76	135,49	-28,06	1,20	-4,69	0,17	0,21	0,3
A24	05 02 2016	554	8,01	103,7	<LD	30,06	155,23	14,88	40,54	3,99	5,47	58,85	412,71	-23,52	0,84	-4,46	0,16	2,21	0,3
A25	05 02 2016	934	7,36	201,3	<LD	83,66	225,41	40,01	51,27	2,83	45,76	96,83	747,07	-24,15	1,40	-4,14	0,19	1,40	0,3
C17	04 02 2016	75	7,13	48,8	<LD	0,52	<0,01	<0,01	0,95	2,72	4,17	6,82	63,97	-31,38	0,92	-5,34	0,19	0,54	0,3

Sample Name	Sampling date	CE (µS/cm) lab	pH lab	HCO_3^-	F^- (mg/l)	Cl^- (mg/l)	NO_3^- (mg/l)	SO_4^{2-} (mg/l)	Na^+ (mg/l)	K^+ (mg/l)	Mg^{2+} (mg/l)	Ca^{2+} (mg/l)	TDS (mg/l)	^2H	error	^{18}O	error	^3H	error
		Réf 20°C	Unité pH	(mg/l)										‰	^2H	‰	^{18}O	TU	^3H
C18	04 02 2016	131	7,19	85,4	<LD	0,49	<0,01	<0,01	1,05	5,46	7,03	12,30	111,72	-31,12	0,50	-4,95	0,15	-0,66	0,3
C 19	04 02 2016	16	6,01	12,2	<LD	0,16	<0,01	<0,01	0,71	1,01	0,92	1,83	16,82	-32,79	1,32	-4,22	0,15	0,08	0,3
C20	04 02 2016	13	7,22	8,2	<LD	0,35	<0,01	<0,01	0,77	0,57	0,45	1,10	11,43	-30,69	1,30	-5,25	0,12	0,32	0,3
C21	04 02 2016	91	7,39	51,2	<LD	3,79	<0,01	<0,01	2,66	3,44	4,23	7,71	73,03	-31,17	0,92	-5,53	0,13	0,51	0,3
C22	04 02 2016	45	7,19	24,4	<LD	0,45	<0,01	<0,01	0,88	6,38	1,63	2,18	35,92	-30,26	1,14	-4,71	0,14	0,09	0,3
C23	04 02 2016	565	7,21	317,2	<LD	4,67	<0,01	2,38	4,33	4,60	37,13	50,29	420,60	-31,46	0,84	-4,74	0,18	0,35	0,2
C24	05 02 2016	17	7,69	9,8	<LD	0,74	<0,01	<0,01	1,00	0,88	0,53	1,69	14,63	-28,03	1,49	-4,36	0,19	1,60	0,3
C25	05 02 2016	95	7,53	61	<LD	0,48	<0,01	<0,01	0,85	10,16	3,67	6,88	83,05	-32,14	0,45	-5,61	0,16	-0,25	0,2
C26	05 02 2016	384	7,22	207,4	<LD	7,30	<0,01	11,89	11,46	10,95	16,30	36,00	301,29	-38,00	1,27	-6,48	0,16	0,83	0,3
C27	05 02 2016	595	7,41	298,9	<LD	8,73	8,33	8,88	6,40	10,35	32,15	55,55	429,28	-27,92	0,98	-4,18	0,06	0,42	0,3
C28	05 02 2016	204	7,65	115,9	<LD	2,28	0,00	0,29	1,41	13,92	9,99	17,66	161,45	-26,93	1,10	-3,80	0,19	1,19	0,3
C29	05 02 2016	30,5	6,36	16,8	<LD	0,71	1,90	<0,01	1,38	2,50	1,08	1,87	26,24	-27,60	0,90	-4,03	0,12	1,03	0,3
C30	06 02 2016	103,5	6,77	67,1	<LD	1,18	0,88	<0,01	1,82	3,72	5,53	8,94	89,16	-20,56	1,29	-2,79	0,19	2,56	0,3
C31	06 02 2016	611	7,74	329,4	<LD	7,16	<0,01	14,02	61,04	11,98	25,88	25,54	475,01	-38,89	0,46	-5,66	0,08	0,18	0,3
C32	06 02 2016	378	6,96	207,4	<LD	4,92	0,92	15,32	18,78	10,22	21,25	24,86	303,67	-35,48	0,94	-5,58	0,19	0,34	0,3
C33	06 02 2016	55,5	6,89	36,6	<LD	0,36	<0,01	<0,01	1,29	1,58	2,99	5,22	48,05	-25,25	1,40	-3,72	0,18	1,05	0,3
C34	06 02 2016	13,48	5,95	9,1	<LD	0,29	<0,01	<0,01	0,86	0,67	0,45	1,20	12,57	-27,39	0,92	-4,63	0,09	0,01	0,3
C35	06 02 2016	31	6,01	19,3	<LD	0,21	<0,01	<0,01	0,91	3,34	0,89	2,17	26,81	-30,07	1,20	-5,41	0,14	1,07	0,3
C36	17 02 2016	132,2	6,98	83,2	<LD	2,08	0,63	1,12	2,74	4,41	6,49	13,03	113,69	-0,81	1,48	1,34	0,18	3,00	0,3
C37	17 02 2016	594	7,68	252,2	<LD	7,15	5,19	87,22	11,13	7,20	37,32	55,52	462,92	-18,55	1,18	-2,66	0,15	0,77	0,3
C38	17 02 2016	524	7,71	244	<LD	5,98	11,00	2,85	8,80	4,13	18,35	44,42	339,52	-24,14	1,13	-3,57	0,15	2,81	0,3
C39	17 02 2016	565	7,42	268,4	<LD	5,95	7,91	54,30	13,87	6,04	31,76	51,88	440,10	-18,85	0,95	-1,74	0,14	1,86	0,3
C40	17 02 2016	154,3	7,33	103,4	<LD	1,12	<0,01	0,65	2,19	4,99	7,36	16,90	136,61	6,49	0,77	2,91	0,16	4,52	0,3
C41	17 02 2016	287	7,11	170,8	<LD	1,07	<0,01	4,51	1,77	4,41	16,13	30,93	229,63	-34,73	1,48	-5,07	0,17	0,49	0,3
C42	17 02 2016	12,8	6,98	4,1	<LD	0,35	3,04	0,00	1,29	0,32	0,16	0,91	10,17	-28,67	0,08	-4,29	0,17	0,47	0,3
C43	18 02 2016	221	6,77	128,1	<LD	1,37	1,71	1,83	2,76	3,97	13,29	21,05	174,09	-22,78	0,91	-2,49	0,07	1,69	0,3
C44	18 02 2016	39	7,72	10,5	<LD	0,78	12,82	<0,01	4,71	0,57	0,44	2,69	32,51	-26,55	0,92	-4,37	0,04	3,79	0,3